PROTECTIVE VENTILATION VS. HYPERCAPNIA FOR THE ATTENUATION OF VENTILATOR-ASSOCIATED LUNG INJURY

by

Nada Mezher Ismaiel

Submitted in partial fulfilment of the requirements
for the degree of Master of Science

at

Dalhousie University
Halifax, Nova Scotia
August 2011

DALHOUSIE UNIVERSITY

DEPARTMENT OF PHYSIOLOGY AND BIOPHYSICS

The undersigned hereby certify that they have read and recommend to the Faculty of Graduate Studies for acceptance a thesis entitled "PROTECTIVE VENTILATION VS. HYPERCAPNIA FOR THE ATTENUATION OF VENTILATOR-ASSOCIATED LUNG INJURY" by Nada Mezher Ismaiel in partial fulfilment of the requirements for the degree of Master of Science.

Dated: August 10, 2011

Supervisor: _____

Readers: _____

_____

_____

Departmental Representative: _____

DALHOUSIE UNIVERSITY

DATE: August 10, 2011

AUTHOR: Nada Mezher Ismaiel

TITLE: PROTECTIVE VENTILATION VS. HYPERCAPNIA FOR THE ATTENUATION OF VENTILATOR-ASSOCIATED LUNG INJURY

DEPARTMENT OR SCHOOL: Department of Physiology and Biophysics

DEGREE: MSc CONVOCATION: October YEAR: 2011

_____

Signature of Author

DEDICATION

I dedicate this Master of Science thesis to my parents for their continued support.

TABLE OF CONTENTS

LIST OF TABLES

LIST OF FIGURES

ABSTRACT

Mechanically ventilated patients are at risk of developing Ventilator-Associated Lung Injury (VALI). Improved ventilation strategies by lung-protective settings may cause hypercapnia. This study investigated whether attenuation of VALI is attributed to protective ventilation with low tidal volume (V_T) or hypercapnia. Lung injury was induced in rats by instillation of 1.25M HCl. Ten rats each were ventilated for 4 hours with: *Conventional Normocapnia* (highV_T), *Lung-Protective Ventilation* (V_T 8mL/Kg), *Injurious Normocapnia* (highV_T, added dead space), *Conventional Hypercapnia* (highV_T, inhaled CO_2), *Protective Hypercapnia* (V_T 8mL/Kg, inhaled CO_2) and *Permissive Hypercapnia* (V_T 8mL/Kg, hypoventilation). Lung-Protective Ventilation reduced pulmonary edema compared to Conventional and Injurious Normocapnia. Therapeutic hypercapnia reduced alveolar damage and inflammation by reducing IL-6 and MCP-1 in the lung, and IL-1β and TNF-α systemically. Therapeutic hypercapnia may be more effective in attenuating some of the biomarkers of VALI and protecting the lung than protective ventilation alone.

LIST OF ABBREVIATIONS USED

ALI	Acute Lung Injury
ANOVA	Analysis of Variance
AP-1	Activator Protein-1
ARDS	Acute Respiratory Distress Syndrome
BALF	Bronchoalveolar Lavage Fluid
BIPAP	Bi-level Positive Airway Pressure
BSA	Bovine Serum Albumin
CI	Cardiac Index
CMV	Controlled Mechanical Ventilation
CO	Cardiac Output
CO_2	Carbon Dioxide
CRE	c-fos Responsive Element
CV	Conventional Ventilation
DAD	Diffuse Alveolar Damage
DAMPs	Damage-Associated Molecular Pattern molecules
ECG	Electrocardiogram
EDTA	Ethylenediaminetetraacetic Acid Dipotassium Dihydrate
FiO_2	Fraction of Inspired Oxygen
GM-CSF	Granulocyte Macrophage-Colony Stimulating Factor
HCA	Hypercapnic Acidosis
HCl	Hydrochloric Acid
HCO_3^-	Bicarbonate
HR	Heart Rate
ICAM-1	Intercellular Adhesion Molecule-1
1- κB	Inhibitory- kappa B
IL-1β	Interleukin-1β
IL-1RA	Interleukin-1 Receptor Antagonist
IL-4	Interleukin-4
IL-6	Interleukin-6
IL-8	Interleukin-8
IL-10	Interleukin-10
IL-13	Interleukin-13
KC	Keratinocyte Chemoattractant
KCl	Potassium Chloride
LPV	Lung-Protective Ventilation
MAP	Mean Arterial Pressure
MCP-1	Monocyte Chemoattractant Protein-1
MIP-1α/2α	Macrophage Inflammatory Protein-1α or 2α
MMP-9	Matrix Metalloproteinase-9
MODS	Multiple Organ Dysfunction Syndrome
NF-κB	Nuclear Factor- kappa B
NOS	Nitric Oxide Synthase
O_2^{-2}	Superoxide Radical
OD	Optical Density

$PaCO_2$	Partial Pressure of Carbon Dioxide
PaO_2	Partial Pressure of Oxygen
P/F	Partial Pressure of O_2: Fraction of Inspired O_2
PEEP	Positive End-Expiratory Pressure
PHC	Permissive Hypercapnia
PMN	Polymorphonuclear
PSV	Pressure Support Ventilation
RIPA	Radioimmunoprecipitation Assay
RNS	Reactive Nitrogen Species
ROS	Reactive Oxygen Species
RR	Respiratory Rate
TACE	Tumor Necrosis Factor Alpha Conveting Enzyme
THC	Therapeutic Hypercapnia
TLC	Total Lung Capacity
TNF- α	Tumor Necrosis Factor- α
TUNEL	Terminal Deoxynucleotidyl Transferase dUTP Nick End Labeling
VALI	Ventilator-Associated Lung Injury
V_A/Q	Ventilation/Perfusion
V_E	Minute Ventilation
VEGF	Vascular Endothelial Growth Factor
V_T	Tidal Volume
W/D	Wet-to Dry Lung Ratio

ACKNOWLEDGEMENTS

First, I would like to thank my supervisor Dr. Dietrich Henzler for his guidance, support and help throughout the completion of my MSc and the preparation of this thesis.

Thank you to my supervisory committee members Drs. Elizabeth Cowley and Brent Johnston for their helpful suggestions and feedback.

A major thanks goes to Nancy McGrath, Sara Whynot, Dr. Juan Zhou, Mandana Kianian, Raymond Chankalal, Ayham Al-Afif, Dr. Jean Marshall, Carolyn Doucette, Dustin Conrad, Dr. Valérie Chappe and Dr. Zhaolin Xu for their technical assistance. Also, thank you to our collaborators Drs. Haibo Zhang and Arthur Slutsky at the University of Toronto.

I extend my sincere appreciation to my family for their continuous support and encouragement throughout my academic career to date.

This research project was funded by the Canadian Institutes of Health Research Frederick Banting and Charles Best Canada Graduate Scholarship, and the Dalhousie University Faculty of Medicine.

CHAPTER 1 INTRODUCTION

1.1 Acute Lung Injury

1.1.1 Definitions and Prevalence

Acute Lung Injury (ALI) is a critical condition where damage to the lungs causes a severe impairment in gas exchange and hemodynamic deterioration, eventually leading to systemic inflammation and hypoxemic respiratory failure (Rubenfeld et al. 2005). Based on a survey in the United States, in North America ALI is estimated to develop for 79 in every 100,000 individuals (Rubenfeld et al. 2005). On average, the mortality rate of ALI patients is approximately 38.5% (Rubenfeld et al. 2005), and has been reported to be as high as 50% in Europe (Brun-Buisson et al. 2004). The criteria for ALI diagnosis are defined by the acute onset of injury with a ratio of arterial partial pressure of oxygen to fraction of inspired oxygen (PaO_2:FiO_2) equal to or less than 300 mmHg (normally at 500 mmHg), and the presence of bilateral pulmonary infiltrates of non-cardiogenic origin (Bernard et al. 1994; Ware and Matthay 2000). The bilateral chest infiltrates are not consistent with left atrial hypertension, and therefore suggest the presence of non-cardiogenic pulmonary edema (Ware and Matthay 2000).

Acute Respiratory Distress Syndrome (ARDS) is the more severe form of ALI, and is defined by a PaO_2:FiO_2 ratio that is equal to or less than 200 mmHg, along with the criteria used for ALI diagnosis (Ware and Matthay 2000). In addition to the impaired gas exchange and hemodynamic compromise that is characteristic of ALI, ARDS is marked by a hypoxemic state that is more severe than that of ALI (Thomsen and Morris, 1995). ARDS is a more complex manifestation of ALI, and approximately 20-50% of

ALI patients progress to ARDS within seven days of developing ALI. In the United States, the ARDS mortality rate is estimated at approximately 41%, and almost 58% in Europe (Rubenfeld et al. 2005; Brun-Buisson et al. 2004).

1.1.2 Causes of Acute Lung Injury

Acute Lung Injury may be directly caused by pneumonia, aspiration of acidic gastric content or inhalation of toxic substances, and indirectly by sepsis and physical trauma, among other conditions (Ware and Matthay, 2000). The resulting ALI leads to severe oxygenation impairment, and thus patients require ventilatory support. This is primarily achieved by mechanical ventilation, which is used to restore gas exchange (Tremblay and Slutsky, 2006). However, it is now accepted that mechanical ventilation itself, while supportive, has the potential to exacerbate the existing lung injury, and may contribute to morbidity and mortality associated with ALI (Tremblay and Slutsky, 2006). This exacerbated state has been termed Ventilator-Associated Lung Injury (VALI), and is primarily caused by the addition of positive or negative pressure to the lungs during ventilation (Pinhu et al. 2003).

1.1.3 Ventilator-Associated Lung Injury

VALI subjects the injured lungs to further damage by four primary mechanisms: volutrauma, barotrauma, atelectotrauma, and biotrauma. Volutrauma is the injury caused by mechanical ventilation using high tidal volumes (V_T) (Dreyfuss et al. 1988). Volutrauma has been shown to be injurious to the lungs by causing overdistention

(hyperinflation), often to the total lung volume capacity (TLC) (Pinhu et al. 2003; Dreyfuss et al. 1988). Clinical trials have demonstrated that ventilation with a V_T of 12 ml/kg predicted body weight produced volutrauma, and resulted in morbidity and mortality in ventilated ALI and ARDS patients (Petrucci and Lacovelli, 2004; ARDS Network, 2000). Volutrauma is typically accompanied by barotrauma, a mechanism of injury caused by ventilation with high inspiratory plateau pressures (Oeckler and Hubmayr, 2007). Barotrauma causes severe damage to the connective tissue matrix around alveolar spaces, and leads to the leakage of various substances into extra-alveolar spaces, including proteins and air (Oeckler and Hubmayr, 2007). Together, volutrauma and barotrauma are the adverse effects of ventilatory attempts to restore physiologic gas exchange in the short-term, but actually cause VALI in the long-term.

Atelectotrauma is another common mechanism of VALI, and is characterized by alveolar collapse resulting from cyclic opening and closing of alveoli during mechanical ventilation (Pinhu et al. 2003). The continuous recruitment and derecruitment of alveoli and small airways leads to airway collapse, and thus no gas exchange can occur at these collapsed and/or occluded airways. As such, pulmonary gas exchange deteriorates further and contributes to the potentiation of VALI. Positive-End Expiratory Pressure (PEEP) is often applied during mechanical ventilation in order to prevent repeated opening and closing of airways and ultimately improve gas exchange. However, PEEP itself, if applied excessively and continuously, has the potential to produce barotrauma by damaging the alveolar barrier membranes (Oeckler and Hubmayr, 2007).

The VALI resulting from volutrauma, barotrauma and atelectotrauma is accompanied by excessive stress, strain and physical damage to epithelial cells. This

activates various chemical mediators that promote cell and tissue inflammation, a phenomenon known as biotrauma (Pinhu et al. 2003; Oeckler and Hubmayr, 2007). These chemical mediators are bioactive molecules involved in complex signaling pathways. Ultimately, biotrauma is an outcome of widespread inflammation by the release of additional cytokines and chemokines from leukocytes and epithelial cells, formation of reactive biological species (oxygen- and nitrogen-based), and activation of mediators that promote cell death, including tumor necrosis factor-α (Oeckler and Hubmayr, 2007).

1.1.4 Local and Systemic Manifestations of VALI

Mechanical stress on the lungs causes biotrauma on a local (pulmonary) and systemic level. Locally, the release of cytokines, chemokines and other chemoattractant molecules from alveolar macrophages and epithelial cells recruits polymorphonuclear (PMN) cells such as neutrophils, basophils and eosinophils to the lungs (Imanaka et al. 2001). PMN cells infiltrate the lungs by adhering to the endothelial surface of pulmonary capillaries, aggregating and modifying their shape to translocate from the circulation into the lung interstitium (Reutershan and Ley, 2004). Upon entering the lungs, a complex network of cytokines and other pro-inflammatory mediators is released into the airspaces, thereby potentiating the inflammatory state of the lungs. This process involves activation of the transcription factor Nuclear Factor Kappa-B (NF-κB), which mediates the production of pro-inflammatory genes coding for cytokines, chemokines and other inflammatory substances (Fan et al. 2001).

In its inactive state, NF-κB is bound to Inhibitory κB (I-κB) in the cytoplasm, which prevents its translocation to the nucleus. NF-κB activation can be triggered by a

variety of stimuli, including pro-inflammatory signaling molecules (cytokines and chemokines), reactive oxygen species (ROS), and bacterial and viral products at the cell surface and intracellularly by toll-like receptor activation (Barnes and Karin, 1997). Activation of NF-κB is the final stage of the signal cascade initiated at the cell surface, and leads to the phosphorylation of I-κB, followed by its dissociation from NF-κB (Fan et al. 2001). In turn, this leaves NF-κB free to translocate to the nucleus, bind to and transcribe downstream pro-inflammatory mediators such as TNF-α, interleukin (IL)-1β, IL-6, MIP-2α and IL-8. Anti-inflammatory mediators such as IL-1 receptor antagonist (IL-1RA), IL-4, IL-10 and IL-13 are generated in response to the pro-inflammatory agents (Goodman et al. 1996). However, in ALI and ARDS, there is a marked imbalance between pro- and anti-inflammatory cytokines that correlates with the severity of injury and mortality rates (Donnelly et al. 1996). In the lungs, this translates into a disruption in alveolar and endothelial barrier function, and programmed cell death (apoptosis), leading to deterioration of gas exchange, hypoxia, and acute respiratory failure (Ware and Matthay, 2000).

Respiratory failure may also serve as the gateway to multiple organ failure, also known as Multiple Organ Dysfunction Syndrome (MODS). This is by way of a "spillover" of inflammatory mediators from the lungs into the systemic circulation (Plötz et al. 2004; Slutsky and Tremblay, 1998). The release of inflammatory mediators into the circulation from the lungs is facilitated by increased permeability of the alveolar-capillary interface, in addition to the fact that the large surface area of the lungs is exposed to a sizable fraction of the total circulating blood (Tutor et al. 1994; Debs et al. 1998). While the mechanisms of cytokine "spillover" remain unclear, it is possible that the

translocation of cytokines into the systemic circulation is mediated by the increase the permeability of the pulmonary endothelium. Under physiologic conditions, healthy pulmonary endothelium plays an important role in filtering the blood before it enters the systemic circulation (Orfanos et al. 2004). Since lung injury has been associated with extensive damage to endothelial cells (Orfanos et al. 2004), it is possible that damage to the endothelium mediates cytokine spillover from the lungs into the circulation. Effectively, this causes a systemic inflammatory response in mechanically ventilated ARDS patients, with elevated levels of tumor necrosis factor alpha (TNF-α), IL-6, IL-8, and IL-1β in bronchoalveolar lavage fluid (BALF) (Meduri et al. 1995). Though biotrauma plays a key role in potentiating VALI, it may not be the only factor associated with MODS secondary to mechanical ventilation. It is likely that multiple factors are involved in exacerbating the systemic inflammatory response associated with VALI.

VALI has been shown to have downstream systemic effects on distal organs by compromising hemodynamic function. This is especially evident in the effects of mechanical ventilation on cardiac output, which is markedly reduced during ventilation (Slutsky and Tremblay, 1998). A reduction in cardiac output markedly decreases intestinal, hepatic and renal perfusion, leading to the dysfunction and potential failure of those organs. A limitation in organ perfusion impairs oxygen delivery to the distal organs, potentially leading to dysfunction in these tissues (Love et al. 1995; Gammanpila et al. 1977). While a direct relationship between mechanical ventilation and MODS is yet to be established, several studies have shown that varying the mechanical ventilation settings reduces the likelihood of developing MODS secondary to VALI, ultimately

reducing ALI/ARDS patient mortality rates (ARDS Network, 2000; Amato et al. 1998; Hickling et al. 1994).

1.2 Mechanical Ventilation

1.2.1 Definition and Context

Mechanical ventilation is the process whereby positive pressure is applied from a machine through the trachea in order to adequately provide fresh gas and ventilate the lungs. Mechanical ventilation is widely used in clinical practice to provide ventilatory support to critically ill patients. While these patients are typically admitted for conditions such as sepsis, trauma, or post-operative care, respiratory failure secondary to such conditions is not uncommon. For that reason, mechanical ventilation is the first standard of care to provide ventilatory support (Task Force on Guidelines, Society of Critical Care Medicine, 1991).

1.2.2 Modes of Ventilation

There are several modes of mechanical ventilation used to manage ALI and ARDS patients. Mechanical ventilation can provide additional support for spontaneously breathing patients, as well as patients that rely completely on mechanical breathing. Patients that exhibit some spontaneous breathing efforts can receive varying degrees of pressure support ventilation (PSV) to supplement their respiratory function. Patients that require complete artificial ventilation undergo controlled mechanical ventilation (CMV), a strategy in which the peak airway pressure, respiratory rate and tidal volume are set by the ventilator (Hooper, 1998).

To facilitate CMV in spontaneously breathing patients, neuromuscular blocking agents are sometimes used to abolish spontaneous breathing efforts and facilitate lung ventilation solely by the machine (Papazian et al. 2010). This has the added advantage of allowing more manipulation of the patient's respiratory mechanics through changes in ventilator settings. A recent multicenter study demonstrated that the use of cisatracurium besylate (a neuromuscular relaxant) in patients with early and severe ARDS undergoing CMV was effective in improving the adjusted 90-day survival rate, and did not cause respiratory muscle weakness when discontinued (Papazian et al. 2010). This suggests that the use of neuromuscular blockade to facilitate CMV may improve the outcome of lung injury for ventilated patients. In the application of CMV and PSV, Dembinski et al. (2002) also showed a better outcome of VALI with an improvement in the ventilation/perfusion (V_A/Q) distribution in CMV compared with PSV in a pig model of ALI caused by repeated lung lavage. However, in that model, PSV appeared to be more effective in improving pulmonary gas exchange (Dembinski et al. 2002). Interestingly, Putensen et al. (1999) showed that PSV with preserved spontaneous breathing is beneficial for ARDS patients, particularly because it improves pulmonary gas exchange by altering the V_A/Q distribution in the ventilated lung. These studies demonstrate that both CMV and PSV contribute to the development and exacerbation of VALI.

1.2.3 Ventilation Strategies

CMV settings have been extensively studied and refined in an attempt to find the best means of restoring gas exchange and improving the outcome of VALI in patients. The conventional ventilation (CV) strategy constitutes the use of high tidal volumes

ranging from 10 to 15 ml/kg predicted body weight (Determann et al. 2010; Amato et al. 1998; ARDS Network, 2000; Broccard et al. 1998; Marini, 1996). Large tidal volumes are traditionally used in the ventilatory management of ALI and ARDS patients in order to achieve adequate pH and arterial partial pressures of carbon dioxide ($PaCO_2$) and oxygen (PaO_2) (ARDS Network, 2000). Since large volumes are achieved by large inspiratory pressures, conventional ventilation often produces lung overdistention, leading to VALI by way of barotrauma, volutrauma, and a potentiated inflammatory response. Severe pulmonary inflammation has the potential to spread to other organ systems and has been associated with MODS, however this relationship has yet to be confirmed (Tremblay et al. 1997; Parker et al. 1993). These findings have also been demonstrated experimentally in large and small animal models, including rats, mice, rabbits and sheep (Dreyfuss et al. 1988; Veldhuizen et al. 2001; Wilson et al. 2003; Bellardine et al. 2006; Savel et al. 2001).

These outcomes prompted intensive care clinicians to adopt the use of lower tidal volumes to promote lung-protective ventilation (LPV). This includes mechanical ventilation with tidal volumes ranging from 5 to 8 ml/kg predicted body weight and low plateau pressures (ARDS Network, 2000; Broccard et al. 1998; Brower et al. 1999). This ventilation strategy was incorporated into the standard management of ALI/ARDS patients to reduce VALI by decreasing the ventilation stress caused by excessive lung stretch (ARDS Network, 2000). While LPV indeed reduced lung stretch, it also proved effective in attenuating pulmonary inflammation by reducing the release of pro-inflammatory substances and improved fluid clearance from the lungs, which improved

the patient mortality rate (Hickling et al. 1990; Hickling et al. 1994; Ware and Matthay, 2001). However, ventilation with low V_T tended to result in a decreased arterial oxygenation, increased $PaCO_2$, leading to respiratory acidosis (Hickling et al. 1990; Hickling et al. 1994). Meanwhile, an experimental model of VALI using rabbits showed that LPV can improve oxygenation, hemodynamic stability and acid-base homeostasis (Savel et al. 2001). Overall, experimental models of VALI in rats, mice and rabbits are in agreement with clinical trials demonstrating the potential for LPV to attenuate the deleterious effects of VALI (Frank et al. 2002; Wilson et al. 2003; Savel et al., 2001).

The low V_T used in LPV can produce hypercapnia (high $PaCO_2$), where the $PaCO_2$ rises spontaneously due to the accumulating CO_2 as an outcome of a decrease in minute ventilation (Hickling et al. 1994; Kavanagh and Laffey, 2006). This phenomenon has since been termed permissive hypercapnia (PHC), and is named accordingly because it is a tolerated side effect of LPV that has gained acceptance as a therapy for managing ALI/ARDS patients (Ismaiel and Henzler, 2011). The effects of PHC have never been directly examined clinically or experimentally. However, several clinical studies have investigated LPV with permissive hypercapnia as a tolerated side effect (Hickling et al. 1990; Hickling, 1992; Hickling et al. 1994; Bidani et al. 1994). Though the direct effects of PHC remain unclear, PHC has been associated with a reduction in lung stretch, and improved patient survival (Hickling et al. 1994; Bidani et al. 1994).

Realizing the potential benefits of PHC, hypercapnia may no longer be viewed as a side effect, but instead as a helpful ventilation strategy (Kavanagh and Laffey, 2006). This sparked interest in investigating the effects of therapeutic hypercapnia (THC), where a small fraction of inhaled CO_2 is added to the gas mixture during ventilation, or

physiologic dead space is added (Kavanagh and Laffey, 2006; Ismaiel and Henzler, 2011). This is used to "deliberately" increase the $PaCO_2$ and induce hypercapnia exogenously. The concept of THC remains experimental, since there is evidence supporting and rejecting the effects of THC. THC was shown to attenuate pulmonary inflammation and free radical production, and preserved pulmonary mechanics in an ischemia-reperfusion-induced lung injury model in the rabbit (Laffey et al. 2000b) (Figure.1). *In vitro*, alveolar macrophages incubated with CO_2 to induce significant hypercapnia (60-146 mmHg) showed a remarkable decrease in the production of free radical compounds, particularly the superoxide radical (O_2^-) (Kogan et al. 1996). The effects of THC thus far have been attributed to the acidotic state that results from hypercapnia, termed hypercapnic acidosis (HCA) (Reviewed in Kavanagh and Laffey, 2006), and is characterized by the decrease in intracellular pH due to the accumulating CO_2 (Reviewed in Ismaiel and Henzler, 2011). HCA has been associated with a reduction in pulmonary inflammation, and cell death (Laffey et al. 2000b) (Figure.1), and protects other organ systems in several experimental models of ALI, including that induced by sepsis, ischemia-reperfusion, and mechanical ventilation (Reviewed in Ismaiel and Henzler, 2011).

1.3 Hypercapnia and Hypercapnic Acidosis

1.3.1 Anti-Inflammatory Effects

Several studies have demonstrated the anti-inflammatory effects of HCA. Laffey et al. (2000b) showed a reduction in IL-1β and TNF-α in BALF collected from injured rabbit lungs treated with HCA. In this study, the pH was approximately 7.00 after 90

minutes of protective ventilation (V_T=7.5 ml/kg) with inspired CO_2 (Laffey et al. 2000b). In cultured human pulmonary artery endothelial cells incubated with endotoxin, HCA inhibited the activation of NF-κB by a mechanism that reduced IκB degradation (Takeshita et al. 2003). This decreased the transcription of intracellular cell adhesion molecule (1-CAM) and IL-8 (Figure.1), and limited neutrophil adherence to pulmonary endothelial cells (Takeshita et al. 2003). HCA also reduced neutrophil counts in BALF and reduced alveolar wall thickening and inflammatory cell infiltration in a rat model of ALI induced by intratracheal instillation of endotoxin (Laffey et al. 2004).

HCA has been reported to inhibit the production of nitric oxide (NO) and other NO metabolites such as peroxynitrite and nitrotyrosine in lung homogenates compared to untreated control animals, demonstrating a reduction in reactive nitrogen species (RNS) (Nichol et al. 2010). This may be mediated by a mechanism that inhibits nitric oxide synthase (NOS), thus reducing pulmonary oxidative reactions (Nichol et al. 2010). Kristof et al. (1998) provide evidence for this by demonstrating that knocking out inducible Nitric Oxide Synthase (iNOS), which produces NO, reduces the susceptibility to endotoxin-induced ALI in mice. Shibata et al. (1998) also showed that HCA attenuates the production of RNS. In that study, a model of isolated rabbit lung was used to show that HCA reduces the activity of the xanthine oxidase enzyme, which is responsible for the production of reactive oxygen and nitrogen species (Figure.1). These studies suggest an important role for HCA in the attenuation of pulmonary inflammation by reducing the production and release of pro-inflammatory mediators, as well as the production of NO and its metabolites.

Conversely, treatment with inhaled NO improved the histopathologic outcome, lung leukocyte counts, and reduced pulmonary oxidant stress in a rabbit model of saline lavage-induced ALI (Floretto et al. 2011). In a swine model of sepsis-induced ALI, pretreatment with inhaled NO also reduced the production of the superoxide anion and neutrophil counts in lavage fluid (Bloomfield et al. 1997). Therefore, the role of NO in ALI remains elusive, given the evidence implicating NO as a biomarker of ALI and as a potential therapy.

To better model clinical sepsis, a cecal ligation model of ALI (secondary to sepsis) showed that HCA protects against ALI in early and prolonged sepsis (Costello et al. 2009). Similarly, Chonghaile and colleagues (2008) demonstrated that HCA substantially reduces bacterial counts in a model of bacterial pneumonia-induced lung injury in rats. In addition, HCA reduced structural lung damage and produced a lower grade of histologic injury compared to normocapnic animals.

Sinclair et al. (2002) used a model of ALI induced by injurious ventilation in rabbits, and showed that HCA reduced pulmonary edema as measured by a decreased wet-to-dry lung ratio postmortem, and reduced protein concentrations in BALF. As well, HCA-treated animals showed lower inflammatory cell infiltration compared to untreated animals (Sinclair et al. 2002).

More recently, Peltekova and colleagues (2010) provide additional evidence highlighting the therapeutic effects of HCA. In that study, a mouse model of ventilator-induced lung injury treated with HCA exhibited a reduction in several key pro-inflammatory mediators, including IL-6, Monocyte Chemoattractant Protein-1 (MCP-1), Matrix Metalloproteinase-9 (MMP-9), and Keratinocyte Chemoattractant factor (KC).

This effect was even more pronounced when HCA was coupled with protective ventilation settings. Inhibition of these inflammatory substances was also noted in a dose-dependent fashion, such that HCA induced with 25% inspired CO_2 had the greatest effect compared to 12% and 5% CO_2, respectively (Peltekova et al. 2010). These effects were reflected in the histopathological evaluation of the lungs, which showed a reduction in PMN cell infiltrates.

Therefore, there is a growing body of experimental evidence demonstrating the anti-inflammatory effects of therapeutic hypercapnia and hypercapnic acidosis, and lends support to its benefits in several experimental models of ALI. In fact, Laffey et al. (2000a) and Nichol et al. (2009) both showed that buffering HCA with sodium bicarbonate actually exacerbates the existing injury in the lungs and myocardium. This was supported by an increase in the wet-to-dry lung ratio and xanthine oxidase activity of the lungs after the HCA was buffered with bicarbonate (Laffey et al. 2000a). These findings suggest an increase in the production of pulmonary edema and reactive molecules with buffering, rendering the effects of HCA ineffective. In turn, this provides further support as to the important role of hypercapnic acidosis in the attenuation of VALI. Taken together, it is clear that therapeutic hypercapnia and the resulting hypercapnic acidosis are closely related, and have been associated with the attenuation of lung injury by reducing various biomarkers of VALI.

1.3.2 Effects on Other Organs

HCA has been shown to exert its therapeutic effects beyond the lungs in other organ systems. Early experiments with HCA in a model of cardioplegia (stopping of the heart during cardiac surgery) demonstrated the ability of HCA to protect the working

myocardium during ischemia-reperfusion injury and under hypoxic conditions (Nomura et al. 1994). Similarly, following ischemia, HCA at a pH of 6.6 was shown to reduce cell death upon reperfusion and protect the ventricular myocardium compared to reperfusion at a pH of 7.6, where significant cell death was noted (Kaplan et al. 1995). This effect was attributed to the inhibition of the Na^+/H^+ exchanger under acidotic conditions, thereby preventing H^+ movement into the extracellular environment (Kaplan et al. 1995). In a canine model of cardiac infarction, HCA also reduced the infarct size during reperfusion (Kitakaze et al. 1997). Findings from these studies highlight the protective effects of HCA in the myocardium.

The protective effects of HCA have also been examined in the central nervous system. Vannucci et al. (1995) demonstrated the neuroprotective effects of HCA induced by therapeutic hypercapnia in a model of ischemia-reperfusion in the brain. In that study, treatment with 6% CO_2 showed the greatest reduction in brain damage in rat pups compared to 3% and 9% CO_2 (Vannucci et al. 1995). In fact, these same effects were exacerbated when hypocapnia was applied. Findings from this study showed that hypercapnia is neuroprotective compared to both hypocapnia and normocapnia in the developing rat brain. Other studies have also evaluated the protective effects of HCA in the brain, including a reduction in neuronal apoptosis, lipid peroxidation, and decreased production of free radical compounds (Xu et al. 1998; Barth et al. 1998). This effect is likely mediated by the inhibition of various biological enzymes that function optimally at physiologic pH. A similar effect has been noted in the liver, where cell death is attenuated in hepatocytes treated with HCA (Gores et al. 1989). Together, these studies

provide sufficient evidence to support the protective role of hypercapnia and hypercapnic acidosis in different organ systems.

1.3.3 Potentially Harmful Effects

While many studies (*in vivo* and *in vitro*) demonstrated the therapeutic potential of hypercapnia and hypercapnic acidosis, others have shown that THC and HCA also have deleterious effects. For example, two *in vitro* studies with rat alveolar epithelial cells showed that treating these cells with CO_2 increases the production of RNS, and increases the expression and activation of iNOS (Lang et al. 2000; Briva et al. 2007). Lang et al. used the terminal deoxynucleotidyl transferase dUTP nick end labeling (TUNEL) stain to show that THC increases cell death in alveolar epithelial cells (Lang et al. 2000). Despite the conflicting results in the application of THC *in vitro*, it is important to possible that these negative effects were observed in alveolar epithelial cells, whereas THC reduced free radical production in alveolar macrophages (Kogan et al. 1996). Therefore, it is possible that THC has different effects on different lung cell populations.

In an *ex vivo* perfused rat lung model of ventilator-induced lung injury, epithelial cell wound healing was impaired under hypercapnic conditions (Doerr et al. 2005). This study suggests that THC does not provide healthy physiologic conditions to facilitate lung cell repair after injury. Two *in vivo* rat models of ALI also provide evidence against HCA. In one study, hydrochloric acid (HCl) was injected intravenously to cause acid-induced lung injury. That study showed that treatment with HCA potentiated the inflammatory response, increased NO production, and caused hemodynamic instability through severe hypotension in the rats (Pedoto et al. 1999). Therefore, Pedoto et al. showed that HCA has global deleterious effects in their model of acid-induced lung

injury. O'Croinin et al. (2008) used a rat model of endotoxin-induced lung injury by intratreacheal *E.coli* instillation to investigate the effects of HCA sustained for two days. In that study, prolonged HCA increased the animals' susceptibility to subsequent bacterial infections, which exacerbated the existing ALI. This effect was likely mediated by the immunosuppressive effects of HCA (O'Croinin et al. 2008). As such, this study provides evidence that prolonged HCA has deleterious effects, but does not provide the same evidence for short-term HCA.

Recent work has also demonstrated that therapeutic hypercapnia does not improve the outcome of lung injury. Treatment with 5% CO_2 in hyperoxic neonatal rats caused the greatest degree of histopathologic damage in the lungs, which were scored based on the presence of inflammatory cells and hemorrhages (MacCarrick et al. 2010). However, therapeutic hypercapnia appeared to reduce the release of pro-inflammatory cytokines IL-1β and TNF-α (MacCarrick et al. 2010). Lang et al. (2005) also provide evidence against hypercapnia (induced permissively, causing acidosis) in a rabbit model of LPS-induced ALI. In that study, rabbits received protective ventilation (V_T= 7 mL/Kg) for 6 hours under normocapnic or hypercapnic conditions. Hypercapnia was shown to increase total protein concentrations and cell counts in bronchoalveolar lavage fluid (BALF) compared to animals under normocapnic conditions (Lang et al. 2005). Hypercapnia also increased pulmonary edema, histopathologic injury, and the expression of iNOS, NO metabolites (nitrite and nitrate) and myeloperoxidase content in the lungs (Lang et al. 2005). Therefore, there is strong evidence against hypercapnia and hypercapnic acidosis in the context of ALI.

Therapeutic hypercapnia has been shown to impair the diaphragmatic muscle function of rats. In that study, Kumagai et al. (2001) showed that diaphragmatic muscle fibers can degenerate following a 6-week exposure of rats in a 10 % CO_2 chamber compared to rats exposed to a 6-week exposure in a normocapnic chamber. This study involved healthy rats, however the findings may have important implications for mechanically-ventilated animals with ALI. This is particularly true at the time of weaning from mechanical ventilation because it requires appropriate diaghragmatic function (Reviewed in (Ijland et al. 2010). Jaber et al. (2008) provide additional evidence for the diaphragmatic impairment under hypercapnic conditions. In that study, ventilated piglets exposed to measured increases in $PaCO_2$ (40, 50,70,90 and 110 mmHg) demonstrated a decrease in the contractile force of diaphragmatic muscle that was directly proportional to the increase in $PaCO_2$. Impaired diaphragmatic activity may represent an important mechanism for worsening VALI as it reduces spontaneous breathing efforts and promotes increased dependence on controlled mechanical ventilation. Therefore, these findings contribute to the current body of literature demonstrating both the potentially benefical and harmful effects of hypercapnia and hypercapnia acidosis.

1.4 Purpose and Hypotheses

1.4.1 Purpose of the Study

To date, multiple studies have demonstrated the potential benefits of lung-protective ventilation, permissive and therapeutic hypercapnia for the attenuation of VALI. These effects have been evaluated in several experimental models of ALI, including ALI induced by mechanical ventilation, pneumonia, sepsis, and ischemia-

reperfusion. However, no study has directly addressed whether the attenuation of VALI is attributed to lung-protective ventilation (with low tidal volumes and pressures) or the resulting hypercapnia (increased $PaCO_2$). In addition, no study has investigated these effects in an acid aspiration model of ALI. For that reason, the purpose of this study was to determine whether the attenuation of VALI is mainly associated with protective ventilation settings or hypercapnia in an aspiration-induced model of ALI. An acid aspiration model of ALI was used as a representation of clinical ALI caused by the aspiration of gastric acids in patients. If the source of attenuation in VALI is indeed an outcome of hypercapnia, is there a difference in the effect of permissive and therapeutic hypercapnia? That is, does therapeutic hypercapnia by inhaled CO_2 gas offer an additional benefit to permissive hypercapnia by endogenous CO_2?

These effects were investigated in a rat model of aspiration-induced ALI with different experimental groups subject to controlled mechanical ventilation with lung-protective settings, permissive hypercapnia and therapeutic hypercapnia. The outcomes of the different ventilation groups were evaluated using parameters of hemodynamics, respiratory mechanics, gas exchange, histology, inflammation, and programmed cell death.

1.4.2 Research Hypotheses

There were three hypotheses in the present study. First, it was hypothesized that hypercapnia protects the lung from VALI by attenuating inflammation and alveolar damage. Second, it was hypothesized that protective ventilation with reduced pressures and tidal volumes attenuates VALI. Finally, it was hypothesized that therapeutic

hypercapnia with inhaled CO_2 is more protective compared to permissive hypercapnia with endogenous CO_2.

CHAPTER 2 MATERIALS AND METHODS

2.1 Rat Handling and Instrumentation

Sixty Male Sprague-Dawley rats (weight, 400-490 g) were obtained from Charles River Laboratories (Saint-Constant, QC, Canada). The rats were maintained at the Carlton Animal Care Facility at Dalhousie University on a 12-hour light/dark cycle. The rats were housed in conventional cages (10.5" W x 19" D x 8" H) in pairs with Beta Chip and hay in the cages. The room temperature was maintained daily at 21-22°C. The rats were given unlimited access to Prolab Rodent Chow and water. All rats received daily health checks by animal care staff at Dalhousie University to ensure the well being of all animals.

All experimental procedures and protocols were conducted with approval of the University Committee on Laboratory Animals and the Carlton Animal Care Facility at Dalhousie University (protocol No. 08-132). Rats were initially weighed using a balance scale (Ohaus, Explorer model E0D110, Parsippany, NJ, USA) to determine appropriate dosing for anesthesia, analgesia and calculating the appropriate tidal volume for ventilation. Rats were anesthetized by intraperitoneal injection of sodium pentobarbital (55 mg/kg). The neck and femoral regions of the body were shaved to facilitate access to those areas for vessel cannulation. The rats were laid in supine position on a Shor-Line stainless steel operating table (22" width x 60" length, distributed by Harvard Apparatus Canada, Saint-Laurent, QC, Canada) with an internal surface heater maintained at 37°C. Additional heat was also provided by an overhead lamp (Burton Medical, Chatsworth, CA, USA) as needed.

During the instrumentation, the rats received oxygen therapy using 100% O_2 delivered from a neonatal ventilator (Evita XL, Draeger Medical Inc., Richmond Hill, ON, Canada). The oxygen was delivered through a tube attached to the facial region of the rats. An incision was made in the right femoral region, and the surrounding tissue was dissected, allowing the isolation of the right femoral artery. A thermocouple temperature probe was carefully inserted into the aorta through the right femoral artery to facilitate the monitoring of body temperature and the measurement of cardiac output (CO) (IT-21, Type T thermocouple copper-constantan, Physitemp Instruments Inc., Clifton, NJ, USA). An incision was then made in the neck, and connective tissue was dissected to expose the left jugular vein. A catheter was then inserted into the left jugular vein and secured to the vessel. The left carotid artery was isolated and cannulated to monitor mean arterial pressure (MAP). Finally, the trachea was isolated, and a tracheostomy was performed by inserting a 14G cannula into the trachea and securing it in place. The temperature probe, two vessel catheters and tracheal cannula were secured in their positions using fine threads tied at the proximal and distal ends of the vessel or trachea.

2.2 Equipment Calibration

ChartPro 6.0 software (ADInstruments, Colorado Springs, CO, USA) was run on a laptop computer (Fujitsu Siemens Lifebook S7110, Germany) and used to calibrate the PowerLab operating system (ADInstruments, Colorado Springs, CO, USA). The physiologic pressure transducers (SensoNor SP 844, ADInstruments, Colorado Springs, CO, USA) for measuring MAP and esophageal pressure were connected to the PowerLab system. Pressure transducers were calibrated with a sphygmomanometer using a two-point calibration for each transducer. The MAP transducer was calibrated from 0 to 100

mmHg, and the esophageal pressure transducer was calibrated from 0 to 100 mmHg, which was then converted on a scale of 0 to 130 cmH_2O units. The pneumotach (Series 8420B, rat and guinea pig-specific, Hans Rudolph Inc., Shawnee, KS, USA) was used to measure spirometry flow and tidal volume (V_T) during each experiment was calibrated using a 100 ml calibration syringe (Series 5510, Hans Rudolph Inc., Shawnee, KS, USA). The syringe was set to measure a 20 ml volume. Twenty ml of air was pushed through the pneumotach and the area under the flow curve was recorded and set to equal 20 ml.

The tissue implantable thermocouple temperature probe was calibrated once per week using a two-point calibration. The temperature-sensitive tip of the probe was submerged into a beaker containing water at 25°C and another beaker containing water at 37°C, while the other end was plugged into an output port connected to the PowerLab operating system. The neonatal ventilator used for oxygen delivery and mechanical ventilation was automatically calibrated daily. The ABL 700 blood gas analyzer and the species adjusted co-oximeter OSM 3 (Radiometer Canada, London, ON, Canada) were automatically calibrated using one and two-point calibrations every 2 hours and 4 hours, respectively. The blood gas measurements obtained from the ABL 700 were automatically adjusted to barometric pressure.

2.3 Physiologic Measurements

2.3.1 Hemodynamics

The arterial catheter was attached to the physiologic pressure transducer calibrated to measure MAP. The thermocouple temperature probe was connected to an output unit, and cardiac output was measured using the thermodilution principle. Briefly, 0.5 ml of saline solution (0.9% NaCl) was administered as an intravenous bolus and temperature

changes were recorded. Cardiac output was computed by the ChartPro software. Two cardiac output measurements were taken at each time point, and the mean was calculated and recorded. Heart rate was measured using three electrocardiogram (ECG) leads positioned according to Einthoven's Triangle (right arm, left arm and left leg). The ECG leads, temperature probe, and MAP transducer were connected to the PowerLab system and data was inputted into the ChartPro 6.0 software for live monitoring and recording. The cardiac output was measured at baseline and at the end of each hour of ventilation. Meanwhile, body temperature, heart rate and MAP were measured at baseline and six times during each hour of ventilation using live recordings.

2.3.2 Respiratory Mechanics

The tracheal cannula was connected to the pneumotach, which was coupled to a signal amplifier (Series 1110, Hans Rudolph Inc., Shawnee, KS, USA). The ventilator was set to deliver mechanical ventilation, and the pneumotach was connected to the ventilator. The ventilator was set in BIPAP (Bi-level Positive Airway Pressure) mode. The inspiratory pressure on the ventilator was set to achieve a tidal volume of 8 ml/kg, PEEP (Positive End Expiratory Pressure) was set to 5 cmH_2O, FiO_2 (Fraction of Inspired O_2) set to 1.0 (100% O_2), and respiratory rate set to achieve a $PaCO_2$ (arterial partial pressure of CO_2) of 40-55 mmHg. The Tinsp (inspiratory time) was adjusted to achieve a 1:1 ratio between inspiratory and expiratory time during ventilation.

This set-up provided live monitoring of airway pressure, tidal volume, flow, and respiratory rate. Elastance, which is the pressure required to displace lung volume, was also measured to indicate changes in the elastic properties of the lung. Mathematically, elastance is defined as the airway pressure divided by the tidal volume (E=P/V). Since

the mechanical ventilator measures airway pressure and tidal volume, the elastance in each group was calculated manually. The elastance was used to measure the presence of ALI, since an increase in elastance indicates that more pressure is required to ventilate with the set tidal volume. This is indicative of ALI because a higher airway pressure suggests that the lung is less compliant to inflate.

Esophageal pressure was measured by inserting a 16G cannula into the esophagus through the oral cavity. A catheter was attached to the physiologic pressure transducer calibrated to measure esophageal pressure, with the distal end inserted into the esophagus through the 16G cannula. Esophageal pressure was monitored to ensure that all spontaneous breathing efforts were eliminated to facilitate controlled ventilation. Tidal volume, flow, airway pressure, respiratory rate, elastance, and esophageal pressure were measured at baseline and six times during each hour of ventilation with live recordings.

2.3.3 Gas Exchange

Blood gases were measured by collecting 0.3 ml of arterial blood and 0.3 ml of venous blood drawn into heparinized syringes. Arterial and venous blood gases and oxymetry were analyzed using the ABL 700 blood gas analyzer and the species adjusted co-oximeter OSM 3. The pH, $PaCO_2$ and PaO_2 in the arterial and venous blood gases were measured at baseline and at the end of each hour of ventilation.

2.4 Experimental Protocol

2.4.1 Sedation Protocol

The venous catheter was connected to a conventional syringe pump (Perfusor Space, Braun Medical, Melsungen, Germany) to facilitate the continuous intravenous

infusion of 20 μg/ml remifentanil and 25 μg/ml pancuronium (diluted in 0.9% NaCl in a 60 ml syringe) at 5 ml/hour. The remifentanil was given at 0.4 μg/kg/min to provide continuous analgesia and sedation, and the pancuronium was given at 0.2 mg/kg/hr to provide neuromuscular blockade to facilitate CMV. The remifentanil was obtained at a concentration of 10 μg/ml, and the pancuronium was obtained at a concentration of 2 mg/ml and were diluted with 0.9% NaCl solution to obtain the final concentration. The intravenous infusion of remifentanil and pancuronium was continuously delivered throughout the duration of the ventilation period.

2.4.2 Acute Lung Injury

After baseline measurements were completed and respiratory paralysis was achieved, acute lung injury (ALI) was induced. Unbuffered hydrochloric acid (pH 1.25) was instilled into the trachea through the 14G cannula at 2.5 ml/kg. The acid was instilled such that 60% of the total volume was delivered to the right lung and 40% of the total volume was delivered into the left lung. First, the tracheal cannula was disconnected from the pneumotach and ventilator. The rat was elevated and tilted to the right side, and the acid designated for the right lung was slowly pushed through a syringe into the trachea. While still tilted to the right, the rat was shaken for approximately 15 seconds to allow the acid to spread evenly throughout the three lobes of the right lung. The trachea was then re-connected to the ventilator, and airway pressure was adjusted to achieve a tidal volume of 8 ml/kg. After ensuring the rat had stabilized after the first acid instillation, the same procedure was repeated for acid instillation into the left lung.

The rats were ventilated with the same BIPAP settings set at baseline with the exception of the airway pressure, which was increased in order to maintain a tidal volume

of 8 ml/kg and $PaCO_2$ of 40-55 mmHg. These settings were maintained for one hour of CMV in order to allow ALI to develop. During that time, six 2-minute data recordings were taken by LabChart, each separated by an 8-minute unrecorded monitoring period. At the end of one-hour of CMV, two cardiac output measurements were taken (as described above). In addition, arterial and venous blood samples were collected in heparinized syringes to test blood gases and oxymetry, and the data were recorded. The extent of the lung injury was evaluated based on a marked decrease in the ratio of arterial partial pressure of O_2 to the FiO_2; PaO_2/FiO_2 or P/F ratio) from baseline. For this study, the development of acute lung injury was considered to be a P/F ratio equal to 300 mmHg or less, as defined clinically (Ware and Matthay, 2000; Hammer, 2000).

2.4.3 Mechanical Ventilation

Once acute lung injury was established, a recruitment maneuver was performed. This was achieved by linking the airway pressure to the PEEP on the ventilator, and then increasing the PEEP from 5 cmH_2O to 7 cmH_2O and ventilating at this PEEP for one minute. The PEEP was subsequently increased from 7 to 9 cmH_2O and held for one minute, and finally increased from 9 to 10 cmH_2O and held for one minute. The recruitment maneuver was performed in order to recruit airways that became closed during the development of ALI. After the recruitment maneuver, the PEEP was once again returned to 5 cmH_2O, and unlinked to the airway pressure.

A total of 60 rats were randomly assigned to six experimental groups (each with 10 animals). The groups varied in the ventilation settings for respiratory rate (RR), V_T, $PaCO_2$, and the addition of inspired CO_2 or dead space. Three groups were ventilated under normocapnic conditions (low CO_2; $PaCO_2$=40-55 mmHg) and three groups under

hypercapnic conditions (high CO_2; $PaCO_2$=60-70 mmHg). While ventilation with a low or 'protective' tidal V_T was targeted at 8.0 mL/kg, ventilation with a high or 'conventional' V_T was defined by a volume high enough to achieve the target $PaCO_2$. Similarly, the low and high respiratory rate settings were defined by a rate necessary to achieve the target $PaCO_2$. Meanwhile, protective and conventional therapeutic hypercapnia groups received inspired CO_2 (1.6%) to increase the $PaCO_2$ to the desired target, and the injurious normocapnia group received 1.0 ml of additional dead space through added rubber tubing. The settings for all groups are detailed in Table 1.

After random assignment to the groups, the rats were ventilated for three hours in each of their respective groups. During each hour of ventilation, six 2-minute data recordings were taken, each separated by an 8-minute unrecorded monitoring period. At the end of each hour, two cardiac output measurements were taken (as described above). Arterial and venous blood was sampled in heparinized syringes to evaluate blood gases and oxymetry, and the data were recorded. At the end of the three-hour ventilation in each group, 1 ml of arterial blood and 1 ml of venous blood were each drawn into syringes containing 0.10 ml ethylenediaminetetraacetic acid dipotassium dihydrate (EDTA) to prevent blood coagulation (EDTA was obtained from Sigma Aldrich, Oakville, ON, Canada). The blood samples were centrifuged (Brinkmann micro centrifuge model 5415, obtained from Eppendorf, Hauppauge, NY, USA) at 5000 rpm for 15 minutes at room temperature, and the resulting supernatant (plasma) was collected in cryotubes. This experimental protocol is summarized in Figure 2.

2.4.4 Tissue Dissection Protocol

After all recordings and measurements were taken, the animals were sacrificed

using 1.0 ml of potassium chloride (KCl) delivered as an intravenous bolus. The table surface heater and the overhead lamp were turned off to prevent early tissue degradation from the heat. The tracheal cannula was detached from the pneumotach and ventilator, and a cuff pressure gauge (VBM Medizintechnik GmbH, Germany) was attached immediately to the trachea with PEEP=20 cmH_2O to maintain lung inflation during the dissection.

The thoracic cavity was opened by a straight incision from the trachea and through the abdominal cavity. The diaphragm was cut and the rib cage was removed, exposing the heart and lungs. The connective tissue surrounding the trachea was removed, and the heart and lungs were excised in a single block while the cuff pressure gauge still maintained the lungs inflated with 20 cmH_2O of pressure. The middle lobe of the right lung was tied with thread, and the left hilus was clamped with a hemostat. The pressure gauge was removed, and broncheoalveolar lavage fluid (BALF) was collected by delivering 2 ml of 0.9% NaCl into the trachea and recovering as much fluid as possible. The BALF was centrifuged for 15 minutes at 5000 rpm, and the resulting supernatant was collected in cryotubes. The right hilus, including the main bronchus and associated vessels, was ligated. The upper and lower lobes of the right lung were cut off and placed in separate cryotubes for future analysis. The middle lobe of the right lung was cut off, placed in a pre-weighed glass scintillation vial, weighed again, and placed in a warming oven at 40°C for 48 hours. After that time, the dried lobe was removed from the oven and weighed. The weight of vial when empty, when containing the wet lung, and when containing the dry lung were all recorded and used to calculate the ratio of the wet to dry lung and used as a measure of pulmonary edema. The weight measurements were

collected using a precision balance scale (Sartoius GmBH, Gottingen, Germany).

The inflation of the left lung was maintained at 20 cmH_2O, and the hemostat was removed. The left lung was perfused with 10 ml of 10% unbuffered formalin injected through the right ventricle of the heart. In its inflated state, the perfused left lung was tied off at the main bronchus using a thread and submerged in 10% formalin. The left kidney was isolated, submerging half of it in 10% formalin and transferring the other half to a cryotube for future analysis. Similarly, the right lobe of the liver was isolated, where half was submerged in10% formalin and the other half transferred to a cryotube for future analysis. Finally, all samples kept in cryotubes (plasma, BALF, lung lobes, kidney and liver) were frozen by submerging them in liquid nitrogen and stored at -80°C until analysis.

2.5 Tissue Processing and Histological Preparation

The left lung was removed from 10% formalin, cut into three pieces (top third, middle third, and bottom third of the lung) representing apical, middle and basal lung sections. The tissue pieces were placed into a plastic cassette, washed twice with 70% ethanol, and embedded in paraffin overnight at 60°C using an automated tissue processor from Leica Micosystems Inc. (Richmond Hill, ON, Canada). The paraffin-embedded tissue blocks were sectioned using a microtome (5 μm section; Jung AG Heidelberg, Germany) and electronic tissue float water bath (model No. 375, Lipshaw MFG Co, Detroit, MI, USA) heated to 44°C. The tissue sections were subsequently transferred onto glass microscope slides and baked in an oven to ensure tissue adhesion to the slides.

The slides were stained with hematoxylin and eosin to evaluate morphological changes and determine the extent of ALI in the ventilated rat lung tissues. Briefly, the

slides were de-paraffinized, washed with xylene, alcohol and distilled water, and stained with freshly filtered hematoxylin for 2 minutes. The excess stain was washed away with water, and Scott's Solution was added for 2 minutes. The solution was rinsed away, and each slide was briefly dipped in a 1% eosin stain solution 13 times to ensure thorough staining. Finally, excess eosin stain was washed away with ethanol and xylene washes. Glass coverslips were mounted onto the slides and sealed with Cytoseal solution (Electron Microscopy Sciences, Fort Washington, PA, USA), ensuring no air bubbles were under the coverslips. The slides were dried overnight under a fume hood and briefly examined to ensure proper staining of cellular structures.

2.6 Histological Scoring and Analysis

The lung tissue samples were scored by a blinded lung pathologist based on the presence of seven criteria: interstitial edema (within lung tissues), alveolar edema, hemorrhaging, polymorphonuclear (PMN) cell infiltrates, atelectasis (alveolar collapse), alveolar damage, and hyaline membranes (fibrous structures lining the alveoli) (Castro, 2006; Henzler et al. 2011). The presence and severity of each criterion was rated from 0 to 3. A score of 0 represents 'no damage present', 1 represents 'mild damage, few lesions', 2 represents 'moderate damage, lesions in every visual field' and 3 represents 'severe damage, lesions ubiquitous'. The arithmetic mean of all subscores was taken as the diffuse alveolar damage (DAD) score for each lung sample.

2.7 Cytokine Analysis

The inflammatory response associated with VALI was evaluated using a 10-plex Procarta Cytokine Assay kit (Affymetrix Inc., Santa Clara, CA, USA). The cytokines and

chemokines measured were interleukin (IL)-1β, ICAM-1, IL-6, TNF-α, GM-CSF, IL-10, RANTES, KC, MCP-1, and MIP-1α. The bronchoalveolar lavage fluid (BALF) and arterial plasma samples collected from all animals at the end of each experiment were analyzed using the cytokine assay kit and Luminex Technology Analyzer and BioPlex Manager software from BIO-RAD (Mississauga, ON, Canada). The Luminex instrument was calibrated before every experiment, and validated once every 30 days. Calibration and Validation kits (BIO-RAD) were used to test and ensure the optimal performance of the Luminex instrument. The instrument was used to run cytokine assays only when the calibration and validation were successful.

The antibody beads (containing beads for the 10 selected cytokines) were loaded into all wells and washed by vacuum filtration. Rat-specific bodily fluid buffer was added to all wells (25 µl). The standards used to calculate cytokine concentrations in the samples were prepared by reconstituting the lyophilized premixed standard powder in 500 µl of rat-specific bodily fluid buffer. A total of 8 standards were prepared starting at 10,000 pg/ml of each analyte and decreasing 4-fold with each standard. All standards and samples were loaded into a 96-well filter plate in duplicates (25 µl/well for a final volume of 50 µl/well). The standards and samples were incubated on a shaker at 500 rpm for 1 hour at room temperature, and subsequently removed from the plate by vacuum filtration. The wells were washed with 1X wash buffer, and the detection antibody was added to the plate (25 µl/well) and incubated on a shaker at 500 rpm for 30 minutes. The antibody was removed by vacuum filtration and the plate was washed with 1X wash buffer. Streptavidin-PE was added to each well (50 µl/well) and incubated on a shaker at 500 rpm for 30 minutes. Finally, the streptavidin-PE was removed by vacuum filtration and

washed with 1X wash buffer. Reading buffer (120 µl/well) was added to all wells and incubated on a shaker at 500 rpm for 5 minutes and then inserted into the Luminex instrument for reading.

A separate standard curve was produced for each cytokine measured, with a limit of detection ≤ 1 pg/ml for each cytokine. Since each standard and sample were assayed in duplicates, the mean of the measured concentrations was taken. The final dilution of sample was 1:2, and the cytokine concentrations were calculated based on the set dilution. To ensure that an adequate standard curve was used for each analyte, the ratio of [observed/expected] x 100 standard concentrations was 100 ± 30, and all standard values were within this range.

2.8 Tissue Homogenization

The right upper lobe was homogenized to probe for caspase-3 activation by western blotting. The right upper lobe was cut into smaller pieces using a razor and placed in a pre-weighed 15 ml Falcon tube. The lung was weighed again and the weight recorded. Ice-cold 1X radioimmunoprecipitation assay (RIPA) buffer (Cell Signaling Technology) was purchased through New England Biolabs (Pickering, ON, Canada). The serine protease inhibitor phenylmethanesulfonylfluoride (1 mM PMSF; Sigma Aldrich, Oakville, ON, Canada) was added to the RIPA buffer prior to use (75µl PMSF/0.01 g of tissue). A tissue homogenizer (PRO200, Monroe, CT, USA) was used on high speed for 45-60 seconds to mechanically break the lung tissue. The homogenized tissue was placed at 4°C with gentle rocking (Rocker 25 from Labnet, Edison, NJ, USA) for 15 minutes, followed by 30 seconds of vortexing and repeated. The homogenates were then subject to 3 cycles of sonication (30 seconds/cycle) using a probe ultrasonic homogenizer (4710

series, from Cole Parmer, Montreal, QC, Canada). The homogenates were centrifuged (MIKRO 120, Hettich, Beverly, MA, USA) at 8000 rpm for 10 minutes at 4°C, and the supernatant transferred into fresh tubes. This supernatant was once again vortexed, centrifuged at 13000 rpm for 20 minutes at 4°C, and the resulting supernatant was collected and stored at -20°C for future protein measurement and western blotting.

2.9 Bradford Protein Assay

A protein assay was performed to determine the protein concentration in the rat lung homogenates (Kruger, 2002). A protein standard curve was created using bovine serum albumin (BSA; 2 mg/ml from BIO-RAD, Mississauga, ON, Canada) with five BSA standards (0, 2, 5, 10 and 15 μg of BSA), run in duplicates. Bradford Reagent Dye (500 μl), double-distilled water, 1X RIPA buffer were added to each standard for a final measuring volume of 1 ml. The lung homogenate test samples were prepared similarly in duplicates, adding 10 μl of protein, double-distilled water, and Bradford Reagent Dye (500 μl) for a final volume of 1 ml. The BSA standards and lung homogenate samples were measured on a 2802 UV/VIS spectrophotometer (UNICO, Dayton, NJ, USA) at 595 nm, and the optical density (OD) values were recorded using the UV/VIS Analyst software. Based on the measured ODs of the standards, a curve was constructed and a linear regression was used to fit the ODs and calculate the R^2 value. An R^2 value between 0.950 and 1.00 was considered adequate for estimating the protein concentrations in the lung homogenates based on the measured ODs. For this study, all standard curves constructed had an R^2 value between 0.960-0.990. The lung protein concentration was calculated, and the loading volume was determined based on loading 50 μg of protein in each well during the western blot.

2.10 Western Blotting for Caspase-3 and Actin

To examine whether apoptotic activity was modified in the rat lung as an outcome of ALI, western blotting was used to probe for caspase-3 activation. This was determined by the expression levels of uncleaved (inactive) and cleaved (active) forms of caspase-3 in the lung homogenates. The lung homogenate samples were prepared based on the determined volumes from the protein assay (50 μg loaded protein) and 5X sample buffer. Prior to loading, the samples were heated for 5 minutes at 85°C to denature the proteins, and the boiled samples were loaded into a 12% SDS-PAGE resolving gel. Alongside the samples, a Precision Plus Kaleidoscope 10-band protein standard (10-250 kD, from BIO-RAD, Mississauga, ON, Canada) was used. The gel gasket chamber was filled with 1X running buffer and connected to a PowerPac HC from BIO-RAD, and run at 90V and 300W for approximately 70 minutes.

Upon protein separation on the gel, the proteins were transferred onto a pure nitrocellulose membrane (Pall Corporation, Pensacola, FL, USA) in the gasket chamber (filled with 1X transfer buffer) for 2 hours at 45V. The membrane was saturated with a 5% milk solution (made with 1X TBS and 0.2% Tween; 1X TTBS) for 1 hour with gentle rocking at room temperature (Stovall Lifescience Inc., Greensboro, NC, USA). The primary polyclonal Caspase-3 antibody (raised in the rabbit) detects the uncleaved 35 kD protein, as well as 17 and 12 kD cleaved fragments. The antibody has species cross-reactivity for human, mouse, rat and monkey (Cell Signaling Technology). The primary antibody was added at 1:1000 dilution prepared with 5% milk and 1X TTBS and incubated overnight at 4°C with gentle rocking.

The primary antibody was removed, and the membrane washed with 1X TBS and

TTBS. The secondary antibody (Anti-rabbit IgG, HRP-linked, Cell Signaling Technology) was added at a 1:1000 dilution prepared with 5% milk and 1X TTBS and incubated for 2 hours with gentle rocking at room temperature. The secondary antibody was removed, and the membrane was washed with 1X TBS and TTBS. The membrane was imaged using the ECL Plus western blot detection system (GE Healthcare, purchased from Fisher Scientific, Ottawa, ON, Canada). The membrane was exposed to film for 10 minutes and subsequently developed.

The primary and secondary antibodies were stripped off the membrane using Restore western blot stripping buffer from Thermo Scientific (from Fisher Scientific, Ottawa, ON, Canada). The membrane was saturated with 5% milk solution and re-probed with an actin antibody as a loading control. The membrane was incubated in a 1:400 dilution of mouse monoclonal antibody of Actin HRP-linked IgG (Santa Cruz Biotechnology Inc., Santa Cruz, CA, USA) overnight at 4°C with gentle rocking. The antibody dilution was prepared with 1X TBS and 0.2% BSA. The actin antibody was removed, and the membrane was washed with 1X TBS and TTBS and imaged using the ECL Plus detection kit. The membrane was exposed to film for 1 minute and subsequently developed.

2.11 Densitometric Analysis of Caspase-3 Expression

The developed films were scanned and analyzed using the Image J software (National Institues of Health, Bethesda, USA). The images were inverted and the density of the uncleaved caspase-3 band (35 kD), cleaved caspase-3 band (17 kD), and background were measured and recorded. The difference between the measured bands and the background was calculated, and the ratio of active: inactive caspase-3 was

determined.

2.12 Statistical Analysis

Two rats were excluded from the Injurious Normocapnia group, and two rats were excluded from the Permissive Hypercapnia group. These animals were excluded due to premature death before the end of the 3-hour ventilation period, and failure to meet the set $PaCO_2$ targets for normocapnia and hypercapnia. Therefore, Conventional Normocapnia, Lung-Protective Ventilation, Conventional Hypercapnia and Protective Hypercapnia each had n=10 per group. Meanwhile, Injurious Normocapnia and Permissive Hypercapnia had n=10 rats per group.

Data are expressed as means ± SD or SEM. All statistical analysis was conducted using the SPSS 10.0 software (Chicago, IL, USA) and the GraphPad Prism 5.0 software (La Jolla, CA, USA). Data sets were tested for normality using the D'Agostino & Pearson Omnibus normality test (Graphpad Prism 5.0), and the data were normally distributed ($p>0.05$). Differences between groups were tested by analysis of variance (one-way ANOVA), followed by Tukey or Dunnett post-hoc tests, or a two-tailed Student's t-test. Two-way ANOVAs were used to test differences between experimental time points (baseline, 1 hour, 4 hours) in each group. The repeated-measures ANOVA was used to compare within-subjects measurements at baseline, after 1 hour and 4 hours and between-subjects interactions. The level of significance was set at $P< 0.05$.

CHAPTER 3 RESULTS

3.1 Hemodynamics

At baseline, all groups had equal hemodynamic functions, with no differences in the MAP, HR and cardiac index (cardiac output normalized to the body surface area of the rat) (CI). One hour (60 min) after induction of acute lung injury (ALI), the groups did not differ in MAP, HR and CI. After 4 hours of ventilation, all groups had equal MAP, HR and CI ($p=0.5435$, $p=0.7254$, $p=0.9524$, respectively). There were no time-dependent changes in MAP, HR and CI at baseline, 1 hour and 4 hours of ventilation in all groups. The MAP, HR and CI measurements at baseline, 1 hour and 4 hours of ventilation for each group are summarized in Table 2, and illustrated in Figure 3, Figure 4, and Figure 5.

3.2 Respiratory Mechanics

At baseline, all groups were ventilated with equal equal V_T, RR, and minute ventilation (V_E),. Elastance was equal in all groups at baseline, demonstrating equal respiratory mechanics in all groups at baseline. One hour after induction of ALI, V_T and RR, and V_E were maintained from baseline, and hence did not differ between groups. The elastance increased significantly in all groups after 1 hour of ventilation ($p<0.0001$) (Figure 9).

3.2.1 Confirmation of Experimental Design

After 4 hours of ventilation in each group, V_T, RR and V_E differed in all groups as per the target group settings. Three groups were ventilated with a conventional V_T (Conventional Normocapnia, Injurious Normocapnia, and Conventional Hypercapnia),

where V_T was increased in order to achieve the target $PaCO_2$ in each group. The three remaining groups were ventilated with a protective V_T (Lung-Protective Ventilation, Protective Hypercapnia, and Permissive Hypercapnia), which was limited to 8 mL/Kg maintained from baseline. After 4 hours of ventilation, the Conventional Normocapnia, Injurious Normocapnia and Conventional Hypercapnia groups had significantly higher V_T compared to Lung-Protective Ventilation, Protective Hypercapnia, and Permissive Hypercapnia ($p<0.0001$) (Figure 6). Meanwhile, the protective V_T in Lung-Protective Ventilation, Protective Hypercapnia, and Permissive Hypercapnia groups also did not differ ($p=0.4726$). The conventional V_T was higher in Conventional Normocapnia compared to Conventional Hypercapnia ($p=0.0032$) (Figure 6). There was a significant interaction between changes in V_T and the ventilation duration ($p<0.0001$), indicating changes in V_T over 4 hours of ventilation.

Respiratory rate was increased in three groups (Lung-Protective Ventilation, Injurious Normocapnia, and Protective Hypercapnia) compared to Conventional Normocapnia, Conventional Hypercapnia and Permissive Hypercapnia groups, which were ventilated with a reduced RR after 4 hours of ventilation ($p<0.0001$) (Figure 7). In addition, there was a significant interaction between the changes in RR and the ventilation duration, indicating changes in RR over time ($p<0.0001$). The changes in V_T and RR resulted in V_E that was significantly greater in Lung-Protective Ventilation and Injurious Normocapnia compared to other groups at the end of ventilation ($p<0.0001$) (Figure 8). There was also a significant interaction between changes in V_E and the ventilation duration, indicating changes in V_E over 4 hours of ventilation ($p<0.0001$). The Injurious Normocapnia group exhibited the highest V_E due to a combination of increased

V_T and RR, which represents a potentially injurious ventilatory mechanism. After 4 hours of ventilation, the elastance increased equally in all groups (p=0.3351). The increase in elastance was significant compared to baseline elastance, but not different compared to elastance after 1 hour of ventilation (Figure 9). The values are shown in detail in Table 3.

3.3 Gas Exchange

Equal gas exchange was achieved at baseline, with physiologic values of pH, PaO_2 and $PaCO_2$ in all groups. The ratio of PaO_2 to the FiO_2 (P/F) ratio was used to evaluate oxygenation. After 1 hour of ventilation, The P/F ratio decreased equally in all groups, however this was not a statistically significant from baseline. At the end of ventilation period (4 hours), the P/F ratio deteriorated further in all groups compared to baseline ($p<0.0001$). All groups developed ALI *per definitionem* (P/F ratio ≤ 300 mmHg) (Table 4) (Figure 10).

The $PaCO_2$ did not significantly in all groups at 1 hour compared to baseline. However, after 4 hours of ventilation, the three normocapnic groups (Conventional Normocapnia, Lung-Protective Ventilation, Injurious Normocapnia) had a $PaCO_2$ between 40-55 mmHg. The three hypercapnic groups (Conventional Hypercapnia, Protective Hypercapnia, Permissive Hypercapnia) had a $PaCO_2$ between 60-70 mmHg (Table 4). The $PaCO_2$ was significantly higher in the hypercapnic groups compared to the normocapnic groups ($p<0.0001$) (Figure 11) but the $PaCO_2$ did not differ within the three normocapnia ($p=0.1723$) or the three hypercapnia groups ($p=0.4158$). There was a significant interaction between the changes in $PaCO_2$ and the ventilation duration ($p=0.0098$), confirming changes in the $PaCO_2$ over 4 hours of ventilation.

Permissive Hypercapnia was the only group to produce profound respiratory acidosis in the rats. This was defined by an arterial pH less than 7.20, and shown by a significantly lower pH in Permissive Hypercapnia compared to Lung-Protective Ventilation (p=0.0264) after 4 hours of ventilation (Figure 12). In addition, only in the Permissive Hypercapnia group was the pH significantly lower after 4 hours of ventilation compared to baseline (7.37 ± 0.08 vs. 7.17 ± 0.11, p=0.0009) (Figure 12). Interestingly, the inhaled CO_2 in Conventional Hypercapnia and Protective Hypercapnia did not induce severe respiratory acidosis. These changes in pulmonary gas exchange are outlined in Table 4.

3.4 Wet-to-Dry Lung Ratio

Lung-Protective Ventilation resulted in a significantly lower wet-to-dry (W/D) ratio compared to Conventional Normocapnia (6.93 ± 0.86 vs. 8.62 ± 1.87, p=0.0186), with a similar difference found between Lung-Protective Ventilation and Injurious Normocapnia (6.93 ± 0.86 vs. 8.43 ± 1.79, p=0.0328) (Figure 13). In addition, the W/D ratio was significantly lower in Protective Therapeutic Hypercapnia compared to Injurious Normocapnia (6.37 ± 2.10 vs. 8.43 ± 1.79, p=0.0428) (Figure 13). Meanwhile, Conventional Therapeutic Hypercapnia and Permissive Hypercapnia produced similar W/D ratios at 7.81 ± 1.56 and 7.44 ± 2.03, respectively.

3.5 Diffuse Alveolar Damage Lung Injury Score

The Diffuse Alveolar Damage (DAD) score was significantly lower in Conventional Hypercapnia compared to Injurious Normocapnia (1.06 ± 0.27 vs. 1.64 ±

0.33, p=0.0317), Conventional Normocapnia (1.06 ± 0.27 vs. 1.49 ± 0.38) (p=0.0097), and Lung-Protective Ventilation (1.06 ± 0.27 vs. 1.44 ± 0.42) (p=0.0247) (Figure 14). The DAD scores for Protective Hypercapnia, and Permissive Hypercapnia were 1.34 ± 0.38, and 1.23 ± 0.47, respectively (Figure 14).

The DAD score was the arithmetic mean of seven subscores, which included alveolar edema, interstitial edema, PMN infiltrates, hemorrhaging, atelectasis, hyaline membranes and alveolar damage. The subscores for hemorrhages and PMN infiltrates are not shown because there were no differences between the groups. The subscores for alveolar edema, interstitial edema, atelectasis, hyaline membranes and alveolar damage are shown in Figure 15. Alveolar edema was lower in Protective Hypercapnia than Permissive Hypercapnia (p=0.0125), however interstitial edema (within lung tissues) was lower in Permissive Hypercapnia compared to Protective Hypercapnia (p=0.0295).

Interstitial edema was lower in Conventional Hypercapnia compared to Injurious Normocapnia (p=0.0152). The alveolar damage subscore was also lower in Conventional Hypercapnia compared to Injurious Normocapnia (p=0.0214), with a similar difference in hyaline membranes (fibrous structures lining alveoli) (p=0.0101). The differences between Conventional Hypercapnia and Injurious Normocapnia in the alveolar damage, interstitial edema and hyaline membrane subscores are also reflected in the DAD score.
The development of hyaline membranes was also greater in Injurious Normocapnia compared to Lung-Protective Ventilation, Protective Hypercapnia and Permissive Hypercapnia (p=0.0292). Atelectasis (alveolar collapse) was lower in Conventional Hypercapnia compared to Conventional Normocapnia and Lung-Protective Ventilation (p=0.0453). The presence of alveolar edema, interstitial edema, hyaline membranes,

atelectasis, alveolar damage, PMN infiltrates, and hemorrhages is also illustrated in representative lung tissues from each group (Figure 16).

3.6 Cytokine Analysis

3.6.1 Plasma Cytokines

Ten inflammatory mediators were measured in the arterial plasma. These mediators were IL-1β, I-CAM, IL-6, TNF-α, GM-CSF, IL-10, RANTES, KC, MCP-1, and MIP-1α. Plasma IL-1β concentrations were lower in Protective Hypercapnia compared to Conventional Normocapnia and Lung-Protective Ventilation (p=0.0042). (Figure 17A). Conventional Hypercapnia decreased IL-1β compared to Conventional Normocapnia (p=0.0196). TNF-α levels were lower in Protective Hypercapnia compared to Conventional Normocapnia (p=0.0194) (Figure 17D). Surprisingly, IL-10 levels were higher in the Conventional Normocapnia group compared to Protective Hypercapnia (p=0.0480) (Figure 17F). Meanwhile, I-CAM, IL-6, RANTES, KC, MIP-1 α and MCP-1 levels did not differ significantly between the groups, and GM-CSF was present in negligible concentrations (<10 pg/ml for all groups) (Tremblay et al. 1997; Venkataraman et al. 2002; Yang et al. 2000; Nanji et al. 1999).

3.6.2 BALF Cytokines

IL-1β, I-CAM, IL-6, TNF-α, GM-CSF, IL-10, RANTES, KC, MCP-1, and MIP-1α. were also measured in bronchoalveolar lavage fluid (BALF) collected from the lungs after 4 hours of ventilation. IL-6 was significantly lower in Conventional Hypercapnia compared to Injurious Normocapnia (p=0.0206), and Conventional Normocapnia (p=0.0202) (Figure 18C). IL-10 levels were higher in Permissive Hypercapnia compared

to Lung-Protective Ventilation (p=0.0244) (Figure 18F). Monocyte Chemotactic Protein-1 (MCP-1) levels were lower in all hypercapnia groups compared to Conventional Normocapnia (p=0.0021), Lung-Protective Ventilation (p=0.0189), and Injurious Normocapnia (p=0.0003) (Figure 18I). IL-1β, I-CAM, TNF-α, RANTES, KC, and MIP-1α concentrations did not differ significantly between all groups. Similar to plasma GM-CSF, the concentration of GM-CSF in BALF was also negligible in all groups (< 10pg/ml) (Tremblay et al. 1997; Beck-Schimmer et al. 1997; Yang et al. 2007; Miyake et al. 2004; Elgrabli et al. 2008).

3.7 Caspase-3 Activation in Lung Homogenates

Caspase-3 activation was measured in lung homogenates as an indication of apoptotic activity (programmed cell death) in the lung. The inactive (uncleaved) form of caspase-3 showed a 35 kD protein (Figure 19). Meanwhile, the prominent form of active (cleaved) caspase-3 showed a 17 kD band (Figure 19). Caspase-3 expression is shown as a ratio of active (17 kD) to inactive (35 kD) caspase-3. An increase in caspase-3 activation was defined by a ratio of active: inactive caspase-3 that is greater than 1.0. While only Protective Hypercapnia showed an increase caspase-3 activation (ratio>1.0) (Figure 20), Lung-Protective Ventilation showed more activation relative to Injurious Normocapia (p=0.0183).

CHAPTER 4 DISCUSSION

This study was designed to investigate whether the attenuation of VALI during protective ventilation is attributed to low tidal volume or the resulting hypercapnia. It was hypothesized that VALI attenuation is primarily attributed to hypercapnia. Rats were used in an acid aspiration model of ALI and assigned to six groups, where V_T settings (protective vs. conventional) and $PaCO_2$ targets (normocapnia vs. hypercapnia) were varied. The effect of permissive (endogenous) and therapeutic (inhaled) CO_2 was also evaluated. The findings indicate that a protective V_T alone only reduced lung edema, but increased apoptosis compared to a high V_T. Meanwhile, hypercapnia reduced several biomarkers of systemic and lung inflammation, suggesting some potential anti-inflammatory effects of hypercapnia via intracellular CO_2-mediated mechanisms.

4.1 Physiologic Effects

All groups were hemodynamically stable at baseline and throughout ventilation, as shown by no differences in MAP, heart rate and cardiac index. This demonstrates that protective ventilation and hypercapnia (permissive and therapeutic) do not compromise hemodynamic stability compared to conventional ventilation and normocapnia, and thus did not affect the hemodynamic outcome of VALI. Sinclair et al. (2002) also showed equal hemodynamic stability in hypercapnic and normocapnic animals. Costello et al. (2009) also showed hemodynamic stability in hypercapnic and normocapnic animals in lung injury secondary to prolonged systemic sepsis. In the same study however, Costello et al. reported that hypercapnia can increase MAP compared to normocapnia in early systemic sepsis. Changes in MAP were not noted in the present study, however this effect

may be specific to the model used (acid apsiration vs. sepsis-induced ALI), or the experimental time course (early vs. late phase of illness). It is possible that no significant hemodynamic changes were observed in our model of aspiration-induced ALI because the injury may have been largely localized to the lung and not systemic enough to cause hemodynamic changes. Therefore, the hemodynamic stability established in hypercapnia and normocapnia in this study is consistent with previous findings.

The increased elastance in all groups after 1 and 4 hours of ventilation confirms the progressive development of ALI (Figure 9). This is because more pressure is required to force air into the lungs and achieve the set tidal volume (protective or conventional). Elastance is inversely related to lung compliance, which is the ability of the lung to recoil to its original volume after inflation (Jonson et al. 1999). A highly compliant lung requires less pressure to inflate, while a reduction in compliance indicates a need for high pressures to inflate the lung adequately. The increased elastance indicates a decreased lung compliance, resulting in a lung which is less compliant to stretch during ventilation. This change in the mechanical properties of the respiratory system has been shown to correlate with the amount and increase of non-aerated lung in other acute lung injury models (Henzler et al. 2005) and can be regarded as a correlate of the severity of lung injury.

Extreme changes in minute ventilation can also contribute to the development of lung injury. Minute ventilation that is too low (as seen in Permissive Hypercapnia) causes hypoventilation leading to alveolar edema (Figure 15), which, along with interstitial edema, contributes to the total lung edema measured by the wet-to-dry lung ratio (Figure 13). Alveolar edema contributes to ALI because fluid accumulation in alveolar spaces

limits the amount of gas that can flow across alveolar walls. Though we did not show that Permisisve Hypercapnia causes atelectasis, this has previously been shown (Fehil et al. 2000) and reviewed by Bigatello et al. (2001). Atelectasis may also result from hypoventilation, and can impair gas exchange and worsen VALI by alveolar collapse, such that fewer alveoli can participate in gas exchange. Therefore, while hypoventilation can reduce excessive lung stretch and tissue tearing during ventilation, it also has the potential to worsen VALI.

While the optimal low (protective) tidal volume is yet to be determined for the attenuation of VALI, Frank et al. (2002) reported a reduction in epithelial and endothelial injury in the lungs of rats ventilated with 3 and 6 mL/Kg. However, Muscedere et al. (1994) ventilated isolated rat lungs with 5-6 mL/Kg. They concluded that ventilation with volumes below the inflection point on the pressure-volume curve (the volume at which the majority of alveoli are open) reduces lung compliance and increases the progression of ALI. This is likely an outcome of atelectasis, which contributes to the exacerbation of VALI. In the present study, atelectasis resulting from a low tidal volume was only present in Lung-Protective Ventilation (compared to Conventional Hypercapnia). Therefore, it is important to define the range of low tidal volumes that may be used in lung-protective settings without causing hypoventilation and atelectasis.

Conversely, minute ventilation that is too high (as seen in Injurious Normocapnia) causes interstitial edema, alveolar damage and hyaline membranes (Figure 15). These changes represent important biomarkers which impair gas exchange and contribute to VALI. Interstitial edema is marked by fluid accumulation within lung tissue, making the lung less compliant to inflate adequately during ventilation. Alveolar damage is the

hallmark of high minute ventilation by causing excessive stretch and tissue tearing in the lung, which destroys the alveolar epithelium. Hyaline membranes are fibrous eosinophilic structures made of fibrin, collagen, elastin and cellular debris (Castro, 2006). The formation of hyaline membranes along alveolar walls disrupts gas exchange by creating an additional barrier through which gas exchange must occur, thereby worsening VALI. Therefore, minute ventilation that is too high exacerbates VALI in an injurious mechanism separate from the injurious mechanism caused by hypoventilation.

These changes in minute ventilation may have also worsened VALI by causing hemorrhages. All groups showed equal lung hemorrhages, suggesting that the ventilation settings in each group may be causing equal amounts of tissue damage by a mechanism that disrupts the alveolar-capillary interface. Damage to the alveolar-capillary interface can facilitate the entry of extracellular fluids and red blood cells into the lung interstitium and alveolar spaces (Marini et al. 2003). Mechanical ventilation settings leading to increased microvascular pressure in pulmonary capillaries are enough to disrupt the alveolar-capillary interface and cause tissue hemorrhages by a process known as Stress Failure (West et al. 1991; Fu et al. 1992). Therefore, it is possible that all groups exhibited equal lung hemorrhages because of a high tidal volume (Conventional Normocapnia, Injurious Normocapnia, Conventional Hypercapnia), high respiratory rate (Lung-Protective Ventilation and Protective Ventilation) and extreme changes in minute ventilation (Injurious Normocapnia and Permissive Hypercapnia). An increased respiratory rate can be particularly important in disrupting the alveolar-capillary interface because it increases cyclic opening and closing of alveoli during ventilation, which causes lung tissue tearing.

While Lung-Protective Ventilation also exhibited high minute ventilation by increased RR (Figure 8), hyaline membranes (Figure 15) and edema (Figure 13) were significantly reduced in this group compared to Injurious Normocapnia. Since both groups were ventilated under normocapnic conditions, the development of hyaline membranes in Injurious Normocapnia may be a function of high tidal volume. The hyaline membrane subscore in Conventional Normocapnia may show some support for this notion since this group also had a high volume, however this was not a statistically significant difference with Lung-Protective Ventilation (Figure 15). Conventional Hypercapnia had a high tidal volume as well, however it produced significantly fewer hyaline membranes and a lower grade of diffuse alveolar damage (DAD) compared to the three normocapnic groups (Figure 14). This may be due to the inhaled CO_2 leading to hypercapnia, suggesting that hypercapnia may have a beneficial effect even in the presence of an injurious ventilation mechanism.

The reduced wet-to-dry lung ratio in Lung-Protective Ventilation compared to Conventional and Injurious Normocapnia suggests that pulmonary edema may also be a function of high tidal volume (Figure 13). This is supported by reduced pulmonary edema in Protective Hypercapnia compared to Injurious Normocapnia, demonstrating the importance of a low (protective) tidal volume for reducing lung edema. This finding also suggests that hypercapnia by inhaled CO_2 does not attenuate edema. Interestingly, both Laffey et al. (2000b) and Sinclair et al. (2002) showed that therapeutic hypercapnia by inhaled CO_2 reduces lung edema (lower wet-to-dry ratio) compared to normocapnia. The wet-to-dry lung ratio is a gross assessment of total lung edema, however it can be an effective technique for estimating fluid content in the lung.

Meanwhile, the detailed assessment of lung edema by the alveolar and interstitial edema subscores does not support for the findings of the wet-to-day ratio. We show that Protective Hypercapnia reduced alveolar edema compared to Permissive Hypercapnia, however Protective Hypercapnia produced more interstitial edema than Permissive Hypercapnia (Figure 15). The increased alveolar edema in Permissive Hypercapnia may be due to hypoventilation leading to atelectasis and fluid accumulation in collapsed alveoli. Both Permissive and Protective Hypercapnia had a low (protective) tidal volume, Protective Hypercapnia did not cause hypoventilation because of the increased RR as well as the flow of inhaled CO_2, which may have maintained proper inflation of alveoli. However, the continuous flow of CO_2 gas in addition to the oxygen from the ventilator may have pushed some fluid into the lung interstitium, causing interstitial edema. This likely did not occur in Permissive Hypercapnia because of the endogenous CO_2, causing less interstitial edema in that group.

Lung edema is believed to be an outcome of impaired fluid clearance from the lungs during ventilation, which has been shown in rats and in patients with ALI and ARDS (Lecuona et al. 1999; Ware and Matthay, 2001). This effect has been attributed to the endocytosis of the Na^+/K^+ ATPase in the membranes of alveolar epithelial cells (Lecuona et al. 2007; Dada et al. 2007). Endocytosis of the Na^+/K^+ ATPase has been described by the PURED (Phosphorylation-Ubiquitination-Recognition-Endocytosis-Degradation) pathway, and may be used to explain impaired fluid clearance during ventilation (Lecuona et al. 2007; reviewed in Ismaiel and Henzler, 2011). High tidal volume in conventional ventilation or hypoventilation in Permissive Hypercapnia can impair gas exchange, leading to hypoxia (Dada et al. 2003; Lecuona et al. 2007). Hypoxia

can initiate the phosphorylation and ubiquitination of the Na^+/K^+ ATPase, leading to its internalization and lysosomal degradation (Dada et al. 2007). With fewer Na^+/K^+ ATPases, Na^+ ion transport across the alveolar epithelium is markedly reduced, thereby reducing water transport by transcellular or paracellular mechanisms and allowing more fluid to accumulate in alveoli.

Alternatively, the epithelial sodium channel (ENaC) and cystic fibrosis transmembrane conductance regulator (CFTR) chloride channel have also been implivated in alveolar fluid clearance (Folkesson et al. 1998; Fang et al. 2005). It is possible that impairment in the expression of these membrane proteins can lead to alveolar fluid accumulation leading to pulmonary edema in the ventilated lung. This has been attributed to the potential downregulation of ENaC in alveolar epithelial type II cells during high tidal volume ventilation by a cGMP-dependent mechanism (Frank et al. 2003). In the present study, this may explain the increased pulmonary edema in the high tidal volume groups (Conventional and Injurious Normocapnia) compared to Lung-Protective Ventilation.

We have clearly demonstrated that mechanical ventilation has the potential to worsen the existing aspiration-induced ALI, leading to VALI that is marked by further deterioration of gas exchange and a less compliant lung. Indeed, gas exchange (measured by the P/F ratio) deteriorated equally in all groups (Table 4). It is possible that this equal deterioration may be attributed to the intitial insult to the lungs (acid aspiration). Since each group was ventilated for only 4 hours, and since all animals received the same dose of acid aspiration, it is likely that the deteriorated P/F ratio is primarily attributed to the aspiration. In addition, a 4-hour ventilation may not have been long enough to

significantly improve gas exchange with the different ventilation settings in each group. While we did not show an improvement in gas exchange, we established an experimental model of aspiration-induced ALI (1.25M HCl at 2.5 ml/kg) such that the injury is progressive over 4 hours without causing hemodynamic instability.

We previously showed that inducing ALI by acid aspiration using 5 mL of 1M HCl caused significant ARDS, where the P/F ratio decreased significantly after 1 hour but did not deteriorate further after 5 hours (Henzler et al. 2011). While that model established lung injury more quickly than the present study, establishing ARDS within 1 hour of ventilation increases the risk for hemodynamic instability and premature death. Our present model is particularly effective because it better reflects clinical aspiration-induced ALI, which develops over several hours as opposed to a single hour.

Despite the changes in $PaCO_2$, physiologic pH was maintained in all groups except for Permissive Hypercapnia, which caused profound respiratory acidosis relative to Conventional Normocapnia and Lung-Protective Ventilation (Figure 12). In the normocapnic groups, physiologic pH (approximately 7.30-7.40 in the rat, Fraser et al. 1978) was maintained by limiting CO_2 accumulation. This was achieved either by increased tidal volume or respiratory rate, which both facilitate CO_2 clearance from the lungs by increasing minute ventilation. Permissive Hypercapnia was induced by decreasing minute ventilation, which lead to hypoventilation and accumulation of endogenous CO_2. Interestingly, the Protective and Conventional Hypercapnia groups (inhaled CO_2) did not induce respiratory acidosis. Hypercapnia by endogenous CO_2 caused respiratory acidosis, however inhaled CO_2 did not affect the pH. This may be an outcome of a compensatory buffering mechanism in the presence of exogenous CO_2 that

is otherwise not present or impaired when the CO_2 originates endogenously and accumulates quickly. It is possible that bicarbonate (HCO_3^-) plays an important role in this compensatory buffering mechanism. While HCO_3^- concentrations were not analyzed in this study, sustained hypercapnia has previously been shown to activate renal acidification processes and prevent hypercapnic acidosis (Battle et al. 1985). This is likely achieved by increasing the secretion of hydrogen ions (H^+) from the collecting duct of the nephron.

CO_2 can be sensed by central and peripheral chemoreceptors (Lahiri and Forster, 2003; Jiang et al. 2005). Central Chemoreceptors (which also sense H^+) are located on medullary neurons in the medulla oblongata, while peripheral chemoreceptors are located in the carotid and aortic bodies (Lahiri and Forster, 2003). CO_2 and H^+ concentrations are specifically monitored by the CO_2/H^+ sensor-receptor (Lahiri and Forster, 2003; Forster and Smith, 2010). This chemosensor plays a key role in quickly detecting and buffering CO_2 in order to prevent H^+ accumulation leading to acidosis. In Permissive Hypercapnia, it is possible that the accumulated endogenous CO_2 impaired or disrupted the function of the CO_2/H^+ receptors. This may have prevented the detection of accumulated CO_2 to activate buffering mechanisms by HCO_3^-, leading to H^+ accumulation and respiratory acidosis. With Protective and Conventional Hypercapnia, inhaled CO_2 may have been immediately detected by the peripheral CO_2/H^+ sensor-receptors. This may have activated downstream buffering mechanisms involving HCO_3^- to increase renal clearance of H^+ and prevent respiratory acidosis. However, the role of the CO_2/H^+ sensor-receptor is still not well understood in the context of Permissive and Therapeutic Hypercapnia.

Perhaps future *in vitro* experiments using alveolar epithelial cells can uncover the role of the CO_2/H^+ receptor and its mechanism of action in preventing respiratory acidosis.

Several other studies have demonstrated that Therapeutic Hypercapnia by inhaled CO_2 leads to respiratory (hypercapnic) acidosis (Laffey et al. 2000b; Sinclair et al. 2002; Peltekova et al. 2010). Meanwhile, we showed that Permissive rather than Therapeutic Hypercapnia caused respiratory acidosis. This difference can be attributed to the fraction of inspired CO_2, which was only 1.6% in this study, but was as high as 5-12% (Sinclair et al. 2002; Laffey et al. 2000b, Peltekova et al. 2010). A low inhaled CO_2 fraction was chosen for this study to cause moderate hypercapnia and evaluate its true effects in the absence of hypercapnic acidosis.

4.2 Systemic and Pulmonary Inflammation

Protective Hypercapnia by inhaled CO_2 reduced both IL-1β and TNF-α in the circulating plasma (Figure 17), suggesting a decrease in some of the important biomarkers of systemic inflammation. This effect may be attributed to the protective tidal volume or the inhaled CO_2. In the case of IL-1β, it is likely due to the inhaled CO_2 because Protective Hypercapnia reduced systemic IL-1β compared to Lung-Protective Ventilation. Both groups had the same tidal volume and only differed in the $PaCO_2$ target (normocapnia vs. hypercapnia). IL-1β was also reduced in Conventional Hypercapnia compared to Conventional Normocapnia, demonstrating a potential anti-inflammatory effect of hypercapnia by inhaled CO_2 that is evident even in the presence of a high tidal volume. IL-1β is synthesized as a proprotein, after which it is cleaved by caspase-1 to produce active IL-1β and released by monocytes, dendritic cells and macrophages

(Eder et al. 2009). IL-1β release can be triggered by a variety of stimuli. In the case of VALI, mechanical stress on the body during ventilation may have produced Damage-Associated Molecular Pattern molecules (DAMPs) that induced IL-1β secretion (Eder et al. 2009; Lotze et al. 2007). It is possible that CO_2 entry across leukocyte cell membranes in Protective Hypercapnia may have disrupted IL-1β cleavage and activation, thereby reducing its release from activated macrophages and monocytes.

TNF-α is another potent pro-inflammatory cytokine that can be released by activated macrophages, T-cells, B-cells and natural killer cells (Pradines-Figueres and Raetz, 1992). TNF-α is initially synthesized as a membrane-anchored proprotein and later proteolytically processed to produce the mature form (Gearing et al. 1994). TNF-α inhibition in Protective Hypercapnia may be attributed to the protective tidal volume or the inhaled CO_2. If it is due to the inhaled CO_2, it is possible that the CO_2 may have interacted with and inhibited the TNF-α converting enzyme (TACE) (Mohan et al. 2002). Inhibition of this enzyme would likely prevent the cleavage and activation of TNF-α, rendering it biologically inactive.

However, if the reduction in TNF-α in Protective Hypercapnia is due to the protective tidal volume, this may have been mediated by a mechanism involving the reduction of pulmonary edema (Figure 13). Dagenais et al. (2004) showed that TNF-α can downregulate ENaC expression in alveolar epithelial cells, thereby reducing alveolar fluid clearance by impairing Na^+ transport. Interestingly however, in this study we did not show a reduction in TNF-α release in Protective Hypercapnia in BALF (Figure 18). This may be due to the activation of TNF-α that peaks approximately 90-120 minutes after the insult to the lungs (Horgan et al. 1993). Since cytokines were sampled 4 hours

after the insult to the lung, peak TNF-α activation may have been missed. Plasma cytokines were specifically sampled after the 4 hours to determine whether 4 hours of ventilation in each group is enough to modulate the inflammatory response associated with VALI.

Surprisingly, the anti-inflammatory cytokine IL-10 was present in higher concentrations in Conventional Normocapnia compared to Protective Therapeutic Hypercapnia (Figure 17). This difference is the reverse of the TNF-α concentrations in those groups. This is particularly surprising because IL-10 has been reported to reduce LPS-induced release of TNF-α and IL-1β from activated monocytes (Wang et al. 1994). Wang et al. (1995) later showed that IL-10 exhibits its anti-inflammatory effects in a mechanism that inhibits NF-κB. Wang et al. (1995) showed that IL-10 inhibited NF-κB translocation into the nucleus, suggesting that IL-10 may have prevented the proteosomal degradation of I-κB and its dissociation from NF-κB.

Our data demonstrate that Protective Hypercapnia can reduce plasma IL-1β and TNF-α, however this reduction is likely not mediated by IL-10-dependent inhibition of cytokine transcription. Rather, this reduction could be mediated by another anti-inflammatory cytokine such as IL-4. While IL-4 does not inhibit NF-κB (Wang et al. 1995), it can effectively inhibit cytokine synthesis in monocytes (Wang et al. 1994). While we did not measure plasma IL-4 levels, it is still possible that IL-4 may have been involved in the inhibition of IL-1β and TNF-α in Protective Hypercapnia in an IL-10-independent mechanism.

Alternatively, previous reports indicate that physical stress caused by mechanical ventilation activates the β-adrenergic signaling system by releasing catecholamines that

bind to β2 adrenergic receptors on leukocytes. This signaling cascade downregulates pro-inflammatory cytokines such as TNF-α, and upregulates anti-inflammatory cytokine activation such as IL-10 (Plötz et al. 2004; Kavelaars et al. 1997). In line with the present findings, Frank et al. (2002) also found elevated IL-10 plasma concentrations in rats ventilated with a high V_T. This is likely due to the activation of innate immune responses that upregulate IL-10 to protect against the injurious ventilation mechanisms (Figure 17). Increasing IL-10 release during Conventional Ventilation may have limited the release of downstream pro-inflammatory cytokines in response to tissue damage not only in the lung, but also in distal organs such as the liver and kidney.

Systemic inflammation is an important component of VALI because it contributes to multiple-organ dysfunction. The changes in IL-1β and TNF-α are likely not an outcome of a "spill-over" of cytokines originating from the lung because these cytokines were equally upregulated in the BALF of all treatment groups. Therefore, the systemic changes in IL-1β and TNF-α may have originated from circulating leukocytes and not from lung-infiltrating immune cells..

IL-6 was lower in the BALF of the Conventional Hypercapnia group compared to Injurious and Conventional Normocapnia (Figure 18). This reflects the same difference found in the DAD lung injury score (Figure 14), and confirms that inhaled CO_2 has some therapeutic potential even in the presence of non-protective (high tidal volume) ventilation settings. Peltekova et al. (2010) also showed a downregulation in IL-6 content in the BALF of mice ventilated with therapeutic hypercapnia (inhaled CO_2) compared to normocapnia using a model of ventilator-induced lung injury. Therefore, our results

demonstrating IL-6 reduction under hypercapnic conditions are supported by previous findings.

This finding may be explained by a modification of IL-6 production in the rat lung. IL-6 is a pro-inflammatory cytokine that can be released from B and T-lymphocytes, activated monocytes and endothelial cells (Kishimoto, 1989; Nishimoto and Kishimoto, 2006). IL-6 plays an important role in T-cell and macrophage differentiation, as well as the production of vascular endothelial growth factor (VEGF) leading to angiogenesis (Nishimoto and Kishimoto, 2006). In the lung, therapeutic hypercapnia may have reduced IL-6 production and release from resident alveolar macrophages and alveolar epithelial cells in a potential mechanism involving CO_2 and IL-6 transcriptional enhancing elements (Kishimoto, 1989). This may be mediated by the inhibiting the binding of NF-κB to IL-6 transcriptional elements such as activator protein-1 (AP-1) and c-fos responsive element (CRE) (Tanabe et al. 1988), resulting in decreased IL-6 transcription by NF-κB and subsequent protein synthesis and release by alveolar macrophages and epithelial cells.

IL-10 levels in BALF were higher in Permissive Hypercapnia compared to Lung-Protective Ventilation (Figure 18). Since IL-10 is anti-inflammatory, this suggests that Permissive Hypercapnia may have an anti-inflammatory effect in the lung. This finding is particularly interesting because Permissive Hypercapnia is the 'tolerated' side effect of Lung-Protective Ventilation. Our data shows that the hypercapnia resulting from protective ventilation may have more benefit for the injured lung than ventilation with the protective tidal volume alone. This benefit is likely mediated by a CO_2-dependent mechanism, since both groups shared the same tidal volume (Figure 6). This finding is

also interesting because Permissive Hypercapnia and Lung-Protective Ventilation have never been directly compared in experimental VALI.

Monocyte Chemotactic Protein-1 (MCP-1) is a potent chemotactic cytokine. MCP-1 can be produced by epithelial cells, monocytes, and endothelial cells (Reviewed in Deshmane et al. 2009). MCP-1 in BALF was significantly lower in all three hypercapnia groups compared to all three normocapnia groups (Figure 18). This suggests that hypercapnia has the potential to reduce the recruitment of monocytes and other immune cells (T-cells, macrophages and dendritic cells) to the injured lung. Interestingly, MCP-1 levels were reduced in Permissive Hypercapnia (endogenous CO_2) Conventional and Protective Hypercapnia (inhaled CO_2) equally. This demonstrates that CO_2 may play a role in reducing monocyte recruitment to the lung, regardless of whether the CO_2 originates endogenously or exogenously. As well, CO_2 appears to reduce monocyte recruitment to the lung independently of tidal volume settings, since all three hypercapnia groups reduced MCP-1 equally. The mechanism of MCP-1 inhibition by CO_2 is unclear, however it likely includes CO_2 disruption of MCP-1 synthesis and release from monocytes. This may be mediated by the enzyme heme oxygenase-1, which has been shown to downregulate MCP-1 expression (Shokawa et al. 2006).

Meanwhile, no differences were found in the levels of I-CAM, GM-CSF, RANTES, macrophage inflammatory protein-1α (MIP-1α), and keratinocyte chemoattractant (KC). This finding was surprising, since many of these biomarkers have previously been implicated in various models of lung injury (Nathens et al. 1998; Frossard et al. 2002; Shanley et al. 1995; Imanaka et al. 2001; Kwon et al. 1995; Yanagisawa et al. 2003). GM-CSF (Granulocyte Macrophage-Colony Stimulating Factor)

was present in extremely low concentrations (<10 pg/ml). However, GM-CSF has been reported to reduce normal neutrophil apoptosis, and has been measured in higher concentrations in the BALF of ALI/ARDS patients with a greater likelihood of survival (Goodman et al. 1999). We also did not show differences in MIP-1α levels in any of the groups. MIP-1α has previously been shown to play an important role in potentiating ALI in a neutrophil-dependent mechanism (Shanley et al. 1995). However, we did not show any differences in the PMN (primarily neutrophil) infiltration subscore in all groups. This may be attributed to the nature of the ALI model, where we used an acid-aspiration model while Shanley et al. (1995) used an IgG complex-mediated alveolitis model leading to ALI. We have previously used an acid aspiration-induced ALI model (Henzler et al. 2011) and also did not show differences in PMN infiltration subscores, suggesting that equal PMN infiltration in all treatment groups may be characteristic of this model of ALI.

ICAM-1 is a cellular adhesion molecule that is expressed on the surface of leukocytes and endothelial cells (Lawson and Wolf, 2009). We did not find differences in soluble ICAM-1 levels in the treatment groups, despite the fact that ICAM-1 expression can be induced by IL-1β and TNF-α, both of which exhibited differences in induction (Yang et al. 2005). We have previously shown no changes in plasma ICAM-1 levels using an acid-aspiration ALI model (Henzler et al. 2011), however Imanaka et al. (2001) showed an increase in plasma ICAM-1 levels during ventilation with a high V_T, indicating the presence of endothelial injury. In the present study, it is clear that ICAM-1 expression is elevated equally in all groups in BALF and plasma. This equal elevation in all groups could be attributed to the initial insult to the lungs by acid aspiration, since all

groups received the same dose and concentration of HCl. In addition, animals may not have been ventilated long enough (only 4 hours) to see effects of individual ventilation strategies on ICAM-1 expression.

4.3 Apoptosis in the Lung

We showed that Lung-Protective Ventilation produced more active caspase-3 compared to Injurious Normocapnia (Figure 20). This finding was unexpected, since protective ventilation settings and hypercapnia were expected to reduce programmed cell death in the lung by decreasing caspase-3 activation. This is based on previous studies showing apoptotic activity in alveolar epithelial cells and endothelial cells in endotoxin-induced ALI (Fujita et al. 1998; Kitamura et al. 2001). In addition, Laffey et al. (2000b) also showed a marked reduction in cell death in rabbits treated with therapeutic hypercapnia and hypercapnia acidosis using the TUNEL stain, with similar findings shown by Tateda et al. (2003) and Kawasaki et al. (2000). However, the TUNEL stain may not be a true indicator of apoptosis because it labels DNA fragments of dead cells in addition to cells in the process of apoptosis. Since cells can die by apoptotic or necrotic mechanisms, TUNEL staining may not be the most effective technique to evaluate apoptosis. Meanwhile, measuring active caspase-3 expression may be a better indicator of apoptotic cell activity.

Our findings may be explained if apoptosis is considered a protective rather than a harmful cellular regulatory mechanism. That is, Lung-Protective Ventilation may have increased apoptotic activity in the lung by caspase-3 activation in order to prevent cell death by necrotic cellular pathways. The fact that Injurious Normocapnia shows the lowest active: inactive caspase-3 ratio (Figure 20) may lend some support for this

concept, because a ratio of active: inactive caspase-3 less than 1.0 indicates less active caspase-3. If Injurious Normocapnia did not activate as much caspase-3 as Lung-Protective Ventilation, cell death in Injurious Normocapnia may have been induced by necrosis as opposed to apoptosis.

Cells of the lung (epithelial cells and fibroblasts) are continuously replaced as aged or damaged cells undergo cell death and new cells differentiate into different types of epithelial cells (Bowden, 1983). Such a process is tightly regulated and involves basal apoptotic activity that creates a balance between the cells undergoing apoptosis and differentiation (Bowden, 1983). The use of a 1:1 ratio to quantify active:inactive caspase-3 reflects this balance between the two biological forms of caspase-3. A ratio less than 1.0 indicates a reduction in active caspase-3 expression. It is interesting to note that both Lung-Protective Ventilation and Injurious Normocapnia produced ratios less than 1.0, indicating a reduction in the basal 1:1 ratio of active:inactive caspase-3 expression. However, caspase-3 activation in Injurious Normocapnia deviates from basal levels more so than Lung-Protective Ventilation (Figure 20). This may be attributed to the injurious nature of mechanical ventilation, which is worse in Injurious Normocapnia than Lung-Protective Ventilation.

Alternatively, it is still possible that there were other undetected differences in cell death in the rat lung, however this cell death may be attributed to necrosis rather than apoptosis. Necrosis may have occurred as an outcome of volutrauma, barotrauma, and biotrauma in all groups, regardless of protective or conventional ventilation settings, normocapnia or hypercapnia, or the source of hypercapnia (endogenous or inhaled CO_2). It is equally possible that no differences in cell death were observed in this study due to

the type of ALI model used and not the ventilation settings. For example, Laffey et al. (2000b) reported differences in cell death in rabbit lungs in an ischemia-reperfusion model of ALI, and Tateda et al. (2003) reported differences in cell death in a murine model of pneumonia-induced ALI. Therefore, the induction of cell death in lung tissue may be more dependent on the lung injury model as opposed to the ventilation settings.

4.4 Permissive vs. Therapeutic Hypercapnia

Although the mechanisms by which hypercapnia occurred were different in Permissive and Therapeutic Hypercapnia, the three hypercapnic groups did not differ in the overall effect on VALI, except for the profound respiratory (hypercapnia) acidosis in Permissive Hypercapnia. Previous studies have shown hypercapnic acidosis to be effective for the attenuation of VALI (Laffey et al. 2000b; Sinclair et al. 2002; Laffey et al. 2004). However, in all these studies, hypercapnic acidosis resulted from Therapeutic and not Permissive Hypercapnia.

In this study, hypercapnic acidosis resulting from Permissive Hypercapnia did not attenuate VALI, since Therapeutic Hypercapnia by inhaled CO_2 appeared to have a greater effect on reducing diffuse alveolar damage as well as some biomarkers of systemic inflammation. However, Permissive Hypercapnia upregulated the anti-inflammatory cytokine IL-10 in the lung, which may suggest some benefit of endogenous CO_2 and potentially hypercapnic acidosis. Meanwhile, previous studies have also described the deleterious effects of hypercapnic acidosis using *in vivo* and *in vitro* models (Lang et al. 2000; Doerr et al. 2005; O'Croinin et al. 2008). Although both *in vitro* and *in vivo* studies are useful elements for investigating experimental ALI and VALI, both systems have their limitations. *In vivo* studies tend to provide more applicable results as

they test concepts in whole organisms, where as *in vitro* studies test the same concepts in isolated cell systems under artificial conditions. Conversely, *in vitro* models are optimal for evaluating cellular effects and mechanisms that are otherwise unclear on a global scale in *in vivo* models. These factors may explain some of the differences between the studies supporting therapeutic potential of hypercapnic acidosis for attenuating VALI, and studies reporting the potentially deleterious effects of hypercapnia and hypercapnic acidosis.

While we have demonstrated some potential benefit of Therapeutic Hypercapnia in an aspiration model of ALI, O'Croinin et al. (2008) demonstrated potential shortcomings. Their findings indicate that therapeutic hypercapnia leading to respiratory acidosis actually worsened VALI by causing immunosuppression in ALI induced by bacterial pneumonia infection. Therefore, Therapeutic Hypercapnia may have some anti-inflammatory effects, but whether these effects are protective may depend on the *in vivo* model of experimental ALI (endotoxin-induced ALI vs. aspiration-induced ALI vs. ventilation-induced ALI).

In vitro, these differences in outcome could be attributed to the difficulty of modeling ALI in culture. This is because most lung cell cultures cannot exactly mimic the lung cell interactions *in vivo*, and therefore may not be reliable models for understanding the effects of hypercapnia not only on lung cell populations, but also on the lung as a whole organ. The conflicting findings regarding the effects of hypercapnia and hypercapnic acidosis may also be attributed to differences in the target $PaCO_2$ range used to achieve hypercapnia and acidosis. We showed that mild hypercapnia ($PaCO_2 \approx$ 70 mmHg) leading to acidosis (Table 4) in Permissive Hypercapnia may not be entirely

protective. Meanwhile, Sinclair et al. (2002) treated with therapeutic hypercapnia ($PaCO_2$ ≈ 95 mmHg) causing more profound hypercapnic acidosis (pH 6.99) and shown effective in attenuating lung injury. These effects could be an outcome of the severity of acidosis, or the method by which hypercapnia was induced (permissive vs. therapeutic). Therefore, more experimental studies are still necessary in order to create a unified understanding of the effects of hypercapnia and hypercapnic acidosis in ALI and VALI.

4.5 Limitations of the Study

4.5.1 Ventilation Settings

While the findings of this study are novel and scientifically applicable, there are several factors that may have limited the study. First, the ventilation settings assigned for each group did not differ sufficiently to produce greater difference in outcomes. The ventilation settings for all groups may have been too injurious to differentiate between those groups designated as 'protective' (Lung-Protective Ventilation, Protective and Permissive Hypercapnia) from the groups designated as 'conventional' (Conventional and Injurious Normocapnia, Conventional Hypercapnia). In this study, a protective V_T was defined as 8 mL/Kg in order to limit lung stretch without causing hypoventilation. However, other studies have used a protective V_T as low as 5-7 mL/Kg predicted body weight (Hickling et al. 1990; ARDS Network, 2000; Ranieri et al. 1999). These studies showed ventilation with V_T between 5-7 mL/Kg to be significantly more protective compared to conventional V_T by reducing lung stretch, inflammation, and improving survival. Therefore, a V_T of 8 mL/Kg may not have been protective enough for the injured lungs in this model of acid aspiration-induced ALI. As a result, this may have diluted the differences between protective and conventional ventilation.

Alternatively, it is also possible that the ventilation settings for all groups may have been fairly protective such that the differences between the 'protective' and 'conventional' groups were lost. In the present study, a 'conventional' V_T was achieved by increasing V_T enough to achieve the target $PaCO_2$, which was approximately 12-13 mL/Kg in the conventional ventilation groups. This coincided with previously reported conventional V_T that were shown to produce VALI in patients (ARDS Network, 2000; Amato et al. 1998). However, other studies previously reported the use of V_T as high as 15 mL/Kg during conventional ventilation of ARDS patients (Kollef and Schuster, 1995; Kacmarek and Venegas, 1987). In addition, a V_T as high as 30 mL/Kg was used in a rat model of ALI as part of a conventional ventilation strategy in order to achieve significant injury compared to protective ventilation with low V_T (Frank et al. 2003). Taken together, these studies suggest the potential need for higher V_T in order to create a conventional ventilation strategy that is more likely to cause VALI. In the present study, the use of V_T less than 15 mL/Kg for conventional ventilation could have made this ventilation strategy somewhat protective.

4.5.2 Ventilation Duration

In this study, all rats were ventilated for one hour after the induction of ALI, and three hours in each of the assigned groups, for a total of four hours of ventilation. This was based on previous studies where four hours of a given ventilation strategy was enough to cause significant changes in gas exchange, inflammation, and lung damage (Rotta et al. 2001; Sinclair et al. 2002; Chiumello et al. 1999). A 4-hour ventilation period was also chosen for this study to minimize the risk for premature death in the animals, which we have shown previously (unpublished data). In the current study, four

hours of ventilation was long enough to detect differences in the inflammatory response, pulmonary edema and diffuse alveolar damage. However, it may not have been long enough to detect differences in gas exchange, hemodynamics and overall attenuation of VALI. For example, Laffey et al. (2004) ventilated rats with therapeutic hypercapnia for 6 hours and showed a significant reduction in pulmonary nitric oxide metabolites, PMN infiltration and alveolar wall thickness in the lung, as well as improved respiratory mechanics and survival rate. In another study, a 5-hour ventilation period in healthy mice was enough to show the potentially deleterious effects of mechanical ventilation. These effects included the induction of ALI by an increase in neutrophil infiltration and protein concentrations in BALF, and an increase in pro-inflammatory cytokines in the lung and systemically (Wolthuis et al. 2009).

There are other studies that ventilated for less than four hours, and still achieved comparable results. For example, a ventilation period of only 90 minutes with protective ventilation and therapeutic hypercapnia significantly reduced IL-1β and TNF-α in BALF (Laffey et al. 2000b). Moreover, a 3-hour ventilation period in a mouse model of ventilator-induced lung injury with protective therapeutic hypercapnia showed a significant decrease in pro-inflammatory cytokine activation and PMN infiltrates in the lung (Peltekova et al. 2010). However, no differences in gas exchange or hemodynamics were noted in that model, similar to the findings of the present study. Meanwhile, mechanical ventilation in intensive care patients is often delivered for up to several days, weeks and even months, depending on the patient's condition. In some clinical studies, a 28-day survival period was used to evaluate the effects of mechanical ventilation

strategies in ALI and ARDS patients (ARDS Network, 2000; Amato et al. 1998; Ranieri et al. 1999). Therefore, there is evidence to suggest that ventilation periods longer and less than 4 hours have the potential to reduce the inflammatory and histopathological markers of VALI in experimental models.

4.5.3 $PaCO_2$ Targets

The $PaCO_2$ targets for normocapnia and hypercapnia were well defined and limited, however they were relatively close in range. Since normocapnia was defined by a $PaCO_2$ of 40-55 mmHg and hypercapnia by a $PaCO_2$ of 60-70 mmHg, this increased the likelihood of overlapping $PaCO_2$ measurements in the different groups. The hypercapnia range was chosen in order to induce hypercapnia without respiratory acidosis, in order to evaluate the true effects of hypercapnia independent of hypercapnic acidosis. This was successfully achieved in Protective and Conventional Hypercapnia (inhaled CO_2) groups, but not in Permissive Hypercapnia (Figure 12).

The normocapnia range was chosen so as to avoid hypocapnia, but still establish a physiologic range of $PaCO_2$. While the $PaCO_2$ target for normocapnia was successfully achieved, it may have been closer to hypercapnia than physiologic normocapnia. This could have made the Injurious and Conventional Normocapnia groups more protective than intended as per the experimental protocol. Therefore, having relatively close $PaCO_2$ target ranges for normocapnia and hypercapnia may have diluted the potentially therapeutic effects of hypercapnia.

Interestingly, Peltekova et al. (2010) used a $PaCO_2$ target for normocapnia similar to that of this study, however the $PaCO_2$ target for hypercapnia was approximately 125 mmHg, demonstrating a substantial difference in the two $PaCO_2$ ranges, and the presence

of hypercapnic acidosis. Alternatively, Hickling et al. (1994) reported a mean $PaCO_2$ of approximately 65 mmHg in ARDS patients ventilated with protective V_T and permissive hypercapnia, and showed improved patient survival. This supports the present study in that a target $PaCO_2$ range of 60-70 mmHg for hypercapnia may offer some benefit.

4.5.4 Rat Strain

In this study, ALI was induced by acid aspiration in male Sprague-Dawley rats. One hour after the induction of ALI, the PaO_2 decreased from baseline in all groups, however ALI *per definitionem* was only established in all groups at the end of ventilation (4 hours) (Table 4). Since it took 4 hours for ALI or ARDS to develop in all groups, it is possible that Sprague-Dawley rats may be somewhat robust and resistant to injury. Several studies have investigated the effects of hypercapnia and hypercapnic acidosis in ALI in different rat strains. Chonghaile et al (2008) also used Sprague-Dawley rats in their model of ALI induced by bacterial pneumonia. In that study, the rats that received E.coli instillation for 6 hours showed a small drop in PaO_2 compared to untreated controls, however this difference was statistically significant (157 ± 6 vs. 114 ± 25 mmHg). This may suggest some level of resistance to infection and injury in Sprague-Dawley rats.

Alternatively, a study using a model of ventilator-induced lung injury in Wistar rats demonstrated more drastic changes than those observed in Sprague-Dawley rats. In that study, the PaO_2 markedly dropped within 40 minutes of injurious ventilation with a high pressure (45 cmH_2O) (139 ± 27 vs. 45 ± 8 mmHg). Interestingly, there was also a drop in the PaO_2 of the rats ventilated with a low (protective) pressure (7 cmH_2O) (133 ± 25 vs. 84 ± 15 mmHg) (Imanaka et al. 2001). Although this drop in PaO_2 was small, it

was significant compared to baseline. While it is not clear whether these effects are due to differences in rat strains or the nature of the ALI model, it is important to consider to that different rat strains may respond differently to lung injury and ventilatory interventions. Experimentally, it is important for animals to develop ALI as per protocol in order to model clinical lung injury and objectively evaluate the effects of a treatment or ventilation strategy on the animals.

4.5.5 Assessment of Survival

After four hours of ventilation the animals were euthanized to eliminate any potential pain and suffering. This prevented assessing the effects of hypercapnia and protective ventilation on the survival of rats in this study. Laffey et al. (2004) demonstrated an improvement in the survival of rats treated with hypercapnic acidosis compared to untreated rats, after all animals were subject to endotoxin-induced ALI (89% vs. 33%). Clinically, the assessment of survival in ALI and ARDS patients is of the utmost importance. As such, protective ventilation and permissive hypercapnia have been reported to improve patient survival (ARDS Network, 2000; Hickling 1994; Amato et al. 1998). This demonstrates the importance of evaluating the effect of ventilatory strategies on the overall survival of the study population. This assessment was not undertaken in this study and thus may have limited the findings.

4.5.6 Representative Lung Sampling

The upper lobe of the right lung was homogenized and used to analyze caspase-3 activation as a measure of programmed cell death in the rat lung. This lobe was chosen because it was large enough to extract enough protein for western blot analysis of

caspase-3. The upper lobe was chosen over the lower lobe because the lower lobe is approximately twice the size of the upper lobe, and would in turn yield far more extracted protein than necessary. However, it is possible that the caspase-3 activity measured in the upper lobe is not representative of caspase-3 activation in the entire right lung, or both lungs, potentially yielding falsely negative results. This is because the lung injury may not have been homogenous throughout the lung, making it difficult to estimate caspase-3 activation throughout the lung. Therefore, non-representative lung sampling may have limited the findings of this study.

4.6 Support for Hypotheses

The first hypothesis stating that hypercapnia protects the lung from VALI was supported with data showing a reduction in alveolar damage and some biomarkers of inflammation in the groups treated with therapeutic hypercapnia. This effect was also observed in ventilation settings that are not considered to be lung-protective. Since inflammation and alveolar damage are important markers of VALI, a reduction in these markers may suggest an attenuation of VALI. The second hypothesis stating that protective ventilation attenuates VALI was only partially supported. Under normocapnic conditions, protective ventilation only reduced pulmonary edema. However, protective ventilation in combination with Therapeutic Hypercapnia reduced inflammation, as well as edema. The third hypothesis stating that Therapeutic Hypercapnia is more protective than Permissive Hypercapnia was also partially supported. Therapeutic Hypercapnia by inhaled CO_2 did not reduce histo-pathologic injury as compared to Permissive Hypercapnia by endogenous CO_2, but maintained physiologic pH and reduced some pro-inflammatory cytokine release.

4.7 Clinical Implications and Conclusions

The findings of this study may be clinically relevant for ALI and ARDS patients that require mechanical ventilation. ALI and ARDS patients receive ventilatory support to restore physiologic gas exchange, however the ventilation settings used to achieve this outcome have the potential to cause VALI. To date, therapeutic hypercapnia has only been studied in experimental models, and has been shown to be protective by reducing inflammation, reactive oxygen and nitrogen species, and cell death. The current study presents clinically relevant findings showing that therapeutic hypercapnia in combination with protective ventilatory settings have the potential to attenuate VALI. These findings may be particularly relevant to patients that develop ALI and ARDS by aspiration of gastric acids. With additional research investigating the effects of therapeutic hypercapnia on VALI, it may become possible to induce hypercapnia in ALI and ARDS patients using a small fraction of inhaled CO_2 to attenuate VALI and improve patient survival.

In conclusion, this study investigated the effects of protective ventilatory settings, Permissive and Therapeutic Hypercapnia on the attenuation of VALI. The effects of these ventilatory strategies were studied in comparison to the effects of normocapnia and conventional ventilation settings. Protective ventilation has the potential to attenuate VALI in a mechanism which reduces pulmonary edema. Hypercapnia may also attenuate VALI, however its effects may be mediated by a mechanism which reduces diffuse alveolar damage, immune cell recruitment, and inflammation. Protective ventilation and hypercapnia did not improve oxygenation, however they also did not cause hemodynamic compromise. Therapeutic Hypercapnia by inhaled CO_2 has the potential to reduce several

biomarkers of systemic inflammation without causing respiratory acidosis. This is the first study to directly compare the effects of Therapeutic and Permissive Hypercapnia, where Therapeutic Hypercapnia maintained physiologic pH without buffering. This study is also the first to evaluate the effects of protective ventilation and hypercapnia together in a rat model of acid aspiration-induced acute lung injury. We have demonstrated the therapeutic potential for inhaled CO_2 and protective ventilatory settings to attenuate VALI and limit some of the biomarkers of inflammation, which should be continually tested in future experimental and clinical trials.

Our results are encouraging, however there are various necessary experiments to validate our present findings and proposed cellular mechanisms. First, a longer ventilation duration (more than 4 hours) may allow us to better evaluate the effects of hypercapnia and protective ventilation on the attenuation of VALI. In addition, analyzing bicarbonate concentrations in arterial blood can help us better understand the compensatory buffering mechanism in therapeutic hypercapnia. Histopatholigic examination of liver and kidney tissues may give us an indication of multiple organ dysfunction secondary to VALI. As well, measuring reactive nitrogen species such as peroxynitrite and nitrotyrosine in urine samples may be useful for attributing some of the effects of VALI to the production of reactive biological species. Finally, measuring total protein concentrations (especially albumin) in BALF can serve as an indicator of vascular leakage of serum proteins into the lungs (suggesting endothelila damage). These experiments may allow us to better understand the global effects of VALI, as well as the potential cellular mechanisms involved in the development and exacerbation of VALI.

REFERENCES

Amato MBP, Barbas CSV, Medeiros DM, Magaldi RB, Schettino GPP, Lorenzi-Filho G, Kairalla RA, Deheinzelin D, Munoz C, Oliveira R, Takagaki TY, Carvalho CRR. Effect of a protective-ventilation strategy on mortality in the acute respiratory distress syndrome. N Engl J Med 1998; 338: 347-354.

ARDS Network. Ventilation with lower tidal volumes as compared with traditional tidal volumes for acute lung injury and the acute respiratory distress syndrome. N Engl J Med 2000; 342: 1301-1308.

Barnes PJ, Karin M. Nuclear factor-kappaB: a pivotal transcription factor in chronic inflammatory diseases. N Engl J Med 1997; 336: 1066-1071.

Barth A, Bauer R, Gedrange T, Walter B, Klinger W, Zwiener U. Influence of hypoxia and hypoxia/hypercapnia upon brain and blood peroxidative and glutathione status in normal weight and growth-restricted newborn piglets. Exp Toxicol Pathol 1998; 50: 402-410.

Battle DC, Downer M, Gutterman C, Kurtzman NA. Relationship of urinary and blood carbon dioxide tension during hypercapnia in the rat: its significance in the elevation of collecting duct hydrogen ion secretion. J Clin Invest 1985; 75: 1517-1530.

Beck-Schimmer B, Chimmer RC, Warner RL, Schemal H, Nordblom G, Flory CM, Lesch ME, Friedl HP, Schrier DJ, Ward PA. Expression of lung vascular and airway ICAM-1 after exposure to bacterial lipopolysaccharide. Am J Respir Cell Mol Biol 1997; 17: 344-352.

Bellardine CL, Hoffman AM, Tsai L, Ingenito EP, Arold SP, Lutchen KR, Suki B. Comparison of variable and conventional ventilation in a sheep saline lavage lung injury model. Crit Care Med 2006; 34: 439-445.

Bernard GR, Artigas A, Brigham KL, Carlet J, Falke K, Hudson L, Lamy M, Legall JR, Morris A, Spragg R. The American-European consensus conference on ARDS. Am J Respir Crit Care Med 1994; 149: 818-824.

Bidani A, Tzouanakis AE, Cardenas VJ Jr, Zwischenberger JB. Permissive hypercapnia in acute respiratory failure. JAMA 1994; 272: 957-962.

Bigatello LM, Patroniti N, Sangalli F. Permissive hypercapnia. Curr Opin Crit Care 2001; 7: 34-40.

Bloomfield GL, Holloway S, Ridings PC, Fisher BJ, Blocher CR, Sholley M, Bunch T, Sugerman HJ, Fowler AA. Pretreatment with inhaled nitric oxide inhibits neutrophil migration and oxidative activity resulting in attenuated sepsis-induced acute lung injury. Crit Care Med 1997; 25: 584-593.

Bowden DH. Cell turnover in the lung. Am Rev Respir Dis 1983; 128: S46-S48.

Briva A, Vadász I, Lecuona E, Welch LC, Chen J, Dada LA, Trejo HE, Dumasius V, Azzam Zs, Myrianthefs PM, Battle D, Gruenbaum Y, Sznajder JI. High CO2 levels impair alveolar epithelial function independently of pH. PLoS one 2007; 2: e1238.

Brochard L, Roudot-Thoraval F, Roupie E, Delclaux C, Chatre J, Fernandez-Mondéjar E, Clémenti E, Mancebo J, Factor P, Matamis D, Ranieri M, Blanch L, Rodi G, Mentec H, Dreyfuss D, Ferrer M, Brun-Buisson C, Tobin M, Lemaire F. Tidal volume reduction for prevention of ventilator-induced lung injury in acute respiratory distress syndrome. Am J Respir Crit Care Med 1998; 158: 1831-1838.

Brower RG, Shanholtz CB, Fessler HE, Shade DM, White P Jr, Wiener CM, Teeter JG, Dodd-o JM, Almog Y, Piantadosi S. Prostective, randomized, controlled clinical trial comparing traditional versus reduced tidal volume ventilation in acute respiratory distress syndrome patients. Crit Care Med 1999; 27: 1492-1498.

Brun-Buisson C, Minelli C, Bertolini G, Brazzi L, Pimentel J, Lewandowski K, Bion J, Romand JA, Villar J, Thorsteinsson A, Damas P, Armaganidis A, Lemaire F. Epidemiology and outcome of acute lung injury in European intensive care units. Intensive Care Med 2004; 30: 51-61.

Castro CY. ARDS and diffuse alveolar damage: A pathologist's perspective. Semin Thorac Cardiovasc Surg 2006; 18: 13-19.

Chiumello D, Pristine G, Slutsky AS. Mechanical ventilation affects local and systemic cytokines in an animal model of acute respiratory distress syndrome. Am J Respir Crit Care Med 1999; 160: 109-116.

Chonghaile MN, Higgins BD, Costello J, Laffey JG. Hypercapnic acidosis attenuates lung injury induced by established bacterial pneumonia. Anesthesiology 2008; 109: 837-848.

Costello J, Higgins B, Contreras M, Chonghaile MN, Hassett P, O'Toole D, Laffey JG. Hypercapnic acidosis attenuates shock and lung injury in early and prolonged systemic sepsis. Crit Care Med 2009; 37: 2412-2420.

Dada LA, Chandel NS, Ridge KM, Pedemonte C, Bertorello AM, Sznajder JI. Hypoxia-induced endocytosis of Na,K-ATPase in alveolar epithelial cells is mediated by mitochondrial reactive oxygen species and PKC-ζ. J Clin Invest 2003; 111: 1057-1064.

Dada LA, Welch LC, Zhou G, Ben-Saadon R, Ciechanover A, Sznajder JI. Phosphorylation and ubiquitination are necessary for Na,K-ATPase endocytosis during hypoxia. Cell Signal 2007; 19: 1893-1898.

Dagenais A, Fréchette R, Yamagata Y, Yamagata T, Carmel JF, Clermont ME, Brochiero E, Massé C, Berthiaume Y. Downregulation of ENaC activity and expression by TNF-alpha in alveolar epithelial cells. Am J Physiol Lung Cell Mol Physiol 2004; 286: L301-L311.

Debs RJ, Fuchs HJ, Philip R, Montgomery AB, Brunette EN, Liggitt D, Patton JS, Shellito JE. Lung-specific delivery of cytokines induces sustained pulmonary and systemic immunomodulation in rats. J Immunol 1998; 140: 3482-3488.

Dembinski R, Max M, Bensberg R, Rossaint R, Kuhlen R. Pressure support compared with controlled mechanical ventilation in experimental lung injury. Anesth Analg 2002; 94: 1570-1576.

Deshmane SL, Kremlev S, Amini S, Sawaya BE. Monocyte chemoattractant protein-1 (MCP): an overview. J Interferon Cytokine Res 2009; 29: 313-326.

Determann RM, Royakkers A, Wolthuis EK, Vlaar AP, Choi G, Paulus F, Hofstra JJ, de Graff MJ, Korevaar JC, Schultz MJ. Ventilation with lower tidal volumes as compared with conventional tidal volumes for patients without acute lung injury: a preventative randomized controlled trial. Crit Care 2010; 14: R1.

Doerr CH, Gajic O, Berrios JC, Caples S, Abdel M, Lymp JF, Hubmayr RD. Hypercapnic acidosis impairs plasma membrane wound resealing in ventilator-injured lungs. Am J Respir Crit Care Med 2005; 171: Epub ahead of print.

Donnelly SC, Strieter RM, Reid PT, Kunkel SL, Burdick MD, Armstrong I, Mackenzie A, Haslett C. The association between mortality rates and decreased concentrations of interleukin-10 and interleukin-1 receptor antagonist in the lung fluids of patients with the acute respiratory distress syndrome. Ann Intern Med 1996; 125: 191-196.

Dreyfuss D, Soler P, Basset G, Saumon G. High inflation pressure pulmonary edema. Respective effects of high airway pressure, high tidal volume, and positive end-expiratory pressure. Am Rev Respir Dis 1988; 137: 1159-1164.

Eder C. Mechanisms of interleukin-1 beta release. Immunobiology 2009; 214: 543-553.

Elgrabli D, Floriani M, Abella-Gallart S, Meunier L, Gamez C, Delalain P, Rogerieux F, Boczkowski J, Lacroix G. Biodistribution and clearance of instilled carbon nanotubes in rat lung. Part Fibre Toxicol 2008; 5:20-32.

Fan J, Ye RD, Malik AB. Transcriptional mechanisms of acute lung injury. Am J Physiol Lung Cell Mol Physiol 2001; 281: 1037-1050.

Fang X, Song Y, Hirsch J, Galietta LJ, Pedemonte N, Zemans RL, Dolganov G, Verkman AS, Matthay MA. Contribution of CFTR to apical-basolateral fluid transport in cultured human alveolar epithelial type II cells. Am J Physiol Lung Cell Mol Physiol 2005; 290: L242-249.

Fehil F, Eckert P, Brimioulle S, Jacobs O, Schaller MD, Mélot C, Naeije R. Permissive hypercapnia impairs pulmonary gas exchange in the acute respiratory distress syndrome. Am J Respir Crit Care Med 2000; 162: 209-215.

Floretto JR, Campos FJ, Ronchi CF, Ferreira AL, Kurokawa CS, Carpi MF, Moraes MA, Bonatto RC, Defaveri J, Yeum KJ. Respir Care 2011; July (Epub ahead of print).

Folkesson HG, Nitenberg G, Oliver BL, Jayr C, Albertine KH, and Matthay MA. Upregulation of alveolar epithelial fluid transport after subacute lung injury in rats from bleomycin. Am J Physiol Lung Cell Mol Physiol 275: L478–L490, 1998.

Forster HV, Smith CA. Contributions of central and peripheral chemoreceptors to the ventilatory response to CO2/H+. J Appl Physiol 2010; 108: 989-994.

Frank JA, Gutierrez JA, Jones KD, Allen L, Dobbs L, Matthay MA. Low tidal volume reduces epithelial and endothelial injury in acid-injured rat lungs. Am J Respir Crit Care Med 2002; 165: 242-249.

Frank JA, Pittet JF, Lee H, Godzich M, Matthay MA. High tidal volume ventilation induces NOS2 and impairs cAMP-dependent air space fluid clearance. Am J Physiol Lung Physiol 2003; 284: 791-798.

Fraser JR, Oliveira PH, Hüttner I. Effect of blood pH on anionic ferritin transport through rat aortic endothelium. Experientia 1978; 34: 1171-1172.

Frossard JL, Saluja AK, Mach N, Lee HS, Bhagat L, Hadenque A, Rubbia-Brandt, Dranoff G, Steer ML. In vivo evidence for the role of GM-CSF as a mediator in acute pancreatitis-associated lung injury. Am J Physiol Lung Cell Mol Physiol 2002; 283: L541-L548.

Fu Z, Costello ML, Tsukimoto K, Prediletto R, Elliott AR, Mathieu-Costello O, West JB. High lung volume increases stress failure in pulmonary capillaries. J Appl Physiol 1992; 73: 123-133.

Fujita M, Kuwano K, Kunitake R, Hagimoto N, Miyazaki H, Kaneko Y, Kawasaki M, Maeyama T, Hara N: Endothelial cell apoptosis in lipopolysaccharide-induced lung injury in mice. Int Arch Allergy Immunol 1998, 117: 202-208

Gammanpila S, Bevan DR, Bhudu R. Effect of positive and negative expiratory pressure on renal function. Br J Anaesth 1977; 49: 199-205.

Gearing AJ, Beckett P, Christodoulou M, Churchill M, Clements J, Davidson AH, Drummond AH, Galloway WA, Gilbert R, Gordon JL. Processing of tumor necrosis factor-alpha precursor by metalloproteinases. Nature 1994; 370: 555-557.

Goodman ER, Striker P, Velavicius M et al. Role of granulocyte-macrophage colony-stimulating factor and its receptor in the genesis of acute respiratory distress syndrome through an effect on neutrophil apoptosis. Arch Surg 1999; 134: 1049-1054.

Goodman RB, Strieter RM, Martin DP, Steinberg KP, Milberg JA, Maunder RJ, Kunkel SL, Walz A, Hudson LD, Martin TR. Inflammatory cytokines in patients with persistence of the acute respiratory distress syndrome. Am J Respir Crit Care Med 1996; 154: 602-611.

Gores GJ, Nieminen AL, Wray BE, Herman B, Lemasters JJ. Intracellular pH during "chemical hypoxia" in cultured rat hepatocytes. Protection by intracellular acidosis against the onset of cell death. J Clin Invest 1989; 83: 386-396.

Hammer J. Acute Lung Injury: pathophysiology, assessment, and current therapy. Paed Resp Rev 2000; 2: 10-21.

Henzler D, Hochhausen N, Chankalal R, Xu Z, Whynot SC, Slutsky AS, Zhang H. Physiologic and biologic characteristics of three experimental models of acute lung injury in rats. Anesth Analg 2011; 112: 1139-1146.

Henzler D, Pelosi P, Dembinski R, Ullmann A, Mahnken AH, Rossaint R, Kuhlen R. Respiratory compliance but not gas exchange correlates with changes in lung aeration after a recruitment maneuver: an exprerimental study in pigs with saline lavage lung injury. Crit Care 2005; 9: 471-482.

Hickling KG, Henderson SJ, Jackson R. Low mortality with low volume pressure limited ventilation with permissive hypercapnia in severe adult respiratory distress syndrome. Intensive Care Med 1990; 16: 372-377.

Hickling KG. Low volume ventilation with permissive hypercapnia in the adult respiratory distress syndrome. Clin Intensive Care 1992; 3: 67-78.

Hickling KG, Walsh J, Henderson S, Jackson R, Low mortality in adult respiratory distress syndrome using low-volume, pressure-limited ventilation with permissive hypercapnia: a prospective study. Crit Care Med 1994; 22: 1568-1578.

Hooper J. Advances in mechanical ventilation. Can J Anaesth 1998; 45: 149-159.

Horgan MJ, Palace GP, Everitt JE, Malik AB. TNF-alpha release in endotoxemia contributes to neutrophil-dependent pulmonary edema. Am J Physiol Heart Circ Physiol 1993; 264: 1161-1165.

Ijland MM, Heunks LM, van der Hoeven JG. Bench-to-bedside review: hypercapnic acidosis in lung injury—from 'permissive' to 'therapeutic'. Crti Care 2010; 14 (Epub Nov).

Imanaka H, Shimaoka M, Matsuura N, Nishimura M, Ohta N, Kiyono H. Ventilator-induced lung injury is associated with neutrophil infiltration, macrophage activation, and TGF-beta 1 mRNA upregulation in rat lungs. Anesth Analg 2001; 92: 428-436.

Ismaiel NM, Henzler D. Effects of hypercapnia and hypercapnic acidosis on attenuation of ventilator-associated lung injury. Minerva Anestesiol 2011; 77:723-733.

Jaber S, Jung B, Sebbane M, Ramonatxo M, Capdevila X, Mercier J, Eldejam JJ, Matecki S. Alterations of the piglet diaphragm contractility in vivo and its recovery after acute hypercapnia. Anesthesiology 2008; 108: 651-658.

Jiang C, Rojas A, Wang R, Wang X. CO2 central chemosensitivity: why are there so many sensory molecules. Respir Physiol Neurobiol 2005; 145: 115-126.

Jonson B, Richard JC, Straus C, Mancebo J, Lemaire F, Brochard L. Pressure-volume curves and compliance in acute lung injury: Evidence of recruitment above the lower inflection point. Am J Respir Crit Care Med 1999; 159: 1172-1178.

Kacmarek RM, Venegas J. Mechanical ventilatory rates and tidal volumes. Respir Care 1987; 32: 466-478.

Kaplan SH, Yang H, Gilliam DE, Shen J, Lemasters JJ, Cascio WE. Hypercapnic acidosis and dimethyl amiloride reduce reperfusion induced cell death in ischaemic ventricular myocardium. Cardiovasc Res 1995; 29: 231-238.

Kavanagh BP, Laffey JG. Hypercapnia: permissive and therapeutic. Minerva Anestesiol 2006; 72: 567-576.

Kavelaars A, Pol M van de, Zijlstra J, Heijnen CJ. Beta-2-adrenergic activation enhances interleukin-8 production by human monocytes. J Neuroimmunol 1997; 177: 211-216.

Kawasaki M, Kuwano K, Hagimoto N, Matsuba T, Kunitake R, Tanaka T, Maeyama T, Hara N. Protection from lethal apoptosis in lipopolysaccharide-induced acute lung injury in mice by a caspase inhibitor. Am J Pathol 2000; 157: 597-603.

Kishimoto T. The biology of interleukin-6. Blood 1989; 74: 1-10.

Kitakaze M, Takashima S, Funaya H, Minamino T, Node K, Shinozaki Y, Mori H, Hori M. Temporary acidosis during reperfusion limits myocardial infarct size in dogs. Am J Physiol 1997; 272: 2071-2078.

Kitamura Y, Hashimoto S, Mizuta N, Kobayashi A, Kooguchi K, Fujiwara I, Nakajima H. Fas/FasL-dependent apoptosis of alveolar cells after lipopolysaccharide-induced lung injury in mice. Am J Respir Crit Care Med 2001; 163: 762-769.

Kogan AKh, Grachev SV, Eliseeva SV, Bolevich S. Ability of carbon dioxide to inhibit generation of superoxide anion radical in cells and its biomedical role. Vopr Med Khim 1996; 42: 193-202.

Kollef MH, Schuster DP. The acute respiratory distress syndrome. N Engl J Med 1995; 332: 27-37.

Kristof AS, Goldberg P, Laubach V, Hussain SNA. Role of inducible nitric oxide synthase in endotoxin-induced acute lung injury. Am J Respir Crit Care Med 1998; 158: 1883-1889.

Kruger NJ. The Bradford method for protein quantitation. In: The protein protocols handbook. (2nd end). Walker JM. (ed.) Humana Press Inc., USA, 2002, pp 15-21.

Kumagai M, Kondo T, Ohta Y, Ishihara T. Size and composition changes in diaphragmatic fibers in rats exposed to chronic hypercapnia. Chest 2001; 119: 565-571.

Kwon OJ, Jose PJ, Robbins RA, Schall TJ, Williams TJ, Barnes PJ. Glucocorticoid inhibition of RANTES expression in human lung epithelial cells. Am J Respir Cell Mol Biol 1995; 12: 488-496.

Laffey JG, Engelberts D, Kavanagh BP. Buffering hypercapnic acidosis worsens acute lung injury. Am J Respir Crit Care Med 2000a; 161: 141-146.

Laffey JG, Tanaka M, Engelberts D, Luo X, Yuan S, Tanswell AK, Post M, Lindsay T, Kavanagh BP. Therapeutic hypercapnia reduces pulmonary and systemic injury following in vivo lung reperfusion. Am J Respir Crit Care Med 2000b; 162: 2287-2294.

Laffey JG, Honan D, Hopkins N, Hyvelin JM, Boylan JF, McLoughlin P. Hypercapnic acidosis attenuates endotoxin-induced acute lung injury. Am J Respir Crit Care Med 2004; 169: 46-46.

Lahiri S, Forster RE II. CO_2/H^+ sensing: peripheral and central chemoreception. Int J Biochem Cell Biol 2003; 35: 1413-1435.

Lang JD Jr, Chumley P, Eiserich JP, Estevez A, Bamberg T, Adhami A, Crow J, Freeman BA. Am J Physiol Lung Cell Mol Physiol 2000; 279: 994-1002.

Lang JD, Figueroa M, Sanders KD, Aslan M, Liu Y, Chumley P, Freeman BA. Hypercapnia via reduced rate and tidal volume contributes to lipopolysaccharide-induced lung injury. Am J Respir Crit Care Med 2005; 171: 147-157.

Lawson C, Wolf S. ICAM-1 signaling in endothelial cells. Pharmacol Rep 2009; 61: 22-32.

Lecuona E, Salidas F, Comellas A, Ridge K, Guerrero C, Sznajder JI. Ventilator-associated lung injury decreases ability to clear edema in rats. Am J Respir Crit Care Med 1999; 159: 603-609.

Lecuona E, Trejo HE, Sznajder JI. Regulation of Na-K-ATpase during acut lung injury. J Bioenerg Biomemb 2007; 39: 391-395.

Lotze MT, Zeh HJ, Rubartello A, Sparvero LJ, Amoscato AA, Washburn NR, Devera ME, Liang X, Tör M, Billiar T. The grateful dead: damage-associated molecular and reduction/oxidation regulate immunity. Immunol Rev 2007; 220: 60-81.

Love R, Choe E, Lippton H, Flint L, Steinberg S. Positive end-expiratory pressure decreases mesenteric blood flow despite normalization of cardiac output. J Trauma 1995; 39: 195-199.

MacCarrick MJ, Torbati D, Kimura D, Raszynski A, Zeng W, Totapally BR. Does hypercapnia ameliorate hyperoxia-induced lung injury in neonatal rats? Lung 2010; 188: 235-240.

Marini JJ. Evolving concepts in the ventilatory management of acute respiratory distress syndrome. Clin Chest Med 1996; 17: 555-575.

Marini JJ, Hotchkiss JR, Broccard AF. Bench-to-bedside review: microvascular and airspace linkage in ventilator-induced lung injury. Crit Care 2003; 7: 435-444.

Meduri GU, Kohler G, Headley S, Tolley E, Stentz F, Postlethwaite A. Inflammatory cytokines in the BAL of patients with ARDS. Persistent elevation over time predicts poor outcome. Chest 1995; 108: 1303-1314.

Miyake M, Morishita M, Ito K, Ito A, Torii S, Sakamoto T. Production of granulomatous inflammation in lungs of rat pups and adults by sephadex beads. Pediatr Res 2004; 56: 205-211.

Mohan MJ, Seaton T, Mitchell J, Howe A, Blackburn K, Burkhart W, Moyer M, Patel I, Waitt GM, Becherer JD, Moss ML, Milla ME. The tumor necrosis factor-alpha converting enzyme (TACE): a unique metalloproteinase with highly defined substrate selectivity. Biochemistry 2002; 41: 9462-9469.

Nanji AM, Jokelainen K, Rahemtulla A, Miao L, Fogt F, Matsumoto H, Tahan SR, Su GL. Activation of nuclear factor kappa B and cytokine imbalance in experimental alcoholic liver disease in the rat. Hepatology 1999; 30: 934-943.

Nathens AB, Bitar R, Watson RWG Issekutz TB, Marshall JC, Dackiw APB, Rotstein OD. Thiol-mediated regulation of ICAM-1 expression in endotoxin0induced acute lung injury. J Immunol 1998; 160: 2959-2966.

Nichol AD, O'Croinin DF, Howell K, Naughton F, O'Brien S, Boylan J, O'Connor C, O'Toole D, Laffey JG, McLoughlin P. Infection-induced lung injury is worsened after renal buffering of hypercapnic acidosis. Crit Care Med 2009; 37: 2953-2961.

Nichol AD, O'Croinin DF, Naughton F, Hopkins N, Boylan J, McLoughlin P. Hypercapnic acidosis reduces oxidative reactions in endotoxin-induced lung injury. Anesthesiology 2010; 113: 116-125.

Nicholson DW, Ali A, Thornberry NA, Vaillancourt JP, Ding CK, Gallant M, gareau Y, Griffin PR, Labelle M, Lazebnik YA, Munday NA, Raju SM, Smulson ME, Yamin TT, Yu VL, Miller DK. Identification and inhibition of the ICE/CED-3 protease necessary for mammalian apoptosis. Nature 1995; 376: 37-43.

Nishimoto N, Kishimoto T. Interleukin 6: from bench to bedside. Nat Clin Pract Rheumatol 2006; 2: 619-626.

Nomura F, Aoki M, Forbess JM, Mayer JE Jr. Effects of hypercarbic acidotic reperfusion on recovery of myocardial function after cardioplegic ischemia in neonatal lambs. Circulation 1994; 90: 321-327.

O'Croinin DF, Nichol AD, Hopkins N, Boylan J, O'Brien S, O'Connor C, Laffey JG, McLoughlin P. Sustained hypercapnic acidosis during pulmonary infection increases bacterial load and worsens lung injury. Crit Care Med 2008; 36: 2128-2135.

Oeckler RA, Hubmayr RD. Ventilator-associated lung injury: a search for better therapeutic targets. Eur Respir J 2007; 30: 1216-1226.

Orfanos SE, Mavrommati I, Korovesi I, Roussos C. Pulmonary endotheliumin acute lung injury: from basic science to the critically ill. Intensive Care Med 2004; 30: 1702-1714.

Papazian L, Forel JM, Gacouin A, Penot-Ragon C, Perrin G, Loundou A, Jaber S, Arnal JM, Perez D, Seghboyan JM, Constantin JM, Courant P, Lefrant JY, Guérin C, Prat G,

Morange S, Roch A. Neuromuscular blockers in early acute respiratory distress syndrome. N Engl J Med 2010; 363: 1107-1116.

Parker JC, hernandez LA, Peevy KJ. Mechanisms of ventilator-induced lung injury. Crit Care Med 1993; 21: 131-143.

Pedoto A, Caruso JE, Nandi J, Oler A, Hoffmann SP, Tassiopoulos AK, McGraw DJ, Camporesi EM, Hakim TS. Acidosis stimulates nitric oxide production and lung damage in rats. Am J Respir Crit Care Med 1999; 159: 397-402.

Peltekova V, Engelberts D, Otulakowski G, Uematsu S, Post M, Kavanagh BP. Hypercapnic acidosis in ventilator-induced lung injury. Intensive Care Med 2010; 36: 869-878.

Petrucci N, Lacovelli W. Ventilation with lower tidal volumes versus traditional tidal volumes in adults for acute lung injury and acute respiratory distress syndrome. Cochrane Database Syst Rev 2004; 2: 1469-1493.

Pinhu L, Whitehead T, Evans T, Griffiths M. Ventilator-associated lung injury. Lancet 2003; 361: 332-340.

Plötz FB, Slutsky AS, Van Vught AJ, Heijnen CJ. Ventilator-induced lung injury and multiple organ failure: a critical review of facts and hypotheses. Intensive Care Med 2004; 30: 1865-1872.

Pradines-Figueres A, Raetz CRH. Processing and secretion of tumor-necrosis factor α in endotoxin-treated mono mac 6 cells are dependent on phorbol myristate acetate. J Biol Chem 267: 23261-23268.

Putensen C, Mutz NJ, Putensen-Himmer G, Zinserling J. Spontaneous breathing during ventilatory support improves ventilation-perfusion distributions in patients with acute respiratory distress syndrome. Am J Respir Crit Care Med 1999; 159: 1241-1248.

Ranieri VM, Suter PM, Tortorella C, De Tullio R, Dayer JM, Brienza A, Bruno F, Slutsky AS. Effect of mechanical ventilation on inflammatory mediators in patients with acute respiratory distress syndrome. JAMA 1999; 282: 54-61.

Reutershan J, Ley K. Bench-to-bedside review: acute respiratory distress syndrome- how neutrophils migrate into the lung. Crit Care 2004; 8: 453-461.

Rubenfeld GD, Caldwell E, Peabody E, Weaver J, Martin DP, Neff M, Stern EJ, Hudson LD. Incidence and outcomes of acute lung injury. N Engl J Med 2005; 353: 1685-1693.

Savel RH, Yao EC, Gropper MA. Protective effects of low tidal volume ventilation in a rabbit model of Pseudomonas aeruginosa-induced acute lung injury. Crit Care Med 2001; 29: 392-398.

Shanley TP, Schmal H, Friedl HP, Jones ML, Ward PA. Role of macrophage inflammatory protein-1 alpha (MIP-1 alpha) in acute lung injury in rats. J Immunol 1995; 154: 4793-4802.

Shibata K, Cregg N, Engelberts D, Takeuchi A, Fedorko L, Kavanagh BP. Hpercapnic acidosis may attenuate acute lung injury by inhibition of endogenous xanthine oxidase. Am J Respir Crit Care Med 1998; 158: 1578-1584.

Shokawa T, Yoshizumi M, Yamamoto H, Omura S, Toyofuku M, Shimizu Y, Imazu M, Kohno N. Induction of heme oxygenase-1 inhiits monocyte chemoattractant protein-1 mRNA expression in U937 cells. J Pharmacol Sci 2006; 100: 162-166.

Sinclair SE, Kregenow DA, Lamm WJ, Starr IR, Chi EY, Hlastala MP. Hypercapnic acidosis is protective in an in vivo model of ventilator-induced lung injury. Am J Respir Crit Care Med 2002; 166: 403-408.

Slutsky AS, Tremblay LN. Multiple system organ failure. Is mechanical ventilation a contributing factor? Am J Respir Crit Care Med 1998; 157: 1721-1751.

Takeshita K, Suzuki Y, Nishio K, Takeuchi O, Toda K, Kudo H, Miyao N, Ishii M, sato N, Naoki K, Aoki T, Suzuki K, Hiraoka R, Yamaguchi K. Hypercapnic acidosis attenuates endotoxin-induced nuclear factor-[kappa]B activation. Am J Respir Cell Mol Biol 2003; 29: 124-132.

Tanabe O, Akira S, Kamiya T, Wong GG, Hirano T, Kishimoto T. Genomic structure of the murine IL-6: high degree conservation of potential regulatory sequences between mouse and human. J Immunol 1988; 141: 3875-3881.

Task Force on Guidelines, Society of Critical Care Medicine: Guidelines for standards of care for patients with acute respiratory failure on mechanical ventilatory support. Crit Care Med 1991; 19: 275-278.

Tateda K, Deng JC, Moore TA, Newstead MW, Paine III R, Kobayashi N, Yamaguchi K, Standiford TJ. Hypoxia mediates acute lung injury and increased lethality in murine legionella pneumonia: the role of apoptosis. J Immunol 2003; 170: 4209-4216.

Thomsen GE, Morris AH. Incidence of the adult respiratory distress syndrome in the state of Utah. Am J Respir Crit Care Med 1995; 152: 965-971.

Tremblay L, Valenza F, Ribeiro SP, Slutsky AS. Injurious ventilatory strategies increase cytokines and c-fos m-RNA expression in an isolated rat lung model. J Clin Invest 1997; 99: 944-952.

Tremblay LN, Slutsky AS. Ventilator-induced lung injury: from the bench to the bedside. Appl Physiol Intensive Care Med 2006; 3: 357-366.

Tutor JD, Mason CM, Dobard E, Beckerman RC, Summer WR, Nelson S. Loss of compartmentalization of alveolar tumor necrosis factor after lung injury. Am J Respir Crit Care Med 1994; 149: 1107-1111.

Vannucci RC, Towfighi J, Heitjan DF, Brucklacher RM. Carbon dioxide protects the perinatal brain from hypoxic-ischemic damage: an experimental study in the immature rat. Pediatrics 1995; 95: 868-874.

Veldhuizen RA, Slutsky AS, Joseph M, McCaig L. Effects of mechanical ventilation of isolated mouse lungs on surfactant and inflammatory cytokines. Eur Respir J 2001; 17: 488-494.

Venkataraman R, Kellum JA, Song M, Fink MP. Resuscitation with ringer's ethyl pyruvate solution prolongs survival and modulates plasma cytokine and nitrite-nitrate concentrations in a rat model of lipopolysaccharide-induced shock. Shock 2002; 18: 507-512.

Wang P, Wu P, Anthes JC, Siegel MI, Egan RW, Billah MM. Interleukin-10 inhibits interleukin-8 production in human neutrophils. Blood 1994; 83: 2678-2683.

Wang P, Wu P, Siegel MI, Egan RW, Billah MM. Interleukin (IL)-10 inhibits nuclear factor kappa B (NF kappa B) activation in human monocytes. IL-10 and IL-4 suppress cytokine synthesis by different mechanisms. J Biol Chem 1995; 270: 9558-9563.

Ware LB, Matthay MA. The acute respiratory distress syndrome. N Engl J Med 2000; 342: 1334-1349.

Ware LB, Matthay MA. Alveolar fluid clearance is impaired in the majority of patients with acute lung injury and the acute respiratory distress syndrome. Am J Respir Crit Care Med 2001; 163: 1376-1383.

West JB, Tsukimoto K, Mathiu-Costello O, Prediletto R. Stress failure in pulmonary capillaries. J Appl Physiol 1991; 70: 1731-1742.

Wilson MR, Choudhury S, Goddard ME, O'Dea KP, Nicholson AG, Takata M. High tidal volume upregulates intrapulmonary cytokines in an in vivo mouse model of ventilator-induced lung injury. J Appl Physiol 2003; 95: 1385-1393.

Wolthuis EK, Vlaar APJ, Choi G, Roelofs JJTH, Juffermans NP, Schultz MJ. Mechanical ventilation using non-injurious ventilation settings causes lung injury in the absence of pre-existing lung injury in healthy mice. Crit Care 2009; 13

Xu L, Glassford AJ, Giaccia AJ, Giffard RG. Acidosis reduces neuronal apoptosis. Neuroreport 1998; 9: 875-879.

Yanagisawa R, Takano H, Inoue K, Ichinose T, Sadakane K, Yoshino S, Yamaki K, Kumagai K, Uchiyama K, Yoshikawa T, Morita M. Enhancement of acute lung injury related to bacterial endotoxin by components of diesel exhaust particles. Thorax 2003; 58: 605-612.

Yang BM, Demaine AG, Kingsnorth A. Chemokines MCP-1 and RANTES in isolated rat pancreatic acinar cells treated with CCK and ethanol in vitro. Pancreas 2000; 21: 22-31.

Yang L, Froio RM, Sciuto TE, Dvorak AM, Alon R, Luscinskas FW. ICAM-1 regulates neutrophil adhesion and transcellular migration of TNF-alpha-activated vascular endothelium under flow. Blood 2005; 106: 584-592.

Yang SR, Wright J, Bauter M, Seweryniak K, Kode A, Rahman I. Sirtuin regulates cigarette smoke-induced proinflammatory mediator release via RelA/p65 NF-κB in macrophages in vitro and in rat lungs in vivo: implications for chronic inflammation and aging. Am J Physiol Lung Cell Mol Physiol 2007; 292: L567-L576.

APPENDIX 1: TABLES

Group	V_T Target (mL/Kg)	RR (min^{-1})	$PaCO_2$ Target (mmHg)	Added CO_2 or dead space
Conventional Normocapnia	High	Low	40-55	
Lung-Protective Ventilation	Low (8.0)	High	40-55	
Injurious Normocapnia	High	High	40-55	1.0 mL added dead space
Conventional Hypercapnia	High	Low	60-70	Inhaled CO_2 (1.6%)
Protective Hypercapnia	Low (8.0)	High	60-70	Inhaled CO_2 (1.6%)
Permissive Hypercapnia	Low (8.0)	Low	60-70	

Table 1. Summary of target ventilation settings, including tidal volume (V_T, mL/Kg), respiratory rate (RR, breaths per minute, min^{-1}), partial pressure of carbon dioxide ($PaCO_2$, mmHg), and the addition of inspired CO_2 gas or dead space for 3 hours of ventilation in each group.

	Group	Baseline	1 Hour	4 Hours
MAP (mmHg)	Conventional Normocapnia	158 ± 13	129 ± 19	116 ± 29
	Lung-Protective Ventilation	152 ± 13	123 ± 16	134 ± 40
	Injurious Normocapnia	156 ± 13	117 ± 20	120 ± 28
	Conventional Hypercapnia	150 ± 13	119 ± 20	121 ± 37
	Protective Hypercapnia	146 ± 13	129 ± 14	140 ± 23
	Permissive Hypercapnia	157 ± 11	119 ± 14	126 ± 28
Heart Rate (BPM)	Conventional Normocapnia	422 ± 36	373 ± 56	428 ± 64
	Lung-Protective Ventilation	418 ± 44	376 ± 68	445 ± 63
	Injurious Normocapnia	401 ± 44	333 ± 39	406 ± 52
	Conventional Hypercapnia	414 ± 43	343 ± 50	411 ± 59
	Protective Hypercapnia	404 ± 41	375 ± 55	420 ± 53
	Permissive Hypercapnia	421 ± 30	365 ± 28	432 ± 55
Cardiac Index ($Lmin^{-1}m^{-2}$)	Conventional Normocapnia	2.55 ± 0.89	2.36 ± 0.75	2.27 ± 0.71
	Lung-Protective Ventilation	2.59 ± 0.64	2.51 ± 0.56	2.19 ± 0.44
	Injurious Normocapnia	2.50 ± 0.55	2.40 ± 0.42	2.22 ± 0.40
	Conventional Hypercapnia	2.46 ± 0.48	2.44 ± 0.67	2.31 ± 0.70
	Protective Hypercapnia	2.47 ± 0.67	2.45 ± 0.59	2.08 ± 0.38
	Permissive Hypercapnia	2.33 ± 0.41	2.75 ± 1.10	2.24 ± 0.85

Table 2. Hemodynamic measurements at baseline, 1 hour and 4 hours of ventilation in each group, including mean arterial pressure (MAP, mmHg), heart rate (beats per minute, BPM), and cardiac index ($Lmin^{-1}m^{-2}$). Values are expressed as mean ± SD.

Table 3. Respiratory mechanics measurements at baseline, 1 hour and 4 hours of ventilation in each group, including tidal volume (V_T, mL/Kg), respiratory rate (RR, breaths per minute, min^{-1}), minute ventilation (V_E, mL/min) and elastance (cmH_2O/L). Values are expressed as mean ± SD.

* p<0.0001 vs. baseline

§ p<0.0001 vs. low VT groups (Lung-Protective Ventilation, Protective Hypercapnia, Permissive Hypercapnia) at 4 hours

\# p<0.01 vs. Conventional Hypercapnia at 4 hours

@ p<0.0001 vs. low RR groups (Conventional Normocapnia, Conventional Hypercapnia, Permissive Hypercapnia) at 4 hours

¶ p<0.001 vs. Conventional Normocapnia, Conventional Hypercapnia, Protective Hypercapnia and Permissive Hypercapnia at 4 hours

	Group	Baseline	1 Hour	4 Hours
V_T (mL/Kg)	Conventional Normocapnia	8.3 ± 0.7	8.2 ± 0.6	13.4 ± 1.2 *§#
	Lung-Protective Ventilation	8.3 ± 0.8	8.1 ± 0.7	8.4 ± 1.4
	Injurious Normocapnia	7.9 ± 0.7	8.6 ± 1.0	12.3 ± 1.4 *§
	Conventional Hypercapnia	8.4 ± 0.9	8.5 ± 0.6	10.9 ± 1.7 *§
	Protective Hypercapnia	8.3 ± 0.5	8.9 ± 1.4	7.8 ± 0.7
	Permissive Hypercapnia	8.3 ± 0.6	8.3 ± 0.7	8.1 ± 1.3
RR (min^{-1})	Conventional Normocapnia	69 ± 14	69 ± 16	42 ± 10 *
	Lung-Protective Ventilation	68 ± 13	68 ± 13	92 ± 14 *@
	Injurious Normocapnia	72 ± 19	72 ± 18	72 ± 16 @
	Conventional Hypercapnia	68 ± 16	69 ± 18	42 ± 11 *
	Protective Hypercapnia	68 ± 13	68 ± 13	68 ± 19 @
	Permissive Hypercapnia	68 ± 11	68 ± 13	52 ± 26
V_E (mL/min)	Conventional Normocapnia	261 ± 61	260 ± 76	254 ± 56
	Lung-Protective Ventilation	256 ± 65	252 ± 64	347 ± 91 *¶
	Injurious Normocapnia	252 ± 67	275 ± 75	367 ± 104 *¶
	Conventional Hypercapnia	258 ± 69	267 ± 76	204 ± 68
	Protective Hypercapnia	261 ± 58	279 ± 73	245 ± 66
	Permissive Hypercapnia	253 ± 36	256 ± 57	191 ± 107 *
Elastance (cmH_2O/L)	Conventional Normocapnia	2.4 ± 0.4	3.8 ± 0.7 *	3.6 ± 1.0 *
	Lung-Protective Ventilation	2.5 ± 0.7	4.2 ± 0.7 *	4.5 ± 0.8 *
	Injurious Normocapnia	2.6 ± 0.5	3.8 ± 0.8 *	4.9 ± 2.3 *
	Conventional Hypercapnia	2.6 ± 0.7	4.3 ± 1.2 *	3.9 ± 1.4 *
	Protective Hypercapnia	2.3 ± 0.5	3.7 ± 0.7 *	4.2 ± 0.8 *
	Permissive Hypercapnia	2.4 ± 0.4	4.1 ± 1.1 *	4.8 ± 1.8 *

	Group	Baseline	1 Hour	4 Hours
pH	Conventional Normocapnia	7.40 ± 0.06	7.35 ± 0.11	7.29 ± 0.14
	Lung-Protective Ventilation	7.38 ± 0.10	7.29 ± 0.05	7.32 ± 0.12
	Injurious Normocapnia	7.37 ± 0.12	7.37 ± 0.13	7.33 ± 0.07
	Conventional Hypercapnia	7.38 ± 0.08	7.33 ± 0.10	7.20 ± 0.11
	Protective Hypercapnia	7.38 ± 0.09	7.36 ± 0.11	7.26 ± 0.11
	Permissive Hypercapnia	7.37 ± 0.07	7.29 ± 0.08	7.17 ± 0.11 *§
P/F Ratio (mmHg)	Conventional Normocapnia	444 ± 60	315 ± 71	222 ± 134 *
	Lung-Protective Ventilation	420 ± 61	247 ± 89	279 ± 111 *
	Injurious Normocapnia	431 ± 92	365 ± 72	242 ± 135 *
	Conventional Hypercapnia	442 ± 84	304 ± 110	242 ± 135 *
	Protective Hypercapnia	414 ± 81	304 ± 120	265 ± 94 *
	Permissive Hypercapnia	421 ± 78	239 ± 68	204 ± 127 *
$PaCO_2$ (mmHg)	Conventional Normocapnia	51 ± 11	53 ± 12	52 ± 9
	Lung-Protective Ventilation	52 ± 17	61 ± 12	48 ± 9
	Injurious Normocapnia	52 ± 19	52 ± 16	55 ± 7
	Conventional Hypercapnia	50 ± 14	53 ± 19	68 ± 8 #@
	Protective Hypercapnia	50 ± 8	52 ± 13	68 ± 15 #@
	Permissive Hypercapnia	50 ± 11	57 ± 11	71 ± 14 #@

Table 4. Gas exchange measurements at baseline, 1 hour and 4 hours of ventilation in each group, including the pH, ratio of the partial pressure of O_2 to the fraction of inspired CO_2 (P/F ratio, mmHg) and partial pressure of CO_2 ($PaCO_2$, mmHg). Values are expressed as mean ± SD.

* $p<0.0001$ vs. baseline

§ $p<0.05$ vs. Conventional Normocapnia and Lung-Protective Ventilation at 4 hours

\# $p<0.001$ vs. baseline

@ $p<0.0001$ vs. normocapnic groups (Conventional Normocapnia, Lung-Protective Ventilation, Injurious Normocapnia) at 4 hours

APPENDIX 2: FIGURES

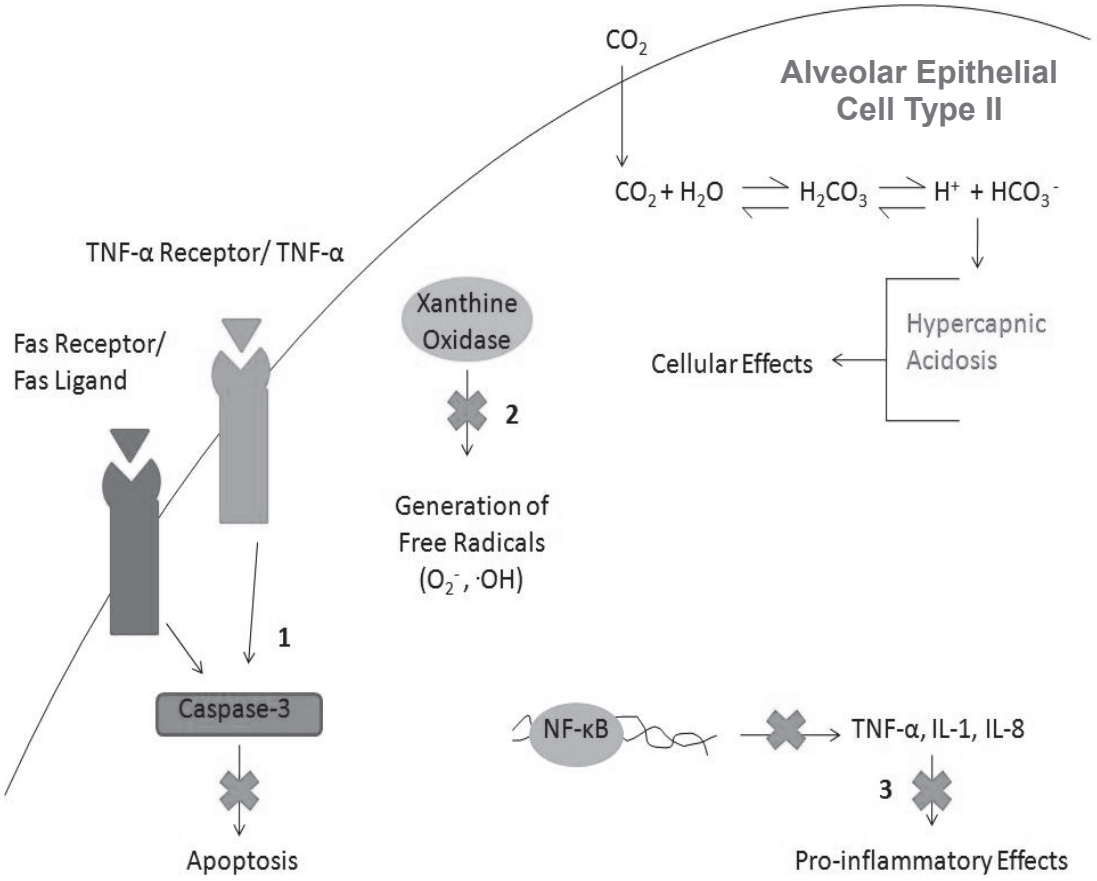

Figure 1. Hypercapnic acidosis (HCA) develops when carbon dioxide (CO_2) accumulates in the cell and reduces intracellular pH. HCA inhibits the apoptotic activity of alveolar epithelial cells by reducing caspase-3 activity (1), reduces free radical production by inhibiting xanthine oxidase enzymatic activity (2), and decreases the production of pro-inflammatory cytokines by inhibiting NF-κB activity (3). OH^-: Hydroxide Radical; O_2^-: Superoxide Radical; TNF-α: Tumor Necrosis-alpha; NF-κB: Nuclear Factor-Kappa B. Modified from Ismaiel and Henzler, Minerva Anesth 2011; 77: 723-733.

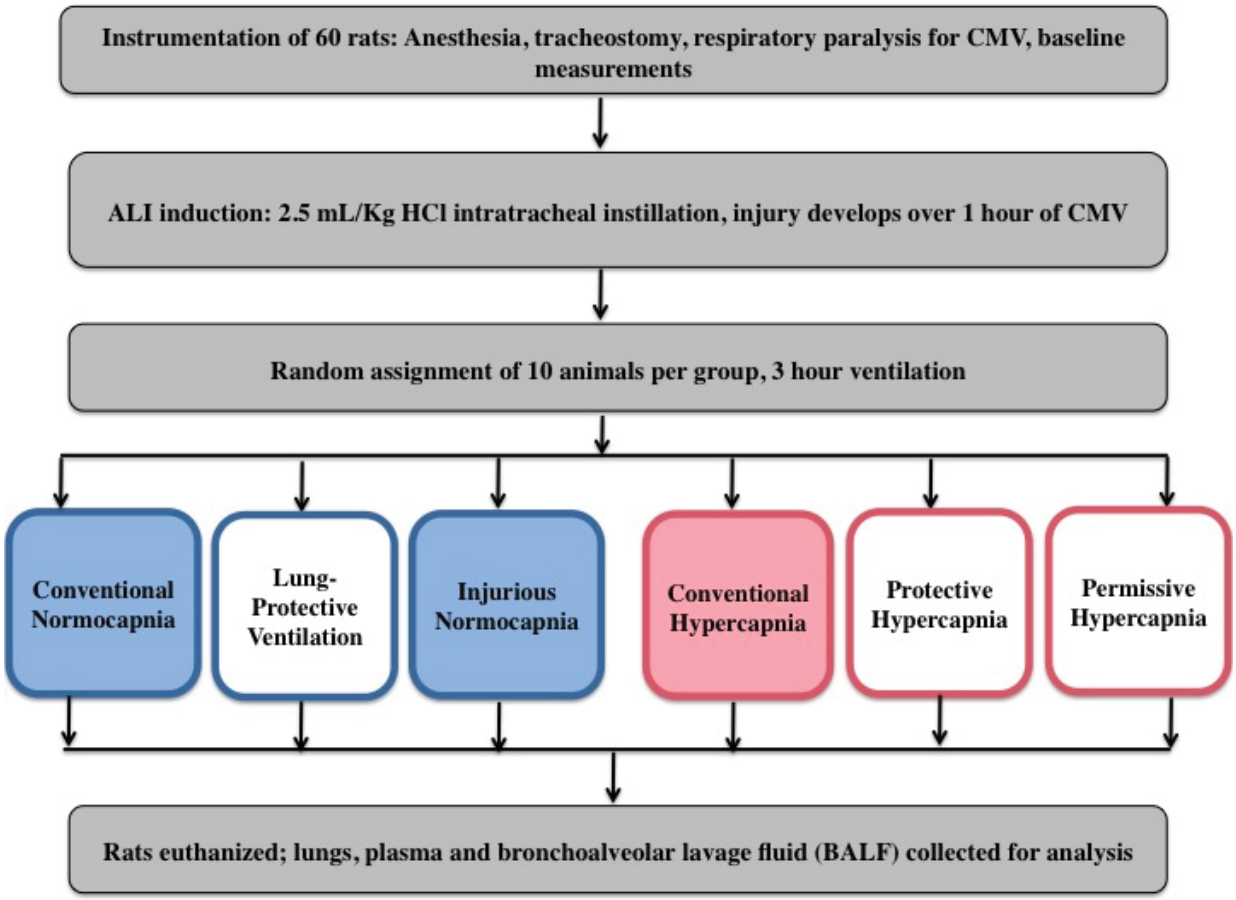

Figure 2. The experimental protocol entails the instrumental of rats (N=60), induction of Acute Lung Injury (ALI) with hydrochloric acid (HCl) and allowing the injury to develop over 1 hour of protective settings under controlled mechanical ventilation (CMV) and respiratory paralysis. After establishment of ALI, animals were randomly assigned to six groups (n=10 per group), ventilated for 3 hours, and samples were collected. Legend: blue border: normocapnia (Partial Pressure of Arterial CO_2, $PaCO_2$ target= 40-55 mmHg); pink border: hypercapnia ($PaCO_2$ target=60-70 mmHg); solid background: conventional ventilation settings (high tidal volume, V_T); blank background: protective ventilation settings (V_T target of 8 mL/Kg).

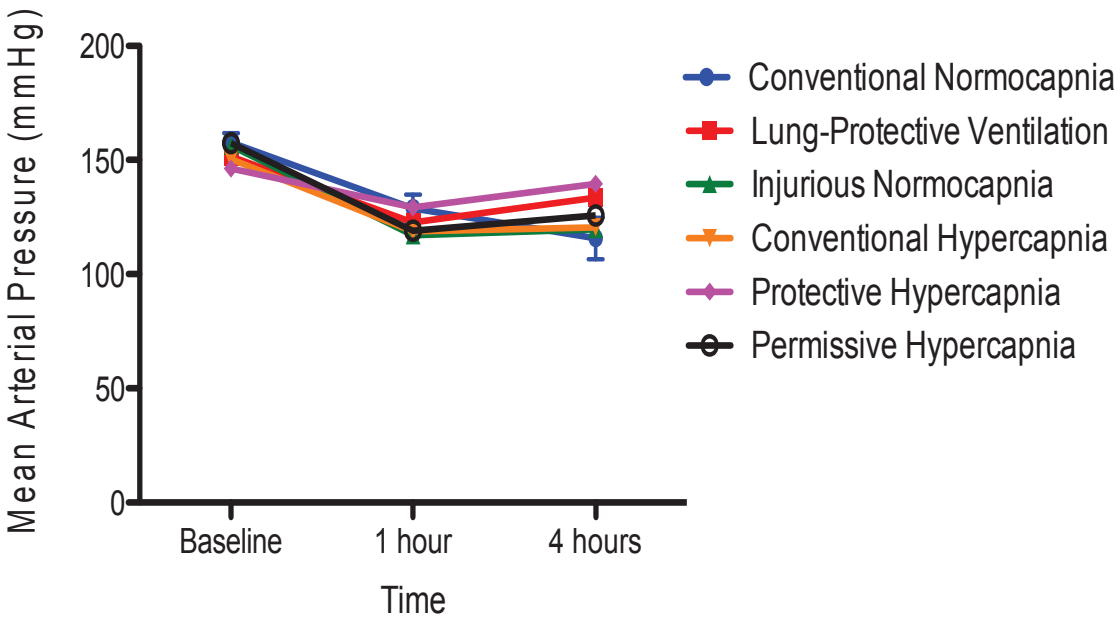

Figure 3. The mean arterial pressure (MAP) at baseline, 1 hour and 4 hours of mechanical ventilation in Conventional Normocapnia, Lung-Protective Ventilation, Injurious Normocapnia, Conventional (Therapeutic) Hypercapnia, Protective (Therapeutic) Hypercapnia and Permissive Hypercapnia. The MAP did not differ among the groups at baseline, 1 hour and 4 hours of ventilation, and there were no time-dependent differences. Values are expressed as mean ± SEM.

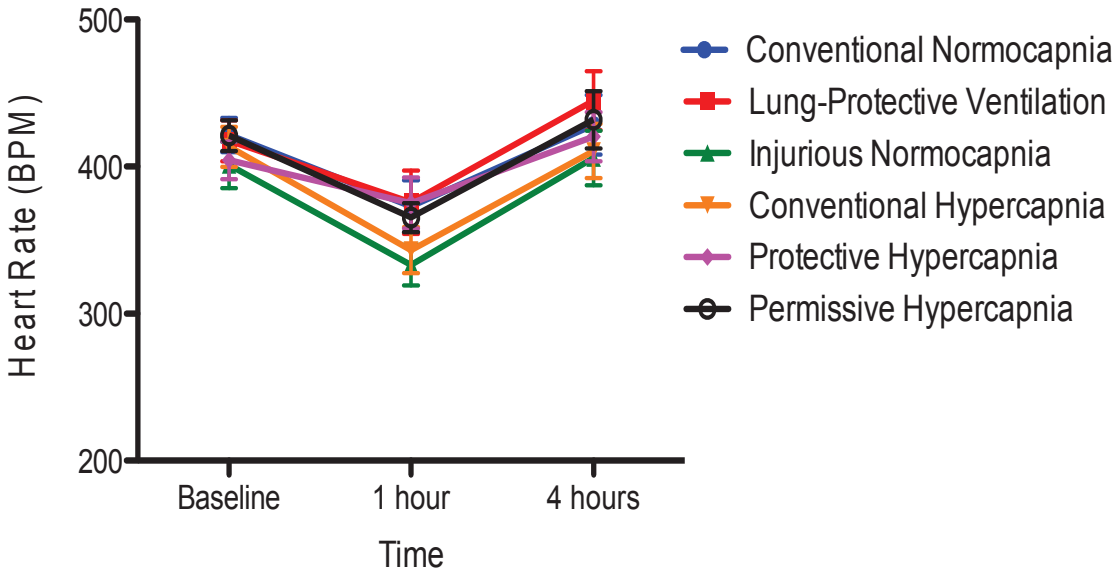

Figure 4. The heart rate (HR) at baseline, 1 hour and 4 hours of mechanical ventilation in Conventional Normocapnia, Lung-Protective Ventilation, Injurious Normocapnia, Conventional (Therapeutic) Hypercapnia, Protective (Therapeutic) Hypercapnia and Permissive Hypercapnia. The HR did not differ among the groups at baseline, 1 hour and 4 hours of ventilation, and there were no time-dependent differences in HR. Values are expressed as mean ± SEM.

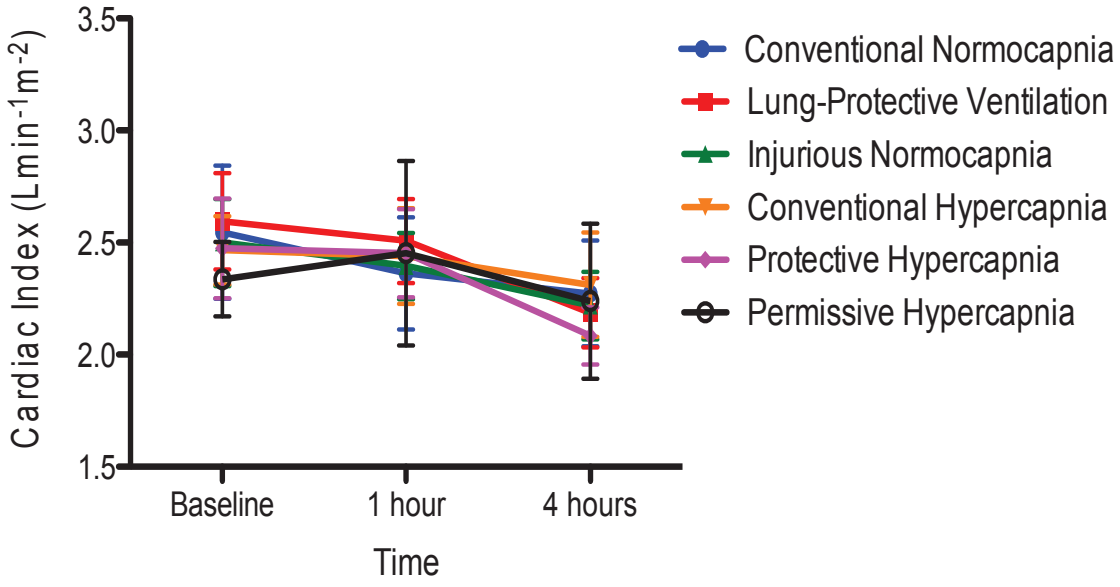

Figure 5. The cardiac index (CI) at baseline, 1 hour and 4 hours of mechanical ventilation in Conventional Normocapnia, Lung-Protective Ventilation, Injurious Normocapnia, Conventional (Therapeutic) Hypercapnia, Protective (Therapeutic) Hypercapnia and Permissive Hypercapnia. The CI did not differ among the groups at baseline, 1 hour and 4 hours of ventilation, and there were no time-dependent differences. Values are expressed as mean ± SEM.

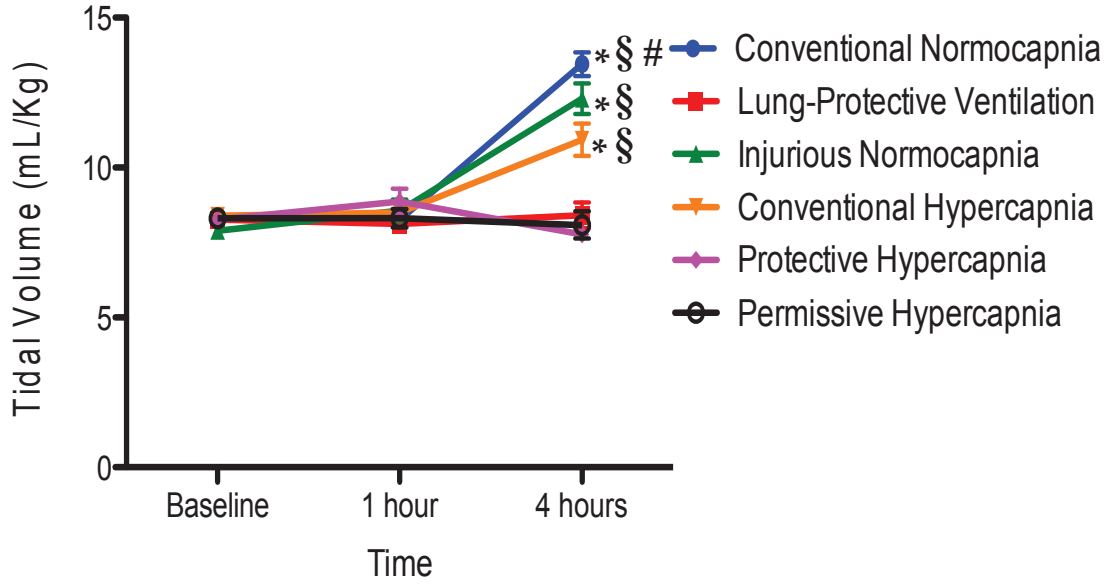

Figure 6. The tidal volume (V_T) at baseline, 1 hour and 4 hours of mechanical ventilation in Conventional Normocapnia, Lung-Protective Ventilation, Injurious Normocapnia, Conventional (Therapeutic) Hypercapnia, Protective (Therapeutic) Hypercapnia and Permissive Hypercapnia. The CI did not differ among the groups at baseline and 1 hour of ventilation. At 4 hours, V_T was higher in Conventional Normocapnia, Injurious Normocapnia and Conventional Hypercapnia compared to Lung-Protective Ventilation, Protective Hypercapnia and Permissive Hypercapnia (§ $p<0.0001$). * $p< 0.0001$ vs. baseline and 1 hour, # $p<0.01$ vs. Conventional Hypercapnia. Values are expressed as mean ± SEM.

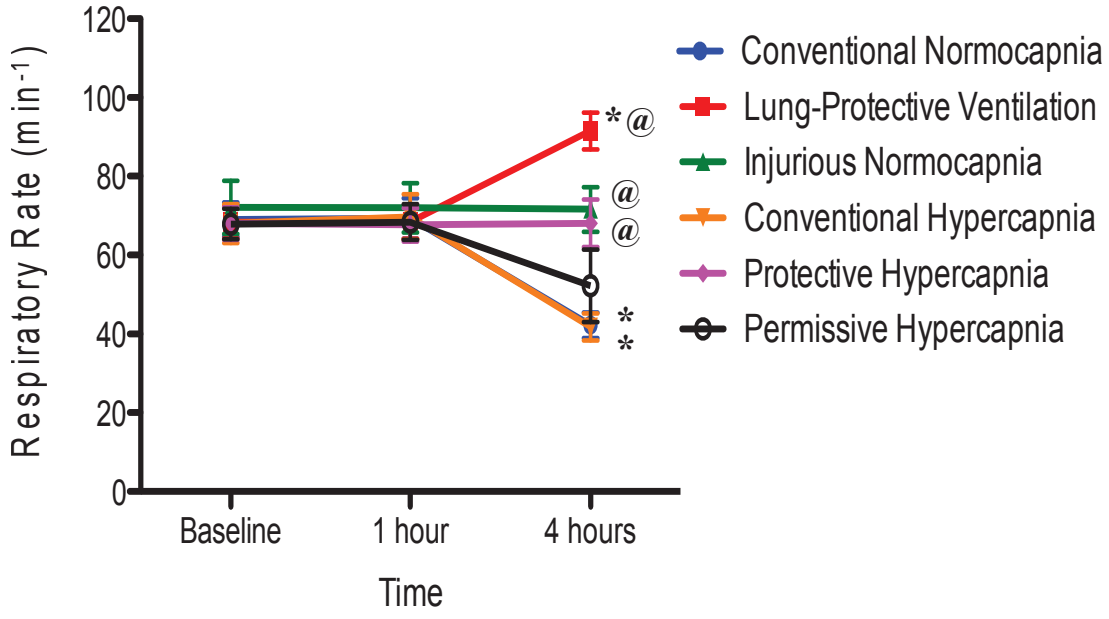

Figure 7. The respiratory rate (RR) at baseline, 1 hour and 4 hours of mechanical ventilation in Conventional Normocapnia, Lung-Protective Ventilation, Injurious Normocapnia, Conventional (Therapeutic) Hypercapnia, Protective (Therapeutic) Hypercapnia and Permissive Hypercapnia. The RR did not differ among the groups at baseline and 1 hour of ventilation. At 4 hours, RR was higher in Lung-Protective Ventilation, Injurious Normocapnia and Protective Hypercapnia compared to Conventional Normocapnia, Conventional Hypercapnia and Permissive Hypercapnia (@ $p<0.0001$). * $p< 0.0001$ vs. baseline and 1 hour. Values are expressed as mean ± SEM.

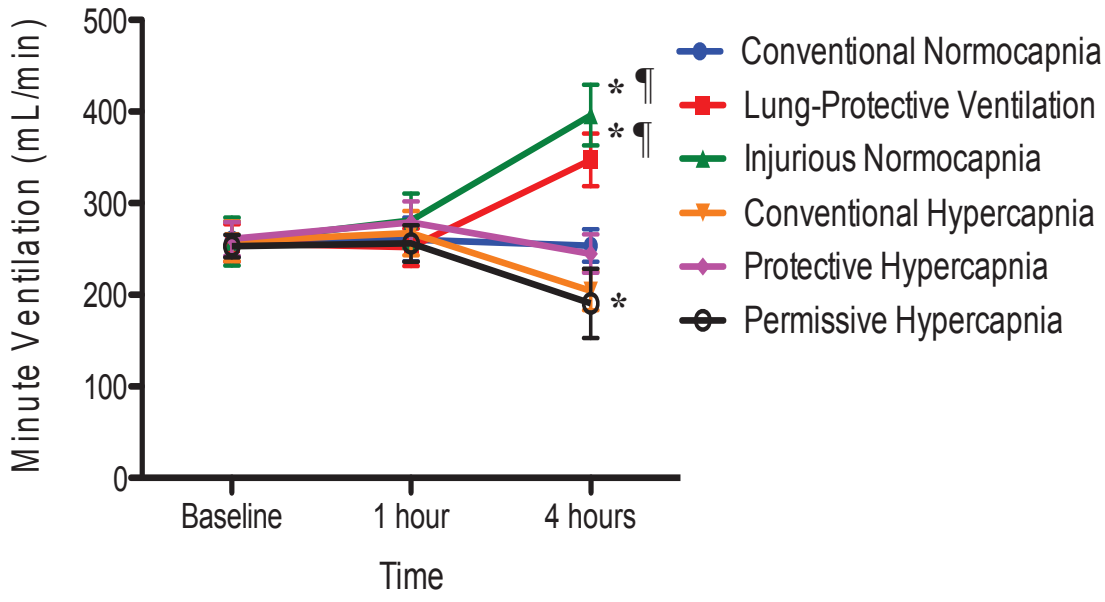

Figure 8. The minute ventilation (V_E) at baseline, 1 hour and 4 hours of mechanical ventilation in Conventional Normocapnia, Lung-Protective Ventilation, Injurious Normocapnia, Conventional (Therapeutic) Hypercapnia, Protective (Therapeutic) Hypercapnia and Permissive Hypercapnia. The V_E did not differ among the groups at baseline and 1 hour of ventilation. At 4 hours, V_E was higher in Lung-Protective Ventilation and Injurious Normocapnia compared to all other groups (¶ $p<0.001$). * $p<0.0001$ vs. baseline and 1 hour. Values are expressed as mean ± SEM.

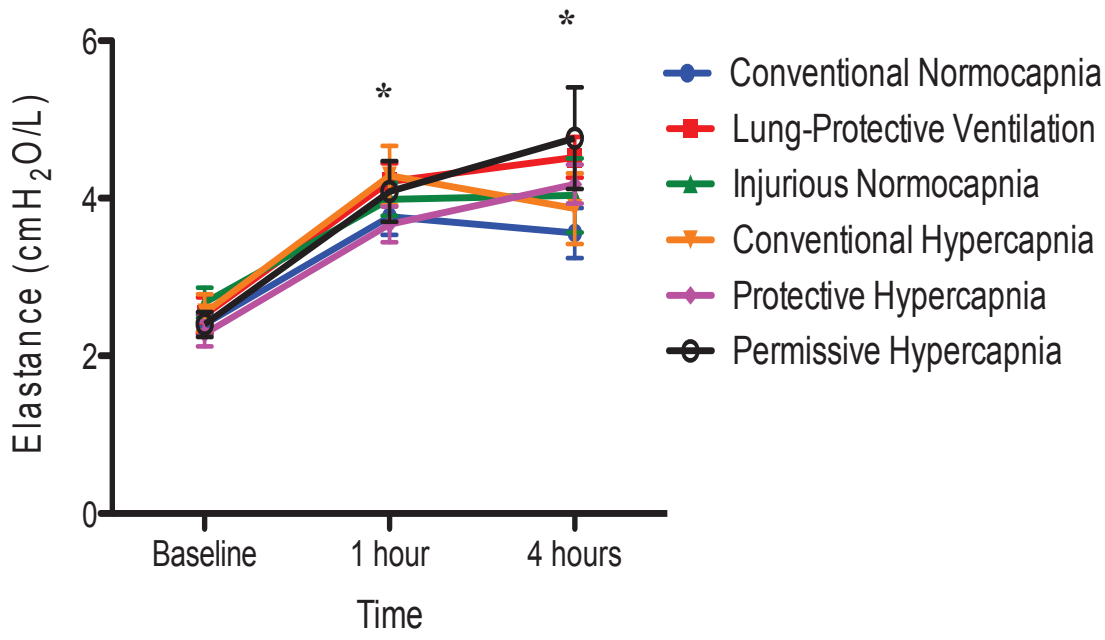

Figure 9. The elastance at baseline, 1 hour and 4 hours of mechanical ventilation in Conventional Normocapnia, Lung-Protective Ventilation, Injurious Normocapnia, Conventional (Therapeutic) Hypercapnia, Protective (Therapeutic) Hypercapnia and Permissive Hypercapnia. The elastance did not differ among the groups at baseline. At 1 hour of ventilation, elastance increased in all groups compared to baseline (* $p < 0.0001$). At 4 hours, elastance increased further in all groups compared to baseline. Values are expressed as mean ± SEM.

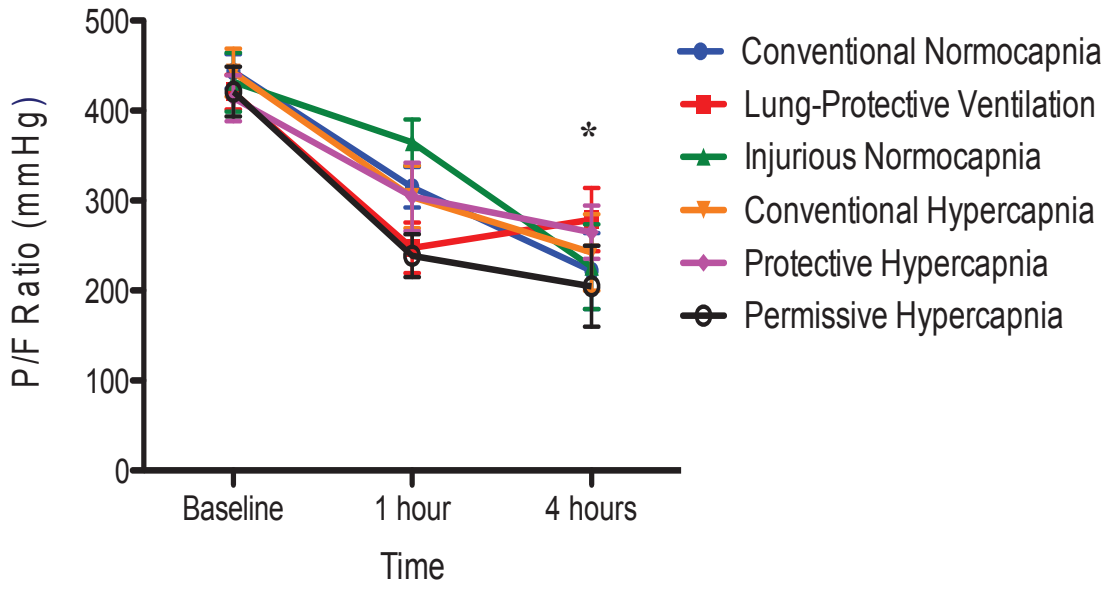

Figure 10. The partial pressure of arterial oxygen (PaO_2) at baseline, 1 hour and 4 hours of mechanical ventilation in Conventional Normocapnia, Lung-Protective Ventilation, Injurious Normocapnia, Conventional (Therapeutic) Hypercapnia, Protective (Therapeutic) Hypercapnia and Permissive Hypercapnia. The P/F ratio did not differ among the groups at baseline. At 1 hour of ventilation, the P/F ratio decreased in all groups compared to baseline, however not significantly. At 4 hours, the P/F ratio decreased further in all groups compared to baseline (* $p < 0.0001$). Values are expressed as mean ± SEM.

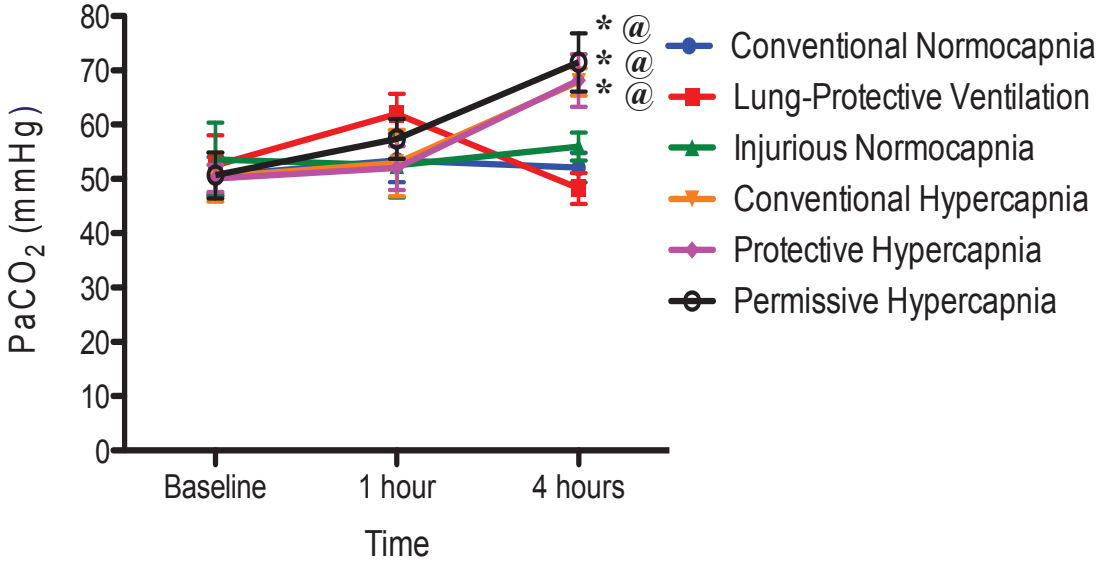

Figure 11. The partial pressure of arterial carbon dioxide ($PaCO_2$) at baseline, 1 hour and 4 hours of mechanical ventilation in Conventional Normocapnia, Lung-Protective Ventilation, Injurious Normocapnia, Conventional (Therapeutic) Hypercapnia, Protective (Therapeutic) Hypercapnia and Permissive Hypercapnia. $PaCO_2$ did not differ among the groups at baseline and 1 hour. The $PaCO_2$ was significantly higher in Conventional Hypercapnia, Protective Hypercapnia and Permissive Hypercapnia at 4 hours compared to baseline (* $p< 0.001$), and compared to Conventional Normocapnia, Lung-Protective Ventilation and Injurious Normocapnia at 4 hours (@ $p<0.0001$). Values are expressed as mean ± SEM.

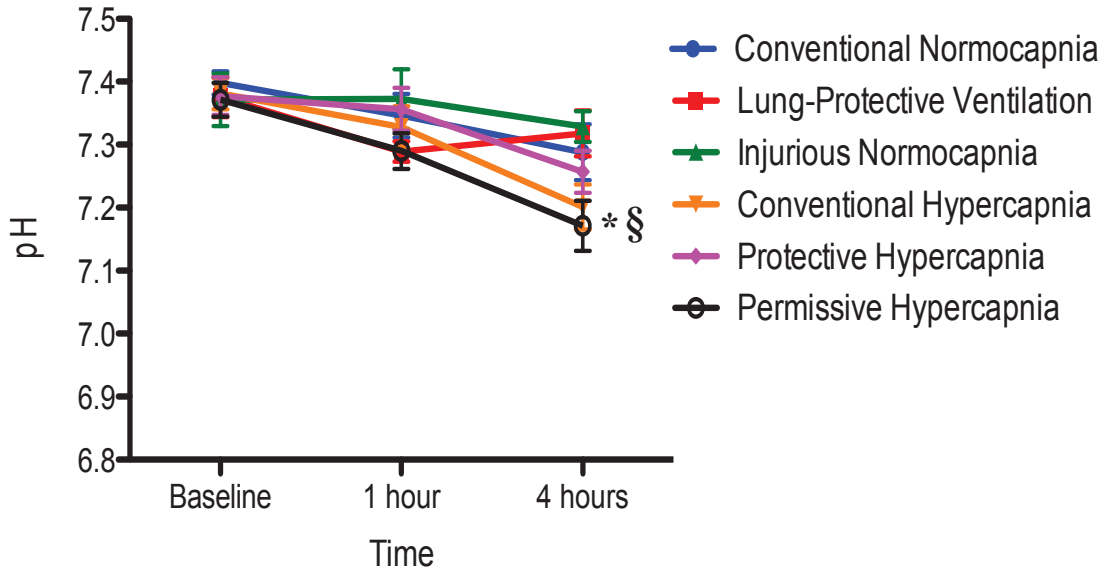

Figure 12. Arterial pH at baseline, 1 hour and 4 hours of mechanical ventilation in Conventional Normocapnia, Lung-Protective Ventilation, Injurious Normocapnia, Conventional (Therapeutic) Hypercapnia, Protective (Therapeutic) Hypercapnia and Permissive Hypercapnia. pH did not differ among the groups at baseline and 1 hour. At 4 hours, pH was significantly lower in Permissive Hypercapnia compared to Lung-Protective Ventilation at 4 hours (§ $p < 0.05$), and compared to baseline pH in Permissive Hypercapnia (* $p<0.0001$). Values are expressed as mean ± SEM.

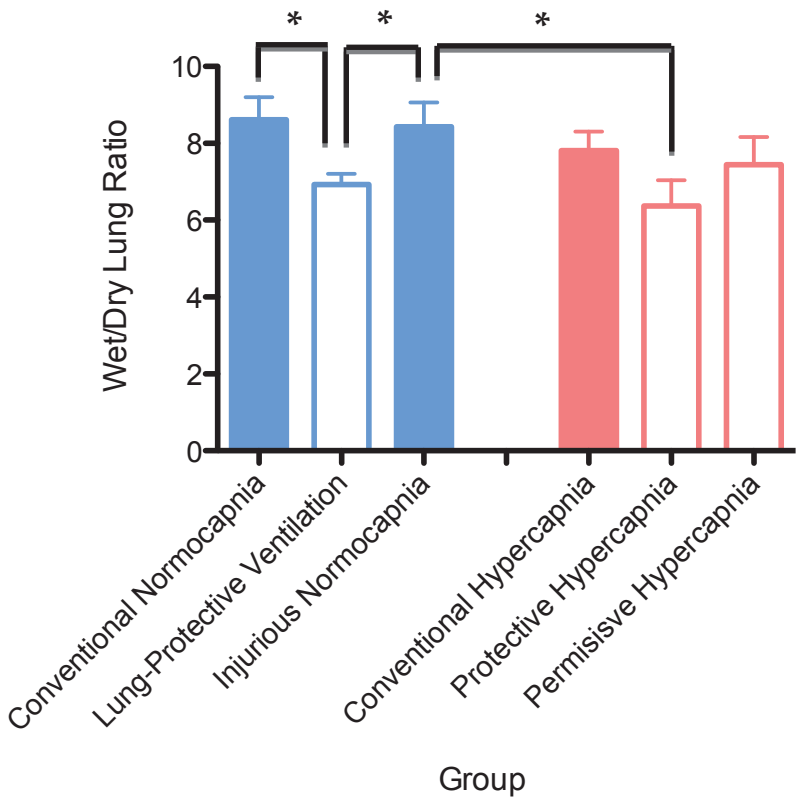

Figure 13. Postmortem Wet-to-Dry Lung Ratio was lower in Lung-Protective Ventilation compared to Conventional Ventilation and Injurious Normocapnia. Protective Hypercapnia produced a lower wet/dry lung ratio compared to Injurious Normocapnia (* $p<0.05$). Legend: blue border: normocapnia (Partial Pressure of Arterial CO_2, $PaCO_2$ target= 40-55 mmHg); pink border: hypercapnia ($PaCO_2$ target=60-70 mmHg); solid bars: conventional ventilation settings (high tidal volume, V_T); open bars: protective ventilation settings (V_T target of 8 mL/Kg). Values are expressed as mean ± SEM.

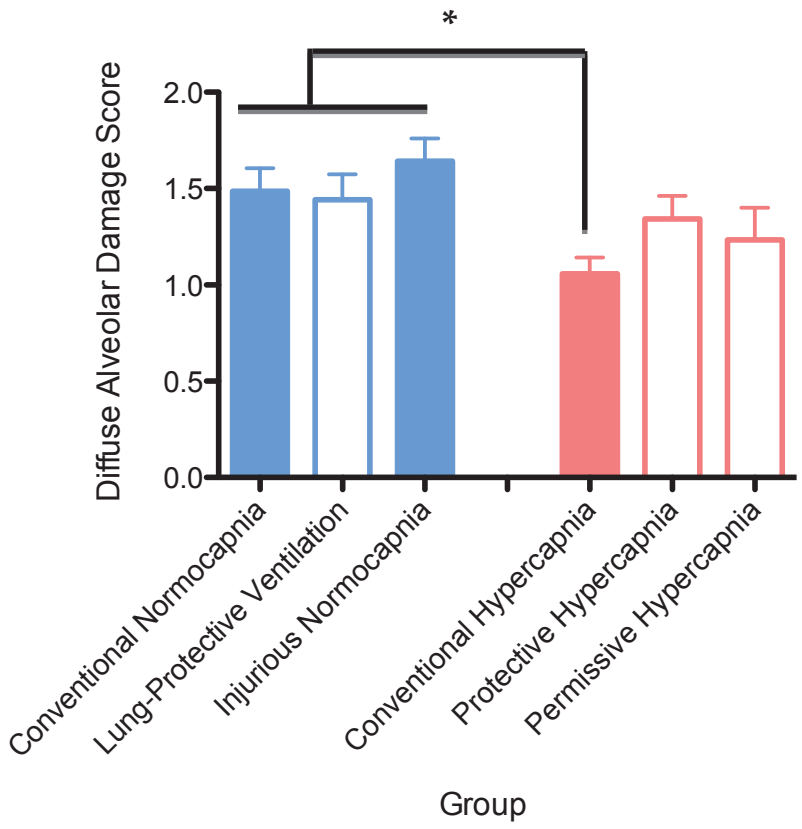

Figure 14. Diffuse Alveolar Damage (DAD) lung injury score was lower in Conventional Injurious Normocapnia, Conventional Normocapnia and Lung-Protective Ventilation (* $p<0.05$). Legend: blue border: normocapnia (Partial Pressure of Arterial CO_2, $PaCO_2$ target= 40-55 mmHg); pink border: hypercapnia ($PaCO_2$ target=60-70 mmHg); solid bars: conventional ventilation settings (high tidal volume, V_T); open bars: protective ventilation settings (V_T target of 8 mL/Kg). Values are expressed as mean ± SEM.

Figure 15. Diffuse Alveolar Damage (DAD) subscores: Interstitial edema, alveolar edema, hyaline membranes, atelectasis, and alveolar damage. Legend: blue border: normocapnia (Partial Pressure of Arterial CO_2, $PaCO_2$ target= 40-55 mmHg); pink border: hypercapnia ($PaCO_2$ target=60-70 mmHg); solid bars: conventional ventilation settings (high tidal volume, V_T); open bars: protective ventilation settings (V_T target of 8 mL/Kg). Values are expressed as mean ± SEM.

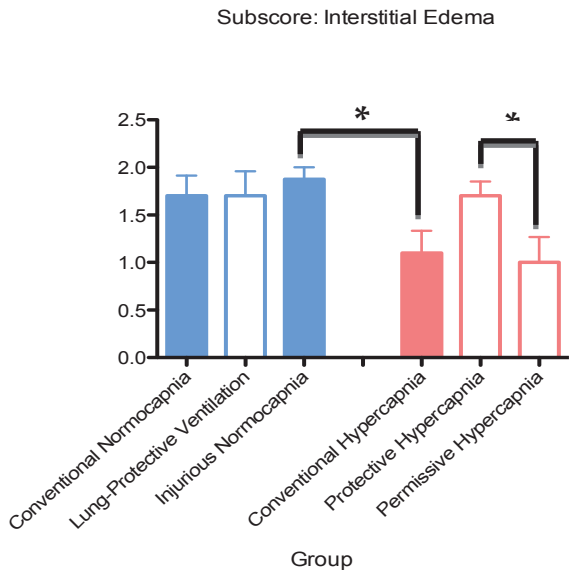
Subscore: Interstitial Edema
2.5
2.0
1.5
1.0
0.5
0.0
*
*
Conventional Normocapnia
Lung-Protective Ventilation
Injurious Normocapnia
Conventional Hypercapnia
Protective Hypercapnia
Permissive Hypercapnia
Group

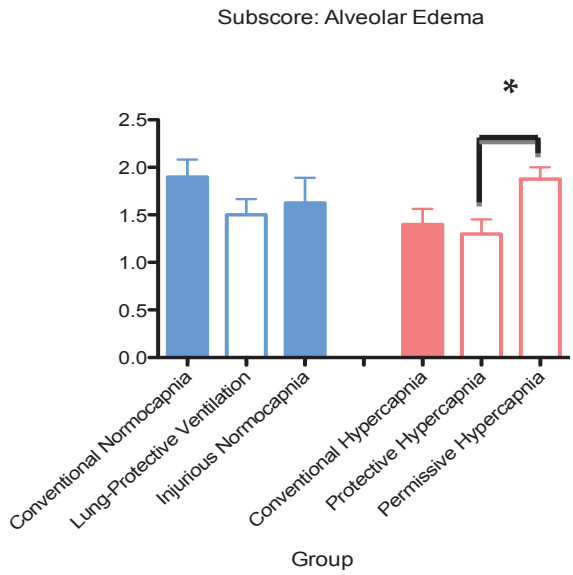
Subscore: Alveolar Edema
2.5
2.0
1.5
1.0
0.5
0.0
*
Conventional Normocapnia
Lung-Protective Ventilation
Injurious Normocapnia
Conventional Hypercapnia
Protective Hypercapnia
Permissive Hypercapnia
Group

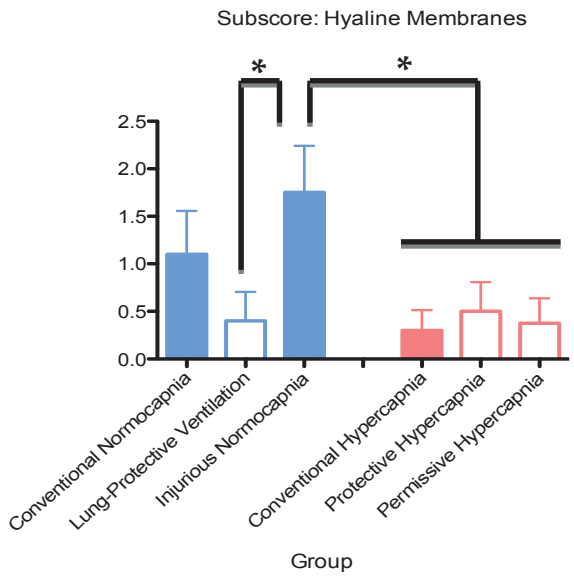
Subscore: Hyaline Membranes
2.5
2.0
1.5
1.0
0.5
0.0
*
*
Conventional Normocapnia
Lung-Protective Ventilation
Injurious Normocapnia
Conventional Hypercapnia
Protective Hypercapnia
Permissive Hypercapnia
Group

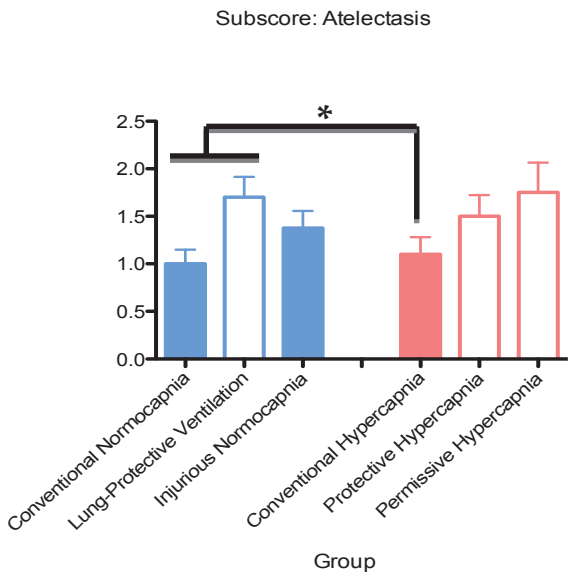
Subscore: Atelectasis
2.5
2.0
1.5
1.0
0.5
0.0
*
Conventional Normocapnia
Lung-Protective Ventilation
Injurious Normocapnia
Conventional Hypercapnia
Protective Hypercapnia
Permissive Hypercapnia
Group

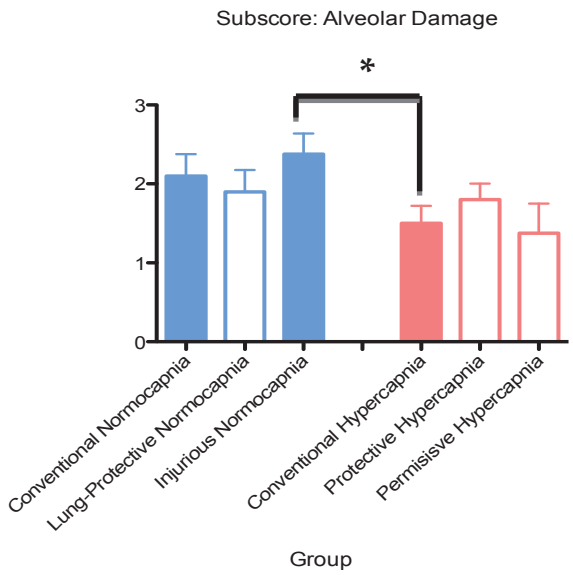
Subscore: Alveolar Damage
*
3
2
1
0
Conventional Normocapnia
Lung-Protective Normocapnia
Injurious Normocapnia
Conventional Hypercapnia
Protective Hypercapnia
Permisisve Hypercapnia
Group

Figure 16. Morphological changes in lung tissue stained with hematoxylin and eosin after 4 hours of ventilation, shown in 40X magnification. Lung tissues show the presence of polymorphonuclear (PMN) cell infiltration **(P)**, atelectasis **(A)**, hyaline membranes **(HM)**, hemorrhages **(H)**, and edema **(E)**.

Conventional Normocapnia

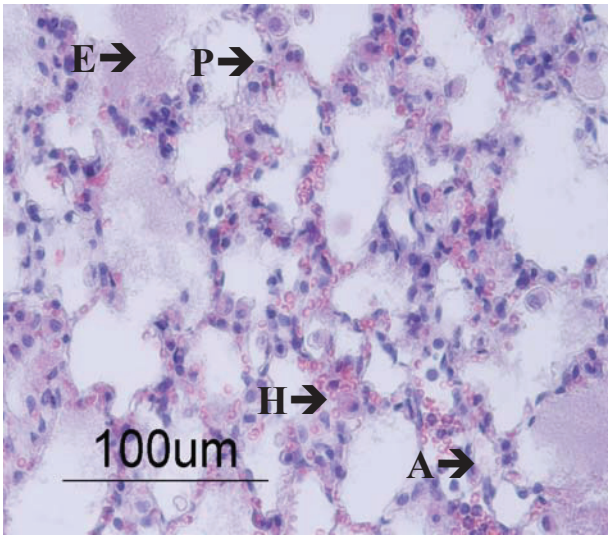

Lung-Protective Ventilation

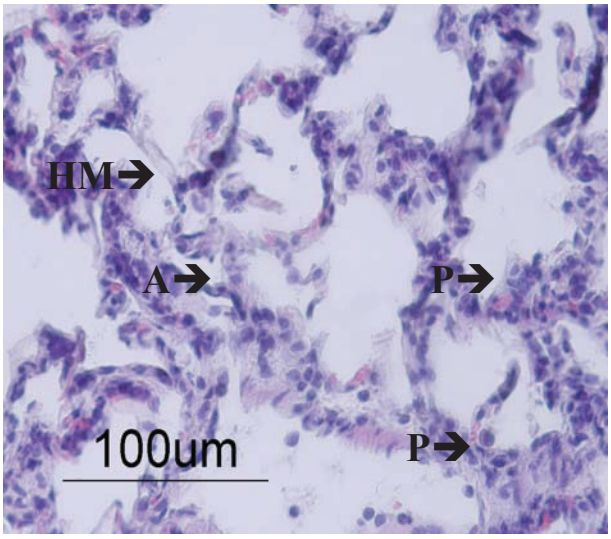

Injurious Normocapnia

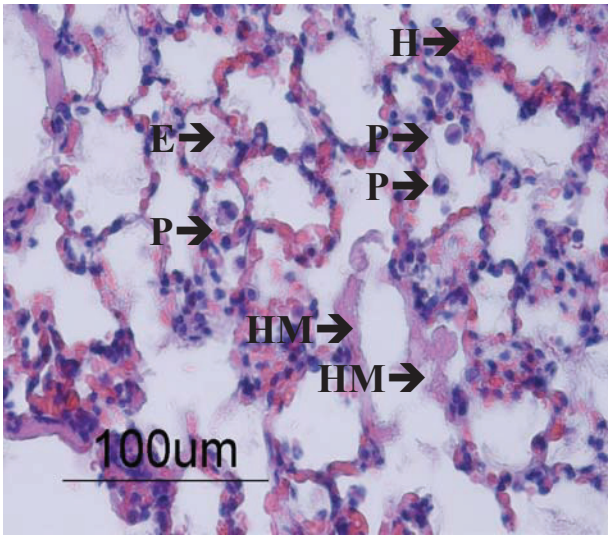

Conventional Hypercapnia

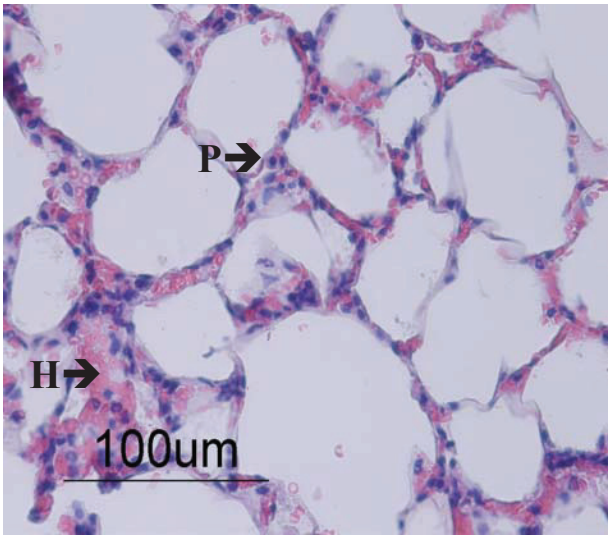

Protective Hypercapnia

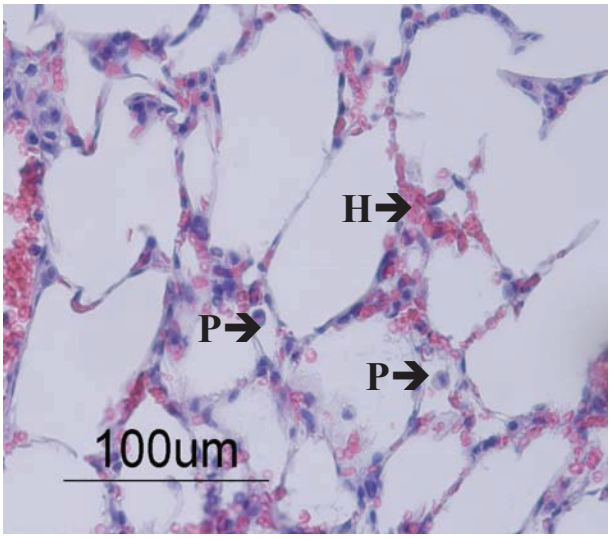

Permissive Hypercapnia

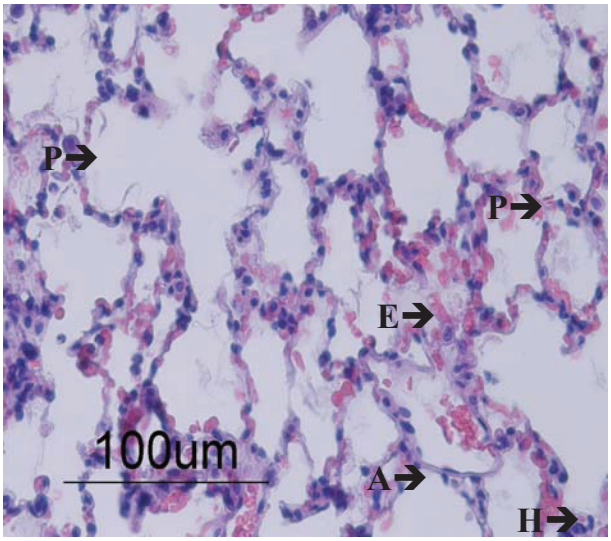

Figure 17. Cytokine and chemokine concentrations in plasma. IL-1β levels were lower in Protective Hypercapnia compared to Conventional Normocapnia and Lung-Protective Ventilation , and lower in Conventional Hypercapnia compared to Conventional Normocapnia **(A)**. TNF-α levels were lower in Protective Hypercapnia compared to Conventional Normocapnia **(D)**. IL-10 was present in higher concentrations in Conventional Normocapnia compared to Protective Hypercapnia **(F)**, (* $p<0.05$). Legend: blue border: normocapnia (Partial Pressure of Arterial CO_2, $PaCO_2$ target= 40-55 mmHg); pink border: hypercapnia ($PaCO_2$ target=60-70 mmHg); solid bars: conventional ventilation settings (high tidal volume, V_T); open bars: protective ventilation settings (V_T target of 8 mL/Kg). Values are expressed as mean ± SEM. (---) indicates normal levels in rat plasma, ND indicates not detectable.

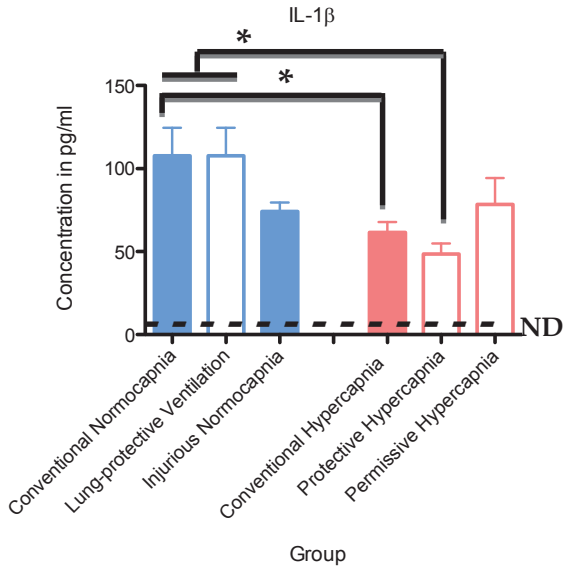
IL-1β
*
*
150
100
50
0
Concentration in pg/ml
ND
Conventional Normocapnia
Lung-protective Ventilation
Injurious Normocapnia
Conventional Hypercapnia
Protective Hypercapnia
Permissive Hypercapnia
Group

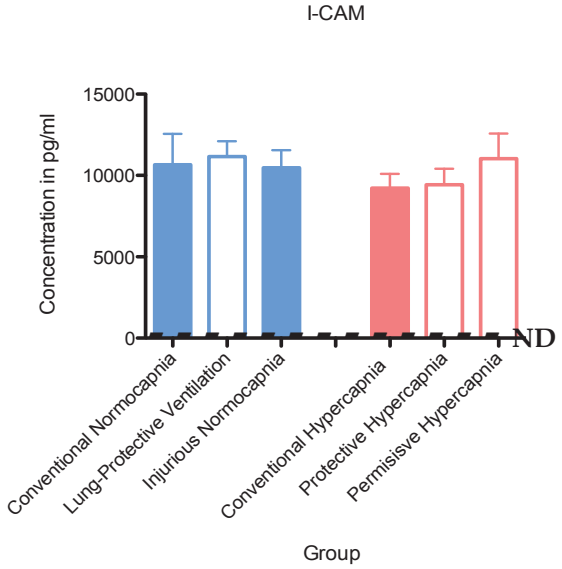
I-CAM
15000
10000
5000
0
Concentration in pg/ml
ND
Conventional Normocapnia
Lung-Protective Ventilation
Injurious Normocapnia
Conventional Hypercapnia
Protective Hypercapnia
Permisisve Hypercapnia
Group

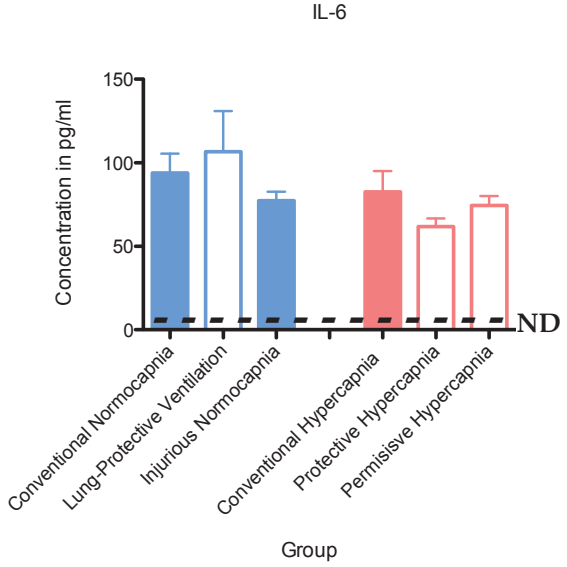
IL-6
150
100
50
0
Concentration in pg/ml
ND
Conventional Normocapnia
Lung-Protective Ventilation
Injurious Normocapnia
Conventional Hypercapnia
Protective Hypercapnia
Permisisve Hypercapnia
Group

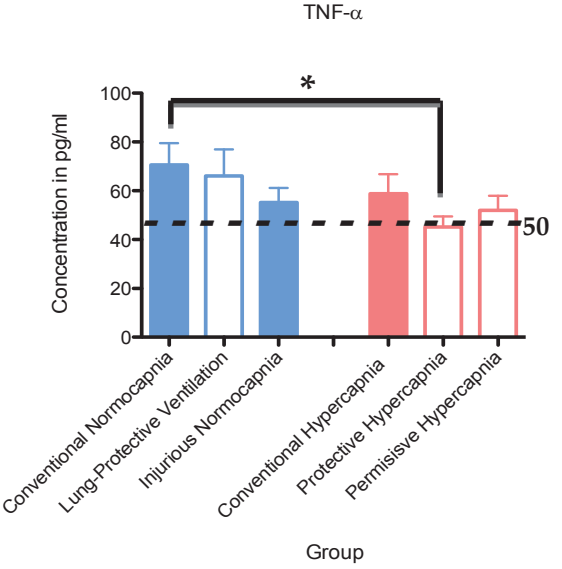
TNF-α
*
100
80
60
40
20
0
Concentration in pg/ml
50
Conventional Normocapnia
Lung-Protective Ventilation
Injurious Normocapnia
Conventional Hypercapnia
Protective Hypercapnia
Permisisve Hypercapnia
Group

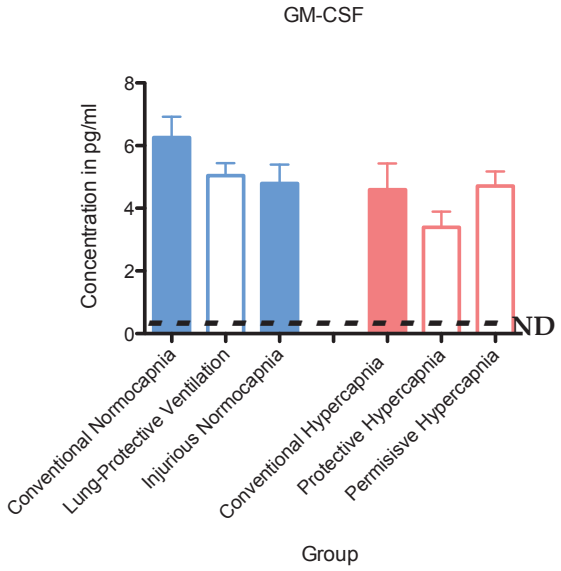
GM-CSF
Concentration in pg/ml
8
6
4
2
0
ND
Conventional Normocapnia
Lung-Protective Ventilation
Injurious Normocapnia
Conventional Hypercapnia
Protective Hypercapnia
Permisisve Hypercapnia
Group

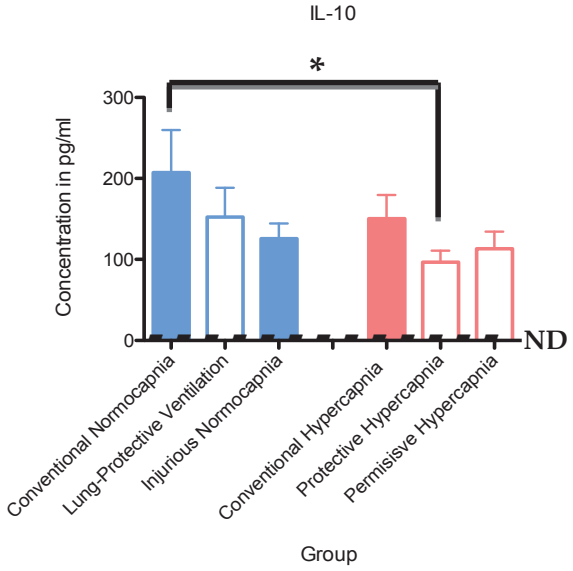
IL-10
*
Concentration in pg/ml
300
200
100
0
ND
Conventional Normocapnia
Lung-Protective Ventilation
Injurious Normocapnia
Conventional Hypercapnia
Protective Hypercapnia
Permisisve Hypercapnia
Group

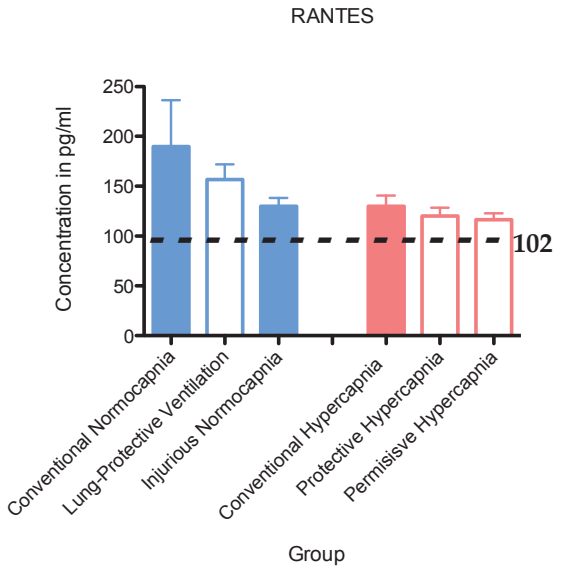
RANTES
Concentration in pg/ml
250
200
150
100
50
0
102
Conventional Normocapnia
Lung-Protective Ventilation
Injurious Normocapnia
Conventional Hypercapnia
Protective Hypercapnia
Permisisve Hypercapnia
Group

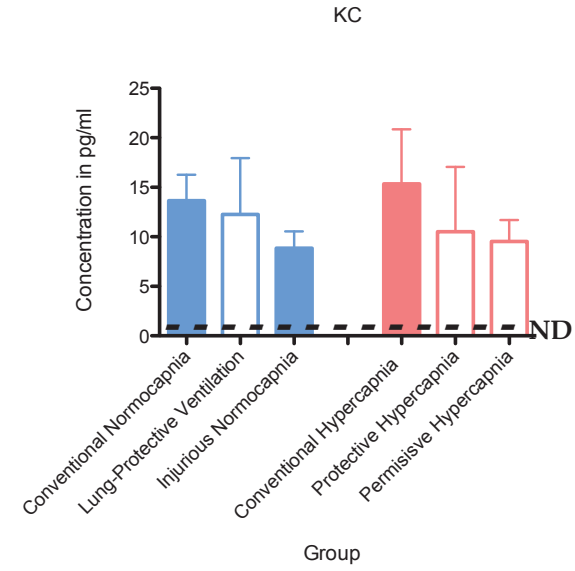
KC
Concentration in pg/ml
25
20
15
10
5
0
ND
Conventional Normocapnia
Lung-Protective Ventilation
Injurious Normocapnia
Conventional Hypercapnia
Protective Hypercapnia
Permisisve Hypercapnia
Group

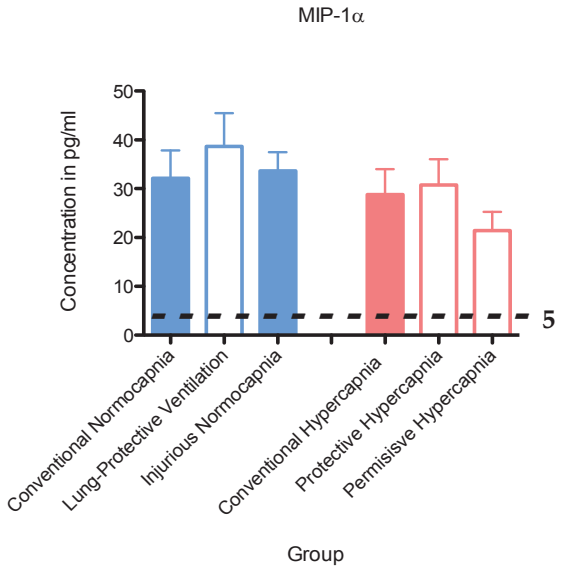
MIP-1α
Concentration in pg/ml
50
40
30
20
10
0
5
Conventional Normocapnia
Lung-Protective Ventilation
Injurious Normocapnia
Conventional Hypercapnia
Protective Hypercapnia
Permisisve Hypercapnia
Group

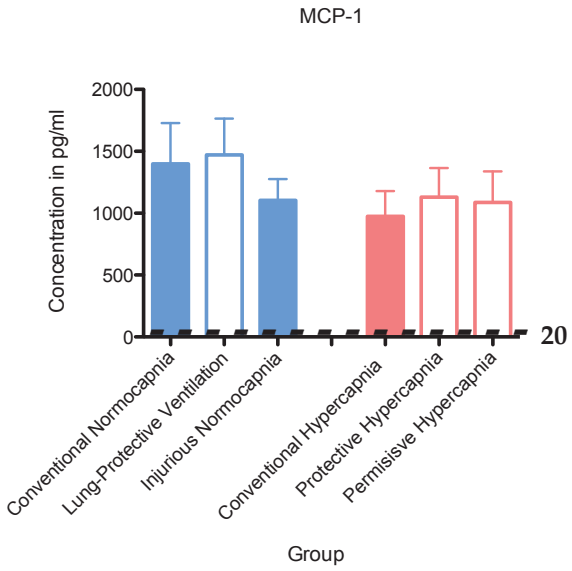
MCP-1
Concentration in pg/ml
2000
1500
1000
500
0
20
Conventional Normocapnia
Lung-Protective Ventilation
Injurious Normocapnia
Conventional Hypercapnia
Protective Hypercapnia
Permisisve Hypercapnia
Group

Figure 18. Cytokine and chemokine concentrations in bronchoalveolar lavage fluid (BALF). IL-6 levels were lower in Conventional Hypercapnia compared to Conventional Normocapnia and Injurious Normocapnia **(C)**. IL-10 levels were higher in Permissive Hypercapnia compared to Lung-Protective Ventilation **(F)**. Monocyte Chemotactic Protein-1 (MCP-1) was lower in all hypercapnia groups (pink) compared to all normocapnia groups (blue) **(J)** (* $p<0.05$). Legend: blue border: normocapnia (Partial Pressure of Arterial CO_2, $PaCO_2$ target= 40-55 mmHg); pink border: hypercapnia ($PaCO_2$ target=60-70 mmHg); solid bars: conventional ventilation settings (high tidal volume, V_T); open bars: protective ventilation settings (V_T target of 8 mL/Kg). Values are expressed as mean ± SEM. (---) indicates normal levels in BALF, ND indicates not detectable .

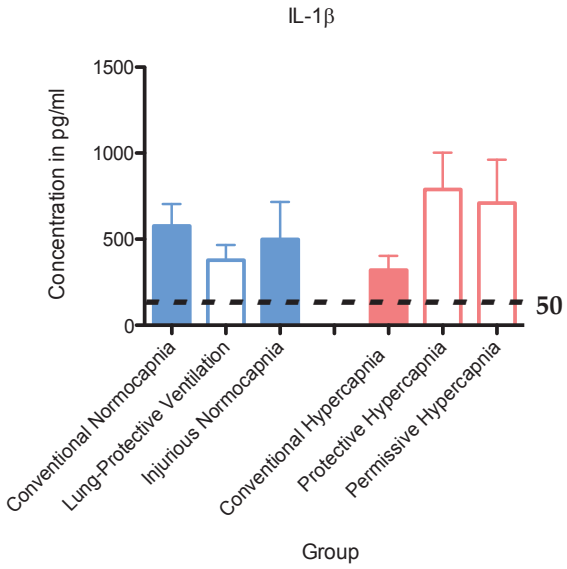
IL-1β
Concentration in pg/ml
1500
1000
500
0
50
Conventional Normocapnia
Lung-Protective Ventilation
Injurious Normocapnia
Conventional Hypercapnia
Protective Hypercapnia
Permissive Hypercapnia
Group

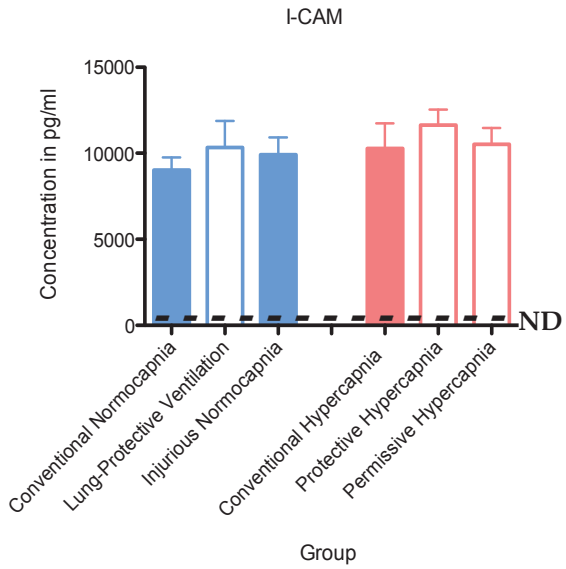
I-CAM
Concentration in pg/ml
15000
10000
5000
0
ND
Conventional Normocapnia
Lung-Protective Ventilation
Injurious Normocapnia
Conventional Hypercapnia
Protective Hypercapnia
Permissive Hypercapnia
Group

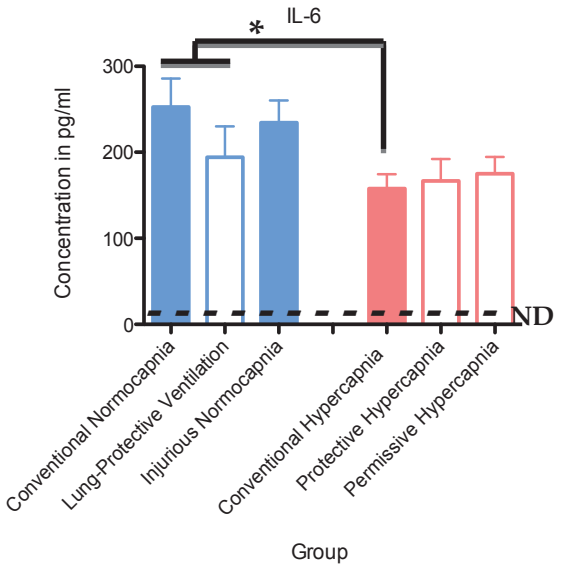
IL-6
*
Concentration in pg/ml
300
200
100
0
ND
Conventional Normocapnia
Lung-Protective Ventilation
Injurious Normocapnia
Conventional Hypercapnia
Protective Hypercapnia
Permissive Hypercapnia
Group

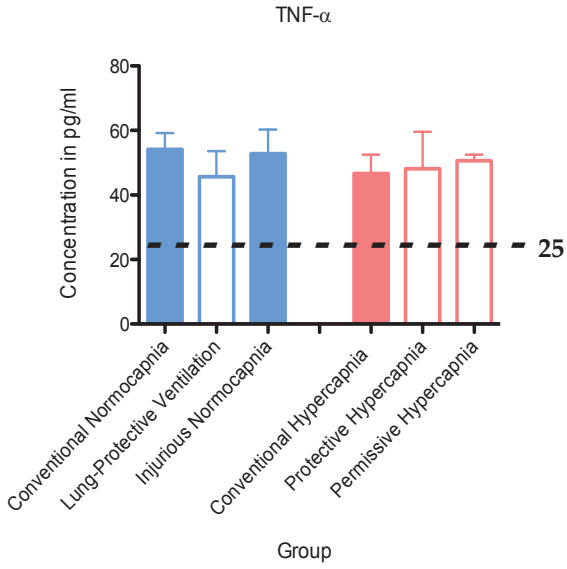
TNF-α
Concentration in pg/ml
80
60
40
20
0
25
Conventional Normocapnia
Lung-Protective Ventilation
Injurious Normocapnia
Conventional Hypercapnia
Protective Hypercapnia
Permissive Hypercapnia
Group

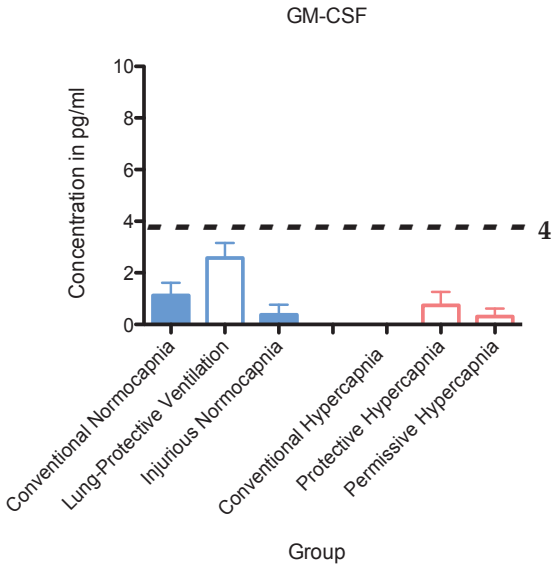
GM-CSF
Concentration in pg/ml
10
8
6
4
2
0
4
Conventional Normocapnia
Lung-Protective Ventilation
Injurious Normocapnia
Conventional Hypercapnia
Protective Hypercapnia
Permissive Hypercapnia
Group

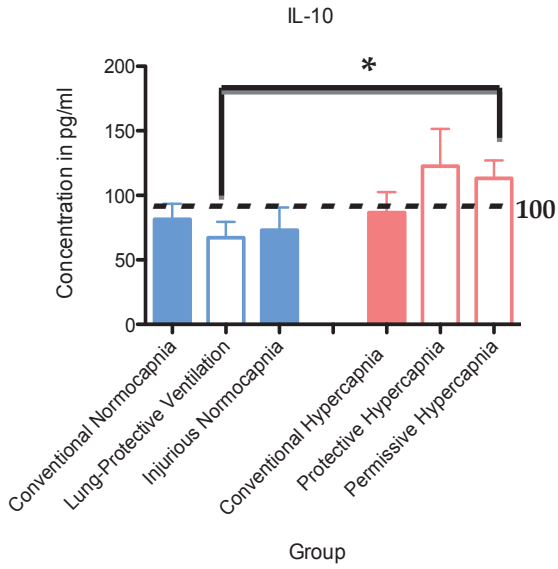
IL-10
Concentration in pg/ml
200
150
100
50
0
*
100
Conventional Normocapnia
Lung-Protective Ventilation
Injurious Normocapnia
Conventional Hypercapnia
Protective Hypercapnia
Permissive Hypercapnia
Group

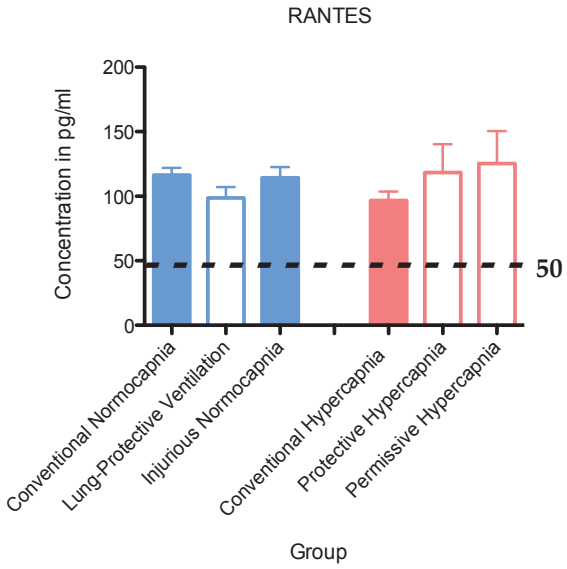
RANTES
Concentration in pg/ml
200
150
100
50
0
50
Conventional Normocapnia
Lung-Protective Ventilation
Injurious Normocapnia
Conventional Hypercapnia
Protective Hypercapnia
Permissive Hypercapnia
Group

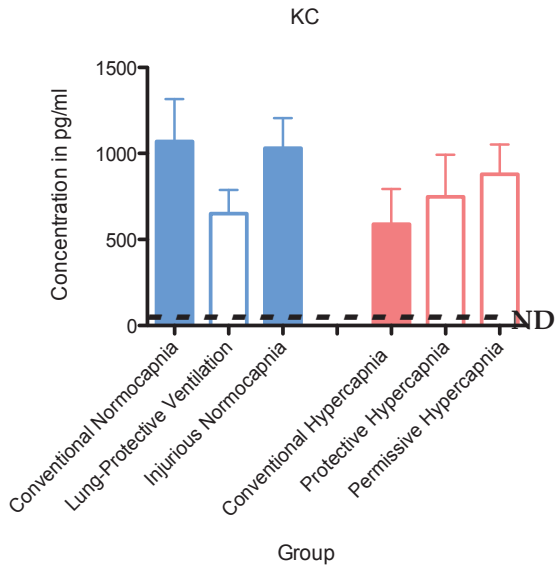
KC
Concentration in pg/ml
1500
1000
500
0
ND
Conventional Normocapnia
Lung-Protective Ventilation
Injurious Normocapnia
Conventional Hypercapnia
Protective Hypercapnia
Permissive Hypercapnia
Group

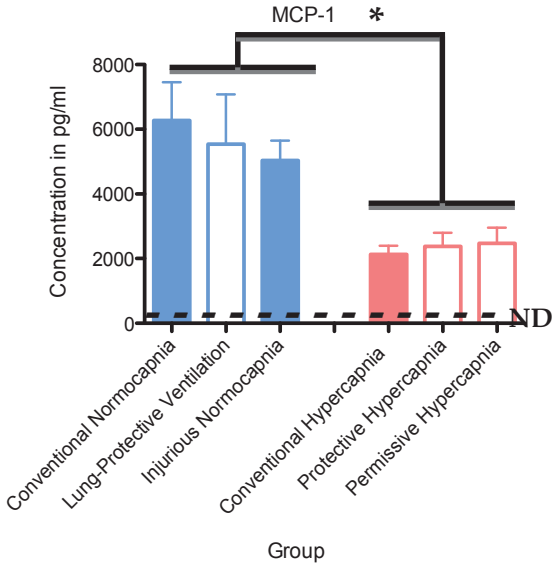
MCP-1
*
Concentration in pg/ml
8000
6000
4000
2000
0
ND
Conventional Normocapnia
Lung-Protective Ventilation
Injurious Normocapnia
Conventional Hypercapnia
Protective Hypercapnia
Permissive Hypercapnia
Group

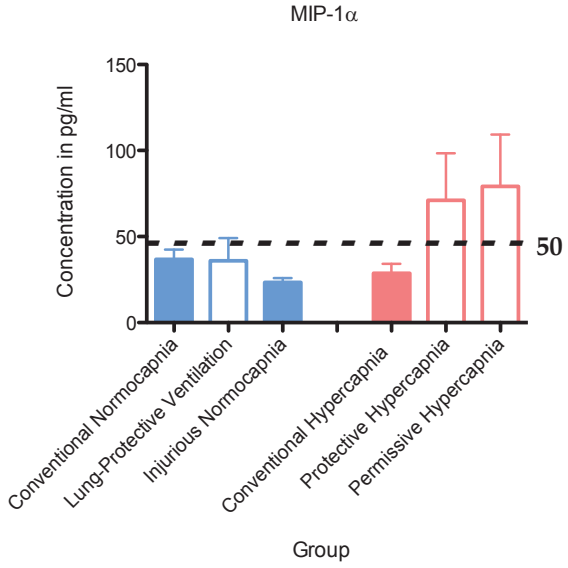
MIP-1α
Concentration in pg/ml
150
100
50
0
50
Conventional Normocapnia
Lung-Protective Ventilation
Injurious Normocapnia
Conventional Hypercapnia
Protective Hypercapnia
Permissive Hypercapnia
Group

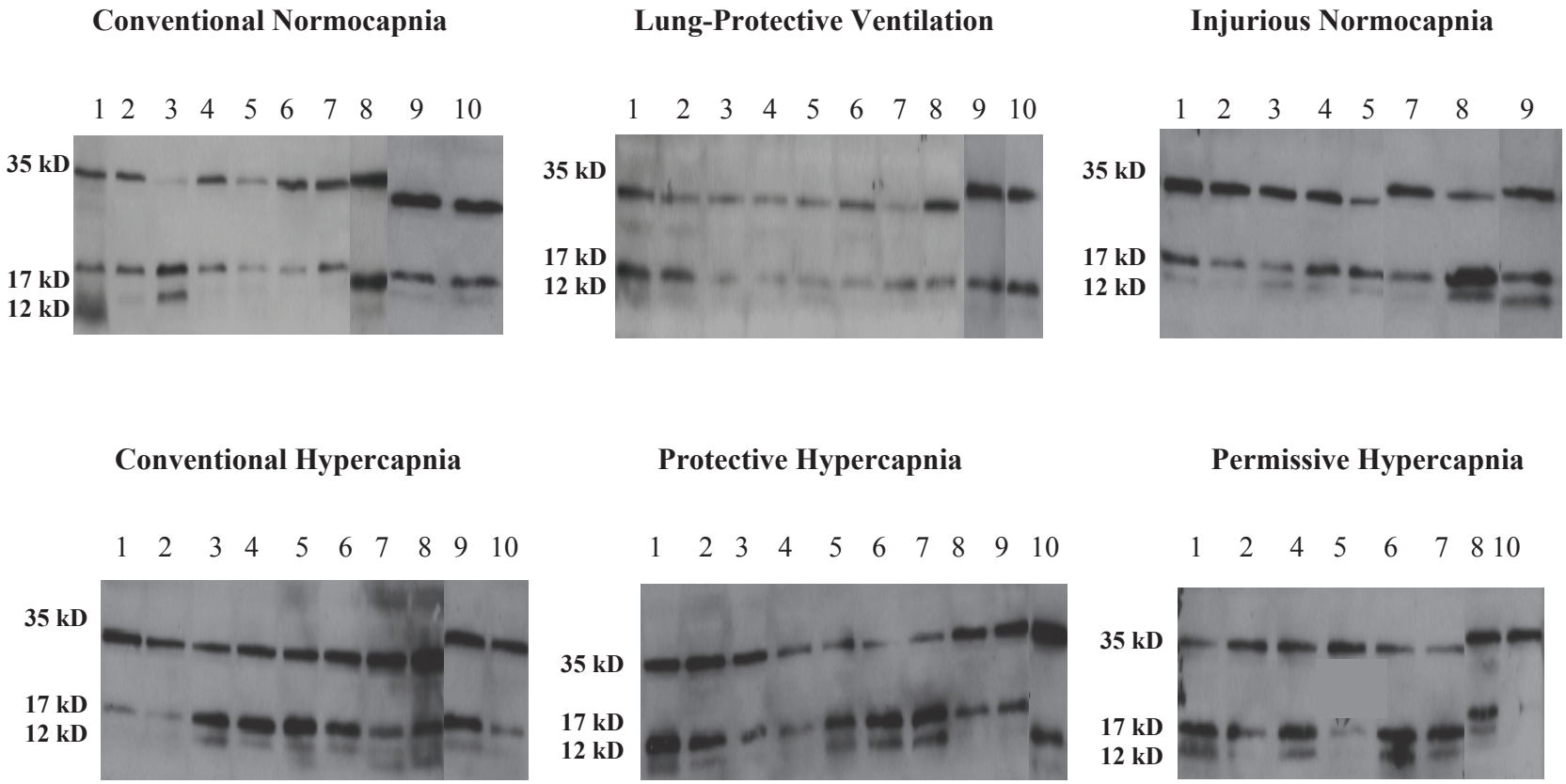

Figure 19. Western blot analysis of caspase-3 expression in lung homogenates. Inactive (uncleaved) caspase-3 (35 kD), active (cleaved) caspase-3 (17 kD and 12 kD) expression was detected. Caspase-3 activation was expressed as the ratio of active (17 kD): inactive (35 kD) caspase-3.

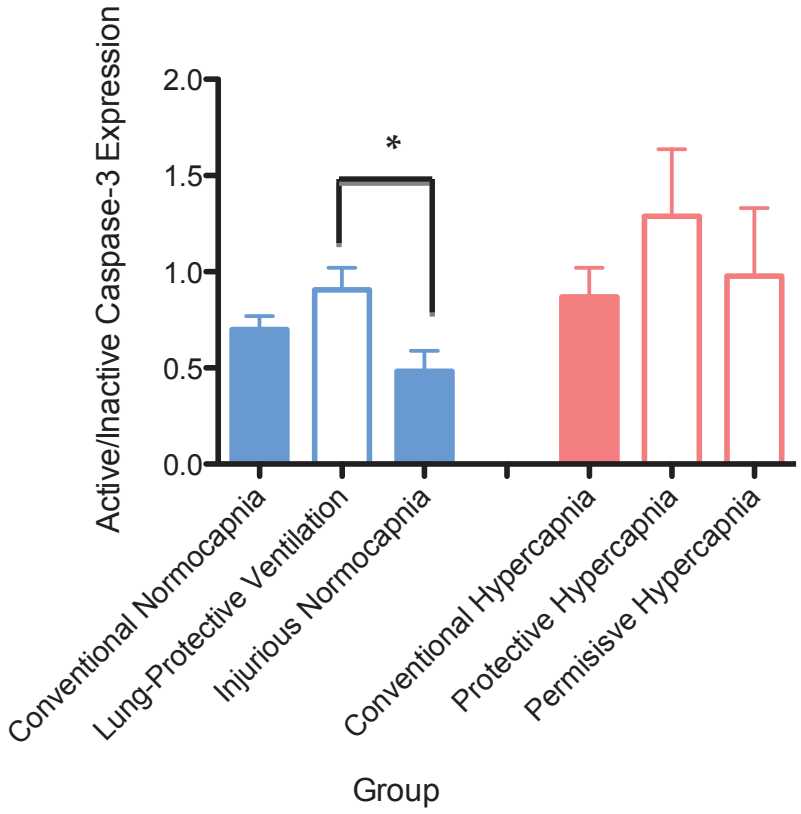

Figure 20. Ratio of active: inactive caspase-3 expression in rat lung homogenates after 4 hours of ventilation, as measured by western blot densitometric analysis. Legend: blue border: normocapnia (Partial Pressure of Arterial CO_2, $PaCO_2$ target= 40-55 mmHg); pink border: hypercapnia ($PaCO_2$ target=60-70 mmHg); solid bars: conventional ventilation settings (high tidal volume, V_T); open bars: protective ventilation settings (V_T target of 8 mL/Kg). Values are expressed as mean ± SEM.